Exploration en conception mécanique préliminaire des compromis entre contraintes architecturales véhicule et performances vibro-acoustiques agrégées

Abdelbasset Hamdi

ECOLE CENTRALE PARIS

THESE DE DOCTORAT

Spécialité :

GENIE INDUSTRIEL – CONCEPTION MECANIQUE

Présentée et soutenue par

Abdelbasset HAMDI

Le 22/01/2008

Pour l'obtention du

GRADE DE DOCTEUR

Exploration in the Preliminary Mechanical Design of Tradeoffs between Automotive Architecture Constraints and Aggregate Noise Performances

---

Exploration en conception mécanique préliminaire des compromis entre contraintes architecturales véhicule et performances vibro-acoustiques agrégées

Composition du jury:

Rapporteur	Zohra CHERFI	UT de Compiègne, Professeur
Rapporteur	Abdessamad KOBI	Université d'Angers, Professeur
Examinateur	Améziane AOUSSAT	ENSAM Paris, Professeur
Examinateur	Eric LANDEL	RENAULT S. A.
Examinateur	Bruno MAHIEUX	TEUCHOS
Examinateur	Nadège TROUSSIER	UT de Compiègne, Maître de Conférences
Directeur de thèse	Bernard YANNOU	Ecole Centrale Paris, Professeur

ECOLE CENTRALE PARIS

Laboratoire de Génie Industriel

Grande voie des Vignes, 92295 Paris

N°2008-06

ECOLE CENTRALE PARIS

THESE DE DOCTORAT

Spécialité :

GENIE INDUSTRIEL – CONCEPTION MECANIQUE

Présentée et soutenue par

Abdelbasset HAMDI

Le 22/01/2008

Pour l'obtention du

GRADE DE DOCTEUR

Exploration in the Preliminary Mechanical Design of Tradeoffs between Automotive Architecture Constraints and Aggregate Noise Performances

---

Exploration en conception mécanique préliminaire des compromis entre contraintes architecturales véhicule et performances vibro-acoustiques agrégées

Composition du jury:

Rapporteur	Zohra CHERFI	UT de Compiègne, Professeur
Rapporteur	Abdessamad KOBI	Université d'Angers, Professeur
Examinateur	Améziane AOUSSAT	ENSAM Paris, Professeur
Examinateur	Eric LANDEL	RENAULT S. A.
Examinateur	Bruno MAHIEUX	TEUCHOS
Examinateur	Nadège TROUSSIER	UT de Compiègne, Maître de Conférences
Directeur de thèse	Bernard YANNOU	Ecole Centrale Paris, Professeur

ECOLE CENTRALE PARIS

Laboratoire de Génie Industriel

Grande voie des Vignes, 92295 Paris

N°2008-06

Remerciements

La présente thèse est le fruit de collaboration entre le Laboratoire de Génie Industriel de l'Ecole Centrale Paris et la société Renault S.A. Je remercie chaleureusement Monsieur Jean-Claude Bocquet, Directeur du Laboratoire, de m'avoir donné la possibilité de mener mes travaux au sein du labo LGI.

Je remercie vivement Monsieur Abdessamad KOBI et Madame Zohra CHERFI pour avoir accepté la tâche ardue de rapporteur.

Tous mes remerciements à Monsieur Améziane AOUSSAT et Madame Nadège TROUSSIER, de me faire l'honneur de participer à mon jury.

Mes remerciements les plus profonds vont à Monsieur Bernard YANNOU, mon encadrant de thèse, Professeur à l'Ecole Centrale de Paris, qui m'a donné, sans compter de son temps, qui m'a soutenu moralement jusqu'aux derniers pas de cette thèse. Il m'a été d'un grand apport pour les choix et les orientations scientifiques. Il a été avec moi d'une grande patience, non sans être toujours exigeant pour une meilleure rigueur scientifique pour mes travaux de recherches. Je lui exprime mon entière reconnaissance.

Je tiens à remercier particulièrement, Monsieur Eric LANDEL, Chef de Service Acoustique à Renault. C'est sous sa direction que la problématique industrielle présentée dans cette thèse a vu le jour, pour être formulée en projet de recherche. Il nous a donné toute sa confiance et son appui afin de mener à bien ces travaux. Il m'a prodigué de son temps précieux, des heures innombrables de réunion, pour m'aider à m'approprier le contexte industriel. A chaque proposition scientifique, de ma part, il a su m'orienter dans mes démarches afin que mes travaux ne soient pas uniquement un exercice théorique de recherche scientifique, mais qu'ils trouvent aussi un terrain d'application le plus proche possible de la réalité industrielle.

Mes remerciements les plus sincères à Monsieur Bruno MAHIEUX, Chef de département dynamique des structures et acoustique à la société Teuchos, pour ses encouragements perpétuels.

Je voudrais remercier aussi tous mes collègues de Renault avec qui j'ai pu travailler ou partager mes idées ; je pense à Christophe DELVAL, Nezam SANEI, Sébastien CHAIGNE, Michel BERGERON et l'ensemble de mes collègues du service acoustique de Renault.

Un grand merci à Sylvie GUILLEMAIN, Anne PREVOT et à l'ensemble du personnel et de mes collègues du labo LGI.

Je salue mes amis Walid BEN-AHMED, Ramzy BOUSSETTA, Mehdi BEN-TAHAR, Ahmed KHAMASSI, Aurelien MOREAU et pardon si j'ai oublié quelqu'un.

Finalement, je voudrai remercier toute ma famille qui m'a soutenue pendant toute la durée de la thèse et qui continue à me soutenir pour la vie.

A mes parents

Contents

List of figures

List of Tables

Introduction

- **Background**

From the early 1990's, the use of ***Concurrent Engineering*** (CE) in various mechanical industries has permitted to realize critical business objectives of shorter development lead times, lower development costs and improved quality. Using CE from the early design stage leads to the **decomposition of the structural part** of the system to design and of its performances. Indeed to work independently, engineers decompose the mechanical system into subsystems. For each subsystem, a primary stage of **volume allocation** must be done. The allocated volume is a geometric design space within which the subsystem design must fit in. Then, using the *V cycle* in the design process, engineers successively decompose the top-level target (or expected) performances into multiple target performances at lower levels. The system-level target performances must be synthesized from the subsystems' target performances; this is, as we will see later, a high value-added process. The **targets** of the system performances must be **decomposed** and **cascaded** from the top-level of the system into the lower levels corresponding to the subsystems and ultimately to the organs and elementary components.

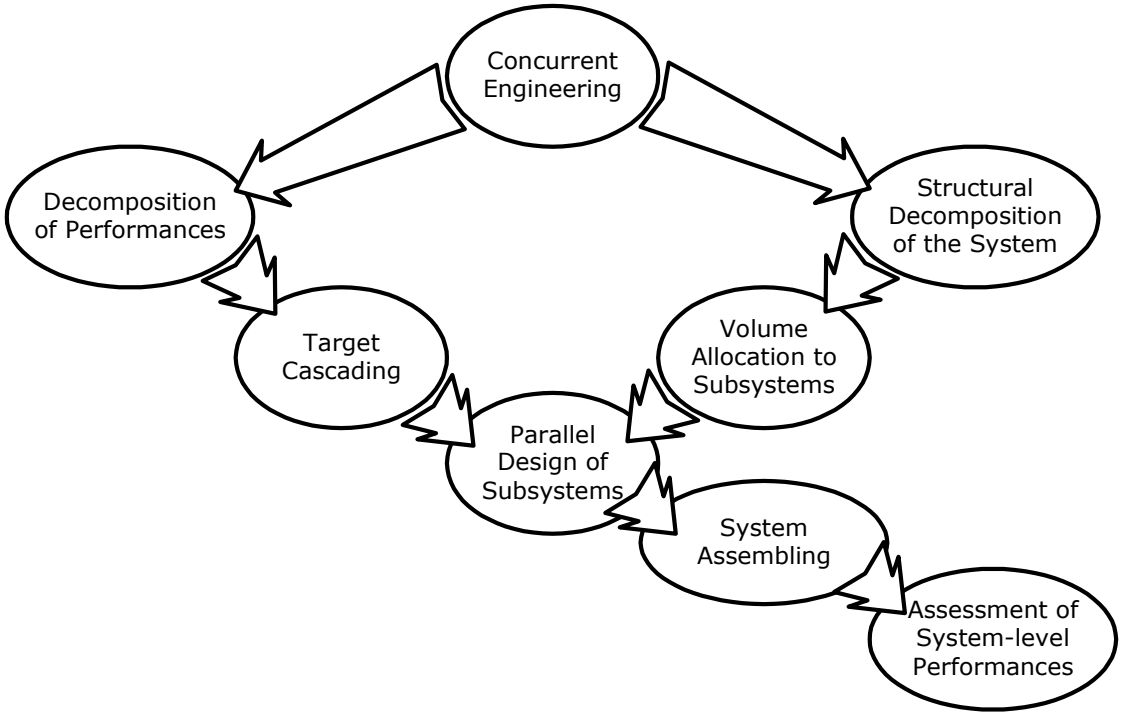

Figure 1 *Concurrent Engineering* implications in the design process of mechanical systems

In this way, engineers can design in **parallel** the subsystems. And, when the design of the subsystems is achieved, engineers numerically check if the **assembling** with the rest of the system is possible. If it is possible, then, engineers can proceed, using CAE[1] tools, to the **assessment** of the **top-level performances** of the system. All this process is summarized in Figure 1.

Despite considerable design integration efforts, this process leads to a **late** assessment of the overall system performances. A late assessment of performances means less possibility for engineers to simulate "what if?" questions and to make evolving the design. Indeed, the design modifications which impact the shape of the subsystems are often too late to take into account and too expensive to integrate.

- **Motivation**

A focus on the concurrent engineering (CE) implications in the preliminary design of mechanical systems let us consider two challenges to tackle with.

The first one is about the decomposition of the system performances. Some questions rise from this issue: Are we able to decompose the targets of the system performances into targets over each of the subsystems? Then, if the design of the subsystems achieves the subsystem targets, are we sure that the system, after assembling, achieves the top-level targets? We refer to **Multidisciplinary Design** and **Analytical Target Cascading** as theoretical backgrounds to deal with this issue.

The second challenge is concerned with the need of **fast**, **surrogate**, and **aggregate** assessment of the subsystem performances to see if the allocated volumes to the subsystems permit the overall design to achieve its targets and consequently, if these primary allocated volumes have finally been well chosen. Although we give targets to the subsystems early in the design stage, it is not guaranteed that a subsystem designed to achieve the targets fits into the allocated volume. Architects of the mechanical system are the engineers who are concerned with system assembling and system architecture from the beginning of the preliminary design stage. Architects allocate the volume that is supposed to guarantee the achievement of the subsystem performances. But, early in the design stage, engineers have no specific tool, other than their experience from previous design cases or benchmarking of existing designs, to negotiate the allocated

[1] Computer Aided Engineering

volume to the subsystems. To be able to efficiently negotiate the volume allocation with the architects, engineers need to assess, even roughly, but quickly, the performances of the subsystems. That is why there is a need, in the preliminary design-stage, of an aggregate and a surrogate assessment of the subsystem performances. The aggregate and surrogate assessment of the performances of the subsystems can help to negotiate more efficiently the primary allocation of the geometric design space. The volume allocation to the subsystem design would be no longer arbitrarily done but it would be afterwards an allocation based on digital assessment (virtual prototyping) of the subsystem performances.

- **Corporate context**

The work resulting in this thesis has been done in close collaboration with industry. The main part of the research has been done at Renault NVH Department in Aubevoye, France, under the industrial supervision of Eric Landel.

- **Industrial application: the case of the preliminary design of automobiles with a focus on noise performance**

The automotive industry is one of the leading industries that adopted CE design. After system decomposition and performance decomposition, the automotive engineers start to concurrently design their subsystems in the geometric design space formerly allocated by the automobile architects: it is the beginning of the preliminary design stage. For an automobile, there are many customer-oriented performances as safety, durability, ride and handling, but we only focus on the quietness. Quietness is rated by the assessment of a mechanical performance that is the noise inside the car. The inside noise is a system-level performance that is decomposed, for the reasons of the CE design, into subsystem-level performances. According to acoustics, the noise inside a cavity which represents the fluid (the air) inside the passenger compartment is due to dynamic coupling between fluid and structure. So, from a mechanical point of view, the noise performance decomposition into subsystem performances (note that subsystems constitute the structure part) leads to assess the vibration performances of those subsystems in order to predict the results of the coupling with the fluid part. Due to this decomposition we come up with a bunch of performances on the subsystem levels.

- Scientific issues

At present time, in automotive industry, volume allocation is performed by vehicle architects within a CAD (Computer Aided Design) environment. But Engineers use a posteriori CAE (Computer Aided Engineering) environments to check that a design is still feasible regarding the mechanical performances they are in charge of.

On the one hand CAD systems are not compatible with the need of a large exploration of the design space in the early design stages. Whereas present CAD software are highly advanced in terms of parametric design, CAD engineers (vehicle architects) in automotive industry still produce most of the time (too much) detailed and "dead" (no high level of parameterization) CAD models with, consequently, no actual possibility to make them varying afterward. The reason is that it is difficult and time-consuming to parameterize the CAD models. Moreover, the design parameterization is dependent of the design discipline. For example, structural design parameters to vary for the crashworthiness performance are not the same for durability performance.

So the first issue is about how to enable a wide variation of the shape parameters and simulate corresponding performances in order to widely explore the design space and to work with the "design uncertainty reduction" paradigm? We will have to choose and adapt a convenient digital environment for allowing variations of the design parameters in preliminary design stage?

On the other hand, architects use CAD environments to "somewhat arbitrary" allocate envelope volumes: an approximate geometric design space in which subsystems of the car must fit. But the allocated volumes can fail to satisfy the demands of performance engineers for more volume. They need a minimum volume in order to guarantee the target achievement of the subsystem performances. Actually, there are too many demands for more geometric design spaces from almost all the design disciplines. But for reason of weight and fuel consumption reduction, subsystems must fit in an ever more narrowed size of the car. Architects allocate more or less design space volumes to the automotive subsystems depending on the argumentations of the engineers for the required volume. Performance engineers have to establish significant relationships between the required volumes and the performance improvement. In order to demonstrate the possible performance improvements, engineers propose some subsystem designs that expand outside the initial allocated volume. In this case, architects need to

know the impact of the proposed design on the other surrounding subsystems represented by their respective allocated volumes.

So the second issue is about how to express the "non-respect of the allocated volume"? And in which design environment can it be represented?

The multiple vibration performances, issued from the decomposition, are the assessment of the multiple dynamic responses of the subsystems, which are subjected to a multiple internal and external excitations of the structure. Each of the response which is a frequency dependent function is subjected to a target. This bunch of vibration performances reduces the ability to focus in a synthetic manner on the vibration performance of the subsystem. So, there is a real need to aggregate vibration performances and their targets into a sole simplified criterion over the subsystem. We recall that a criterion consists of two components: the parameter (or a measure) that is evaluated), and the required standard (threshold).

So the third issue is how to aggregate the multiple vibration performances of a subsystem into one criterion? Can we define a vibration criterion using the aggregate vibration performances? Is the satisfaction of the criterion targets on the subsystems correlated and consistent with the noise targets of the system (e.g. the inside noise in the automobile)? So as to prove that the target decomposition over subsystems was meaningful.

On the other hand, the assessment of the automotive mechanical performances as the noise and vibration performances requires the pre-processing of the CAD models that includes the meshing of the CAD models and the modeling of the boundary conditions. After pre-processing, we obtain finite element (FE) models that are ready for simulation in order to digitally assess the mechanical performances. It currently takes about 6 weeks to prepare the data of the first structures of the automobile (the main frames and panels known as the Body in White "BiW") needed to generate the FEM model, and about 20 minutes for assessing the vibration performances of the BiW that is considered as a subsystem. These two computational times are excessive in the context of preliminary design for quickly exploring large portions of the design space (and then for iterating such a computation).

So the fourth issue is about how to enable fast assessments of mechanical performances. What are pros and cons of using surrogate models (or *metamodels*) for a fast assessment of mechanical performances? Are surrogate models well adapted to the preliminary design stage?

Moreover, engineers lack tools and criteria with which they can negotiate the allocated volume. Then, later in the detailed design stage, when the assessment of the automobile performances by numerical simulations reveals some performance weaknesses of some subsystems, it turns out that negotiations are hard for modifying the structure. The negotiation with the architect of the vehicle project is difficult, especially when the solution proposed by the engineers consists in a modification of the subsystem shape. This modification can lead to an interference of a subsystem with the allocated volumes of other subsystems because it requires design reviews of the other subsystems.

It is up to the mechanical design engineers to negotiate the impact of the modification of the allocated volume on the fulfillment of their design targets. There is no explicit modeling of the tradeoff between a still modifiable volume allocation and the probable mechanical performances of subsystems/components which must fit in this allocated volume. Presently, there is no tool for simultaneously exploring the compliance of both architectural constraints and targets of mechanical performances.

So, the fifth and the last issue is how to enable tradeoffs between architectural constraints and mechanical performances (e.g. noise performances)?

- **Thesis proposal**

Our proposal is to embed all the invoked issues into a methodology (a process) in order to enable the exploration, in the preliminary design, of tradeoffs between automotive architectural constraints and aggregate noise performances. Figure 2 illustrates the proposed process. The main stages of this illustrated process are: the geometry processing that includes the volume allocation stage, the shape and structure parameterization, design criteria building, metamodeling and finally the tradeoff exploration stage.

First, volume allocation and the geometric models of the subsystems are drawn using CAD software. Then, the preprocessing operations are done in order to obtain Finite Elements (FE) meshes. At this stage, apart from the classical operations consisting in cleaning up the geometry, setting up the physical properties, and setting the loads and the boundary conditions, we propose that the allocated volumes represented by CAD models to be meshed using FE shells. This operation enables geometric calculation of the respect of architectural constraints using the simulation models and not the CAD models. We proceed then to the parameterization of the structure and of the shape of the subsystem with the minimal set of meaningful parameters that one would like to make varying in an exploration process. The shape of the subsystem is parameterized using the morphing techniques applied to the FE model. Other parameters of the structure are accessible like the shell thicknesses, the physical properties, and the material properties.

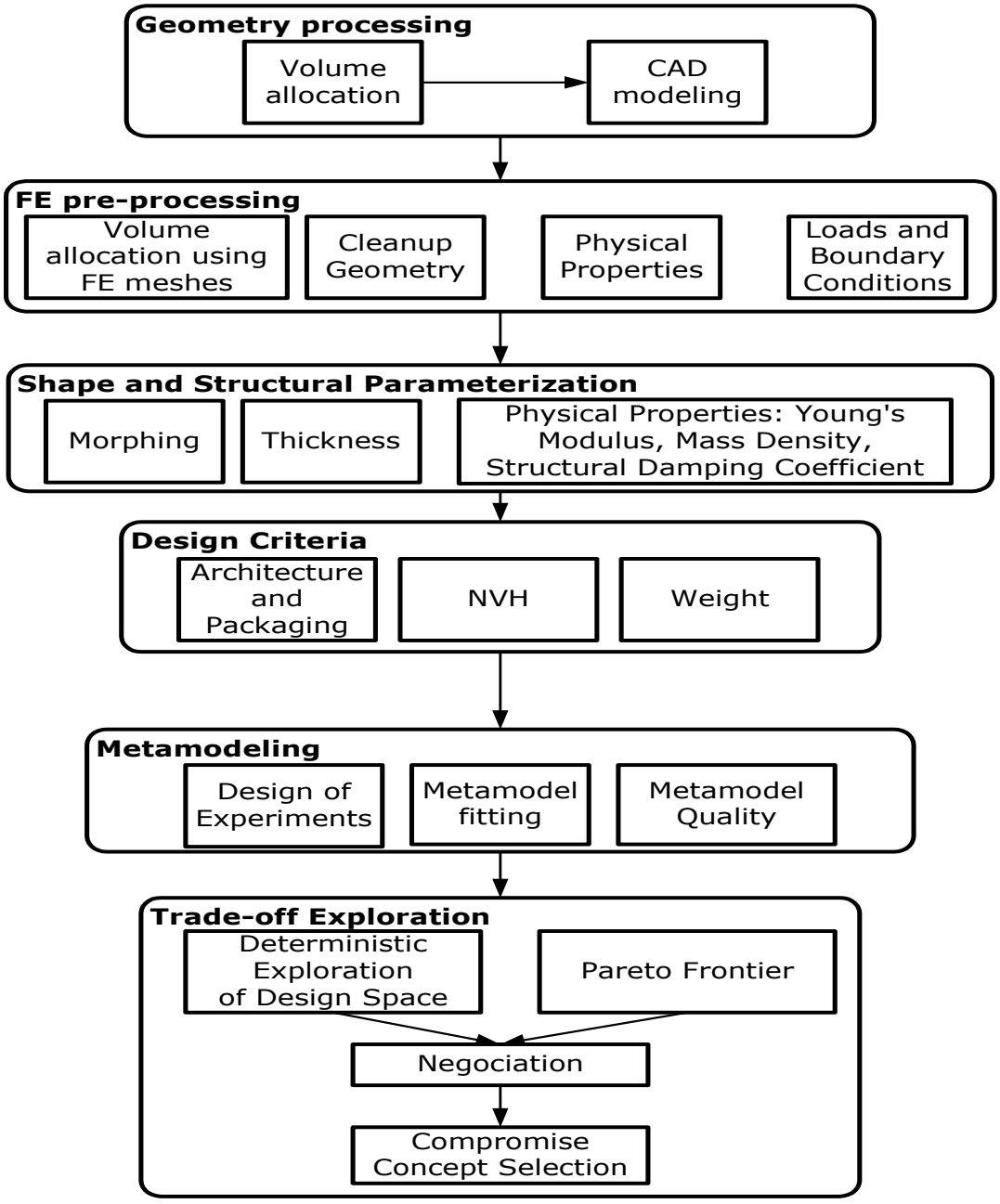

Figure 2. The process to explore the design tradeoffs in the preliminary design stage

For the Design Criteria there was a stage of building up and validation of these criteria. For our design problem we build up two criteria. The first one is a criterion that expresses the "non-respect" of the architectural constraint. It is calculated using the FE mesh of the subsystem model and the mesh of the allocated volume as the maximal depth penetration of both meshes. The second criterion expresses how much the vibration performances of a subsystem is improved in comparison with the targets. To

these two criteria we added a classical but important criterion which is the weight of the structure.

Then we propose to use a surrogate model of the FE simulations in order to reduce the calculation time. So, we build up a MetaModel (MM) that consists of an approximation of the simulation responses using a number of already assessed design points. A Design of Experiments (DOE) is used to better fill the design space for a better approximation with a reduced number of design points. Then the MetaModel (MM) is fitted to the data of the design space filled by the DOE and the MM quality is checked in term of precision of the MM prediction for new design points.

We use then the MM to graphically explore the design space. Then we propose the use of the Pareto Frontier techniques in order to enable tradeoff exploration between the design criteria. By the proposed process, compromise designs are found and adopted to be developed in the next detailed design stage. Finally, it is a posteriori checked that the best compromise which has been chosen really corresponds with a good precision to the expected predicted performances. So, the overall model-based approximation turns out to be reliable.

- **Dissertation Organization**

The thesis is organized along six parts. In **Part I**, we describe the practical motivations from the Renault NVH applications. In this part we investigate the numerical processes used by the NVH engineers for mechanical performance assessments and the design practices of automobile architects for volume allocation. Then we come up with the challenging problem that engineers face in the preliminary design of the vehicle subsystems: the tradeoff between architectural constraints and the respect of mechanical performances. Then we give in **Part II** our proposal that consists in a methodological framework to design a mechanical structure complying with architectural constraints. The stages of the methodology are briefly described and developed in the latter parts. **Part III** corresponds to a stage of modeling of the design problem we face. Firstly, we provide how to tackle with the problem of designing a complex mechanical system especially in the preliminary design stage. Secondly, we establish our proposal for the design criteria that consist of an aggregate performance criterion for noise and vibration and architectural criterion to measure the 'non-respect' of volume envelopes. Finally, we detail how to parameterize the shape of the structure using the morphing techniques. **Part IV** is dedicated to the exploration of design

tradeoffs using surrogate models. We present the metamodels that we build up as an approximation to the FE simulation responses. We describe how the metamodel enables us to graphically explore the design space. Then we present the Pareto frontier techniques that enable us to initiate negotiation between architectural constraints, noise performances and mass. Finally, we illustrate the effectiveness and efficiency of our thesis proposals by a practical case study in **Part V**. The dissertation concludes with a synthesis and a discussion of contributions, work benefits, limitations, related works and future works.

Part I

Practical Motivations from Renault NVH Applications

Part Presentation

The part is intended to present the background and the motivations that rise from the automotive design practices in the preliminary design stage and especially in the NVH department of Renault.

Firstly, we present in **chapter 1** the context of the preliminary design of automotive mechanical structures through a brief presentation of the product development process of automobiles. We describe the design process as it is practiced in the automotive industry, i.e. from a hierarchical point of view by the V cycle and from a chronological point of view by the design workflow. Secondly, we dedicate the **chapter 2** to the **volume allocation** issue. We detail how the car architects allocate volumes in the preliminary design stage and what the pitfalls of the current practices are. Thirdly, the **chapter 3** is intended to the description of the **NVH performance.** We present how the acoustic engineers deal with the design problem, practically how they design the sub-systems of the automobile in order to attenuate the road noise and the engine noise. And we describe the typical simulation and CAE processes for an NVH analysis in automotive industry. By the description of the current practices, we bring out the need for more efficient tools to negotiate the allocated volume for vibrating mechanical sub-systems. Finally, in **chapter 4**, we describe the automotive components or subsystems that we take as case studies in our work.

Chapter 1 Preliminary Design Practices at Renault

In this work, we detail only the design process in its preliminary stages: the stage of interest for the thesis proposal. We detail more in the preliminary stage the aspects that are related to the vehicle architecture and the NVH performance.

1.1 The Product Development Process

The complete vehicle development process requires a combination of many separate activities. In automotive industry a formal design process is implemented to ensure that separate design groups can work on different parts of the development activity in parallel and also ensure that the final combined activity produces a design that meets the performance targets initially set.

The development of a new car can be visualized by two different ways:

- by the **V cycle** described through hierarchical steps defining the way of working for a specific task.
- by the **design workflow** which is a chronological planning of studies that specifies the task timing. The design workflow is a defined series of tasks within an organization to produce a final outcome.

We describe in the following each of the two issues.

1.1.1 The Design V Cycle

The design V cycle itself is a result of Concurrent Engineering and represents the effort to reduce the time to market. In order to reduce delays of development of new vehicles, Renault has adopted a strategy based on splitting the design process into several hierarchical (or multi-levels) steps.

The design process is described by the V cycle model as four loops processes on each level of a hierarchical decomposition of the system. The four V Cycle loops for vehicle level are **Target Setting** (specification), **Cascading** (deployment of the function requirement), **Synthesis** (subsystem and components development validation) and **Confirmation** (system level validation) as shown in Figure 3. The same loops are re-applied at the subsystem and the component levels. This model can be implemented with a variety of different tools and specific applications. The overall requirement is to maintain communication between the independent tasks as soon as the results from each loop become available.

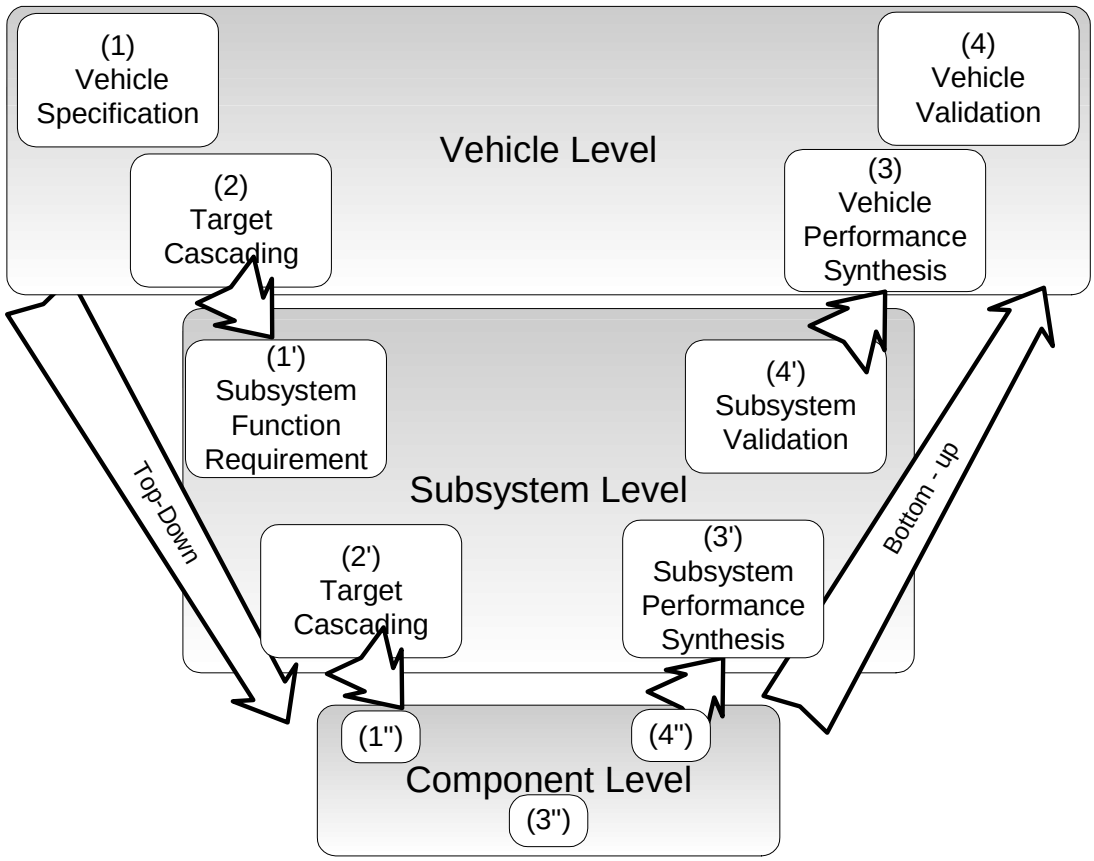

Figure 3. The V cycle for automotive vehicle development

1.1.2 The Design Workflow

The design workflow is a set of specific tasks organized in sequence from a chronological point of view. The design workflow is well established for many industries as well as aerospace or automotive industries and the steps are more known as design stages. Figure 4 illustrates the main design stages in automotive industry. In the product development cycle, the design stages are as follows: conceptual design, preliminary design and detailed design. Then, it follows manufacture and assembly.

At Renault, and in parallel to design stages, the project of a new vehicle is managed by typical milestones. The starting point is the intention letter for the new vehicle model: how can the vehicle be suitable for the market? Then the conceptual design stage starts and it ends with the specification of the project orientations. At this point, the preliminary design stage is initiated and lasts until the contract appointment. In the preliminary design studies, design teams check if the performances are achievable while evolving the digital mock-ups of the vehicle subsystems. Meanwhile, the "pre-project" is transformed into a "project" at the contract appointment. Then the detailed design stage is engaged.

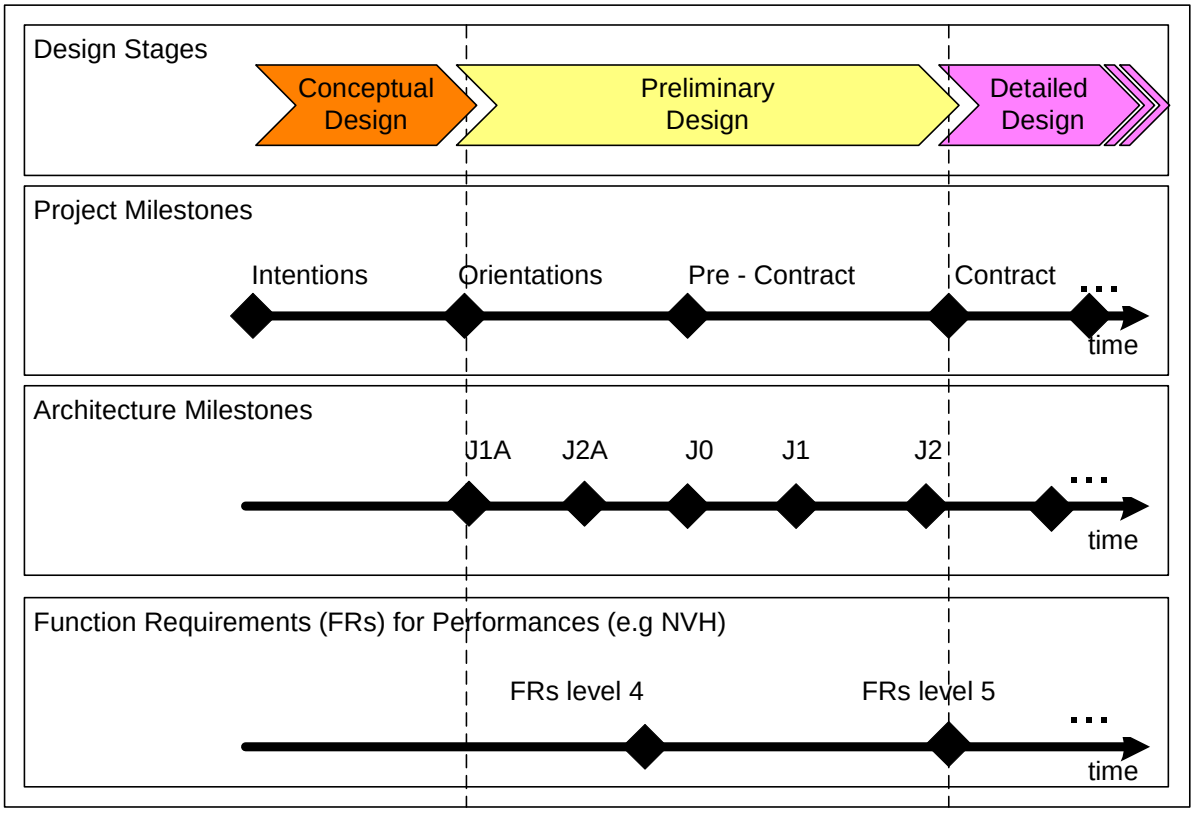

Figure 4. Design stages and project planning of an automobile development at Renault

J1A - One to two design alternatives per structural subsystem are to be studied. Basic design fundamentals are put into a **baseline plan**. **J2A** - A decision milestone: **freezing design alternatives**. Only one design alternative per subsystem (in particular innovating ones) is kept. **J0** - **Initialization** : agreement between the responsible groups for elementary functions, the pilots of customer performances, the stylists of the external and internal design, the responsible for after-sales and the architects of the vehicle, on the studied design alternative and on the schedule of the project milestones **J1** - Design teams (The performance engineers, the elementary function groups, the pilots of customer performances, the stylists, and the manufacturers) provide to the architects, their needs, their constraints and their recommendations on the geometry of the subsystem structures. Architects prepare a first **complete architectural plan** and communicate to design teams the **allocated volumes** to subsystems, the **interfaces** between subsystems and the typical cross sections. **J2** - Design teams review the architectural plan. Architects respond to their expressed needs (modifying allocated volumes if needed). Subsystem interfaces are frozen. Vehicle feasibility is confirmed via a **Digital Mock-up Design**.

Table 1. Architecture milestones during automobile preliminary design stage

FRs level 4 - Function Requirements level 4: For NVH performances, they concern the engine noise, the road noise and the mean frequency noise. Function requirements are expressed in terms of one single value for each noise type. **FRs level 5** - Function Requirements level 5: For NVH performances they concerns the engine noise, the road noise and the mean frequency noise. Function requirements are expressed in the frequency domain as target curves for each noise type.

Table 2. Planning of Function Requirements emission during automobile preliminary design stage

1.2 Vehicle Architecture Versus NVH Performances

As we see from the description of product development, the architects, the engineers in charge of the NVH performance and the other design teams work in parallel and in tandem during the preliminary design stage in order to fix the needed volumes for subsystem structures that guarantee the function requirements for each of the vehicle performances (e.g. the noise performances). In our thesis we focus only on the work of architects and of engineers in charge of the NVH performance (in the following we

simply call them engineers for reason of brevity). We start by providing some definitions of the terms used by architects and engineers during the preliminary design stage.

1.2.1 Definitions

Architecture: In Renault company terminology, architecture means the way of allocating and distributing volumes to subsystems and their components in the vehicle. It also concerns the interface locations between subsystems. In the present work, **architecture** and **topology** have the same meaning.

Architect: he/she is the engineer who cares for the coherence of the car architecture and its subsystems. He/she integrates demands of volume allocations and manages the evolutions of the CAD models of the subsystems of the car.

Baseline plan: The baseline plan is a single plan of geometrical objectives. It gathers technical information and basic geometric function requirements based on prior expressions of the product manager (who decides which vehicle for which market), the engineer teams, the stylists and the manufacturers. It contains the main platform and takes into account the possible variants of the vehicle family and the possible carried-over subsystems from former projects.

Architecture choice: It is a decision made at architecture milestone J2 (see Figure 4 and Table 1). The decision assigns and freezes (1) allocated volumes to subsystems and their components and (2) interfaces between subsystems. A digital mock-up design is presented to confirm the feasibility of the design.

Digital Mock-up: The set of digital data (in opposition to physical prototypes) that permits to address all the performances of the vehicle. A digital mock-up is composed of:

- an assembled digital model of the automotive vehicle
- physical properties of components
- digital data and results from (1) physical tests and (2) simulations that are in agreement with the assembled digital model. Results can be brought from former projects that share the same platform or have enough similarity and consistency with the digital model.
- the results corresponding to the numerical simulations on the present digital model

Digital Mock-up Design Review: (DMDR) is a Renault expression concerning a number of meetings between architects, designer and engineers who are involved in the vehicle project.

NVH performances: it concerns mainly the engine noise, the road noise and mean frequency noise. For our study we focus only on engine noise and road noise. Chapter 3 gives a description of the aforementioned noises.

NVH Function requirements (FRs): they are the targets for the noise and vibration performances. Their contents depend on the level of the hierarchical decomposition of the vehicle and on the position in the vehicle project planning.

Performance engineer: he/she is the engineer who focuses only on the study of the subsystem and the system performance (e.g NVH performance). He/she is responsible for the assessment of the performance and for the setting of the targets to achieve for that performance.

1.2.2 Architecture Versus Noise Performance

The architecture planning is linked to the noise performance planning, especially in the preliminary design stage. We describe hereafter the main tasks of engineers and architects during the preliminary design stage and through the architecture milestones.

At the beginning of the preliminary design stage, there are two to three design alternatives per subsystem. For NVH performances, it is essential to assess each of the alternatives using the available simulation models. For milestone J1A (see Figure 4 and Table 1) for instance, engineers have to evaluate the risks of each of the alternatives and the possible advantages that can be derived from them. Engineers however can not assess the performances at the vehicle level since it is not already completely designed. They only assess at this stage the intrinsic subsystem performances in terms of vibration transfers and attenuation ability of the body and the chassis. We obtain by that first assessment, some rough orientations about the subsystem vibrational behavior. Meanwhile architects set a baseline plan for the entire vehicle.

In accordance with other design teams, a design alternative is chosen for reasons of a better performance and/or lower costs.

Then, the J2A milestone takes place. In parallel, performance engineers work to emit FRs on high level (e.g. system level) performances of the vehicle. For the NVH performances, FRs consist of noise targets mainly for engine noise, road noise and mean frequency noise. It is the FRs level 4 (see Figure 4 and Table 2) which is emitted before

the project milestone of the pre-contract. Although the vehicle level performance can not be assessed at that milestone, FRs are set for the vehicle level. FRs are fixed as target values that, later in the detailed design stage, the vehicle performances must achieve. Setting targets at the vehicle level does not mean that it is possible to immediately assess them but it helps engineers in cascading targets to lower levels for allowing to independently and concurrently (in parallel) design subsystems and components.

For NVH performances, before J2A, engineers try to anticipate the assessment of vibrational performances. To do so, engineers construct and simulate a rough digital mock-up of the car and its subsystems. Then, based on the assessment results, engineers propose structural solutions and orientations to improve the vibration behavior of the structure. A good vibration behavior improves the possibility to finally get a vehicle with noises that respect the FRs. The proposed solutions of the structures are taken into account by the architects to be added to the needed allocated volumes.

J0 is really a starting milestone from the project viewpoint. Decision about leading the project into later stages is made. At that point, if the vehicle design seems to be costly or unable to achieve FRs, project managers may decide to delay by months the contract rendezvous, enabling engineers to rework on the design, or they can decide to entirely abandon the project. If the decision is positive and it is almost the case because of prior preparations, more human resources are allocated to the project. Design teams and architects begin to work about the chosen alternatives for each of the subsystem.

At J1 a first global architecture plan is presented by the architects. The plan includes allocated volumes for subsystem and components. The design teams consider the allocated volumes and start to assess performances of subsystems and components which respect to the proposed allocated volumes.

The architecture milestone J2, that comes days before the contract, is a deadline for engineers. After their studies initiated at J1, performance engineers communicate their conclusions about if the allocated volumes for subsystems were sufficient or not to achieve the FRs level 5 (see Figure 4 and Table 2). If it is not the case, the engineers express their updated needs for more volumes. Then, architects take the expressed needs into account (if it is possible) and achieve a tighter architectural plan. A digital mock-up is presented during a DMDR. Then an architectural choice is fixed.

Chapter 2 Volume Allocation in Preliminary Design

We explain here the problem of the architecture constraint when we assemble (make the packaging[1] of) the mechanical subsystems of the automobile.

First we describe the role of architects, who are responsible for all the digital models in the CAD environment. Then we describe practical aspects of the volume allocation process and what it involves.

2.1 The Role of Vehicle Architects

Vehicle architects are a specific designation from the Renault company to the engineers who are responsible for the digital mock-up and CAD modeling of the automotive components and sub-systems. In preliminary design, architects digitally allocate volumes for each component and subsystem. Along the preliminary design stage, they define and progressively tighten geometric constraints that the components and subsystems must respect. From the beginning, they set rules on how the subsystems and the components have to be designed and positioned in the global architecture of the vehicle. Rules are based on the respect of the intentioned design of the automobile (the overall dimensions) and on the respect of the recommendations expressed by different design teams.

[1] The term packaging is more suitable than assembly. The latter is a more dedicated term for the manufacturing process.

Then, architects set a baseline plan (see Figure 5) and begin to model the design alternatives for each of the subsystem using CAD software.

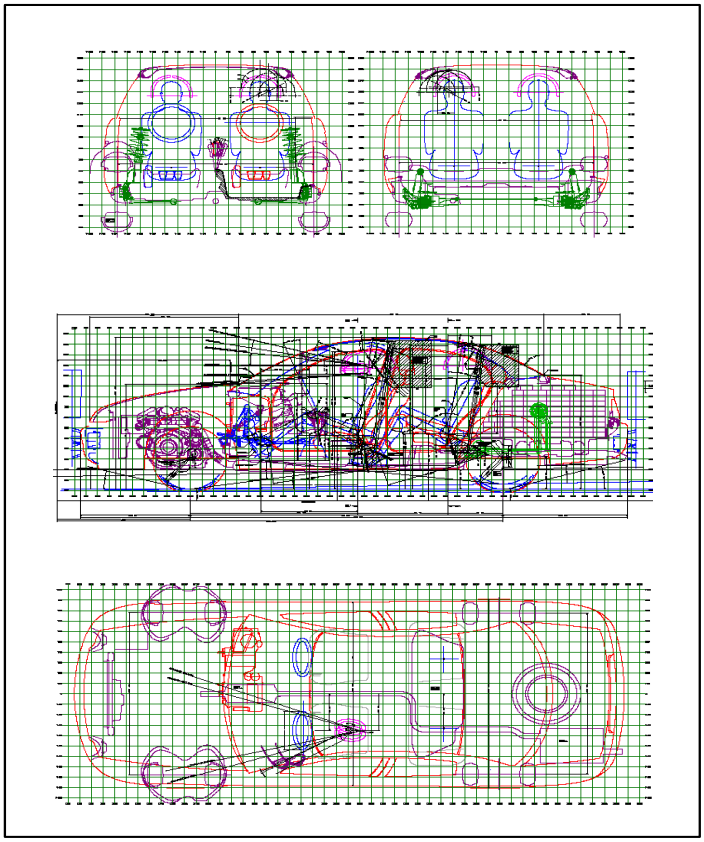

Figure 5. Example of vehicle baseline plan

While architects are modeling components and subsystems, they include to their CAD models the geometric constraints and the allocated volumes. For instance, Figure 6 is a snapshot from CATIA V4 software. It describes some of the geometric constraints that are explicitly drawn. The architects who are responsible for the design of the front subframe, which is a part of the vehicle chassis, must respect the specified geometric constraints. Here, we see specifically the engine limits, the ground clearance, the body limits, the fixation points between the subframe and the body and between the subframe and the suspension triangles. Figure 7 provides a better description of the subframe geometric constraints.

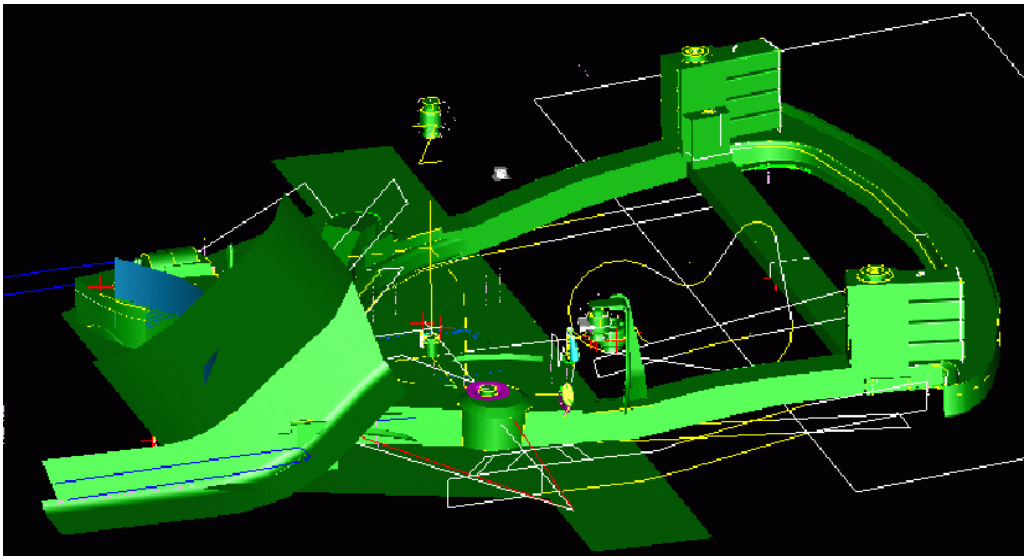

Figure 6. Geometric constraints represented by wire lines and planes in a CATIA V4 environment

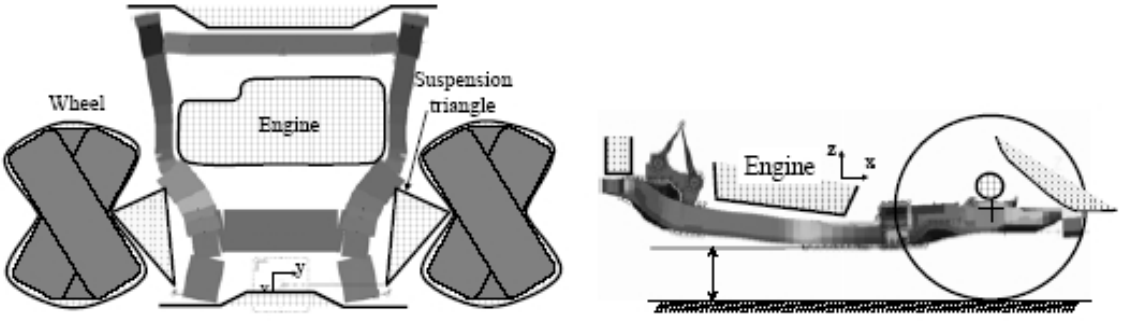

Figure 7. Architectural constraints on the subframe

2.2 Practical Aspects of Volume Allocation

In preliminary design, when no models of a mechanical subsystem or its components are available, architects allocate to them a volume representing the geometric space they might occupy.

To help architects to allocate volumes, at Renault a database called MEREX combines sets of architectural rules. Architects use the database to sketch their first models of the mechanical structures. Also, they often use previous models from former projects as a baseline for the new ones.

The main idea of volume allocation consists in using simplified geometry as lines, surfaces, and volumes to represent the boundaries around the mechanical systems and the space they occupy. In preliminary design, we have not necessarily a detailed geometry of the model. But techniques to perform volume allocation can be different according to the tools used for the purpose. Currently, the allocated volumes are directly represented in CAD software. But, performance engineers are not necessarily familiar with CAD software. They rather simulate the mechanical structures using CAE software. During the transformation of the model from CAD model to CAE model, aspects of volume allocation are purged. So, the engineers have not immediately in their CAE models the information about the allocated volume. We propose a new way to deal with this problem. The allocated volumes can be represented in CAE tools, using FE meshes. We detail the proposal in chapter 12.

Chapter 3 NVH Performances

Car design, however, is a multidisciplinary design. We focus on our work on one discipline which is the vibro-acoustical design more known in automotive jargon as NVH design. The aim of the work is to present a strategy of how to deal, in the preliminary design stage, with the problem of volume allocation and the NVH performance design. The reasoning can be extended, surely with modifications, to other disciplines.

First, we begin to describe **NVH analysis** in automotive industry to grasp the complexity of the problem.

Secondly, we give the **NVH performances** that are mainly assessed in the preliminary design stage of an automobile.

Finally, we describe the **target setting process** for NVH performances.

3.1 NVH Analysis

The NVH Analysis is realized through a frequency response analysis of detailed full vehicle structural-acoustic models [Misra et al. 1999]. In the case of automotive analyses vehicle model includes tires, suspension, powertrain, body and the acoustic cavity. For typical automotive NVH analyses, modes are computed for the entire vehicle structure (including chassis and powertrain) as well as for the acoustic cavity. Both, tactile and acoustic responses to excitation are computed at the areas of interest. Tactile responses include vibrations in the seat, toe pan and steering column, while acoustic responses include sound levels at specific locations in the acoustic cavity [Wolf 1997]. Typical full vehicle NVH simulations involve forces that may be external or internal to the vehicle. External forces include road induced shake/noise and aerodynamic forces due to contact with the surrounding air. Internal forces include powertrain combustion reaction forces, powertrain unbalance forces, tire/wheel unbalance forces, driveline unbalance forces (axle etc.) and brake induced forces.

The NVH analysis as described above is processed during the preliminary design stage.

3.2 NVH Performances of Automobiles

We give here the models used in the preliminary design stage. Then, we present the main NVH performances that we deal with during our study.

- **NVH models**

Depending on the advance of the vehicle preliminary design, NVH analysis can be held on three different models of the automobile.

The first model that can be assessed is the car Body in White (BiW): It is a structural model of the superstructure that includes structure skeleton and main panels. Figure 8 gives an example of BiW model.

Figure 8. Body in white model

The second model is the trimmed body model. It consists of the trimmed structural model (see Figure 9) and the acoustic cavity (see Figure 10). The structural part of the trimmed body includes the structural elements of the BiW, the doors, the seats, the dashboard and the foams. The acoustic cavity is the model of fluid (the air) included inside the vehicle.

The third model type is the vehicle system model (see Figure 11). It includes the trimmed body model plus the trains. The vehicle system model better concerns the detailed design stage than the preliminary design stage.

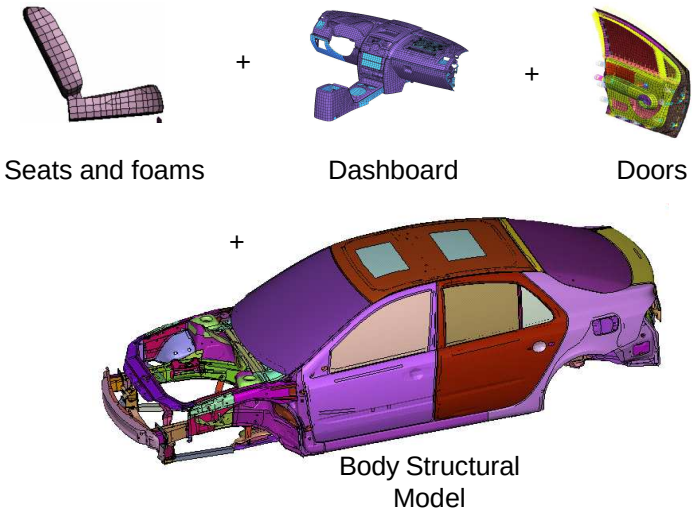

Figure 9. Trimmed body model

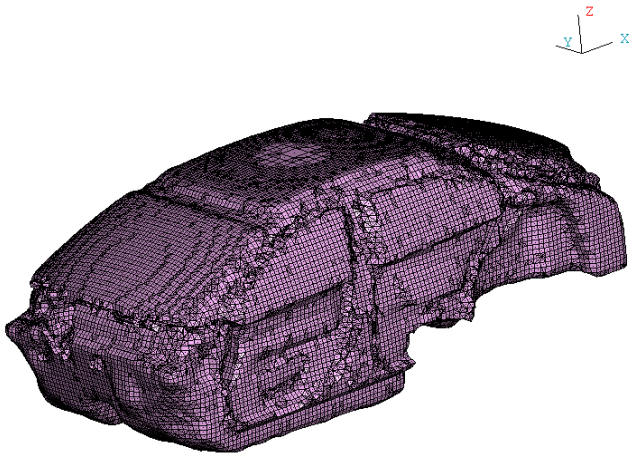

Figure 10. Interior Acoustic cavity

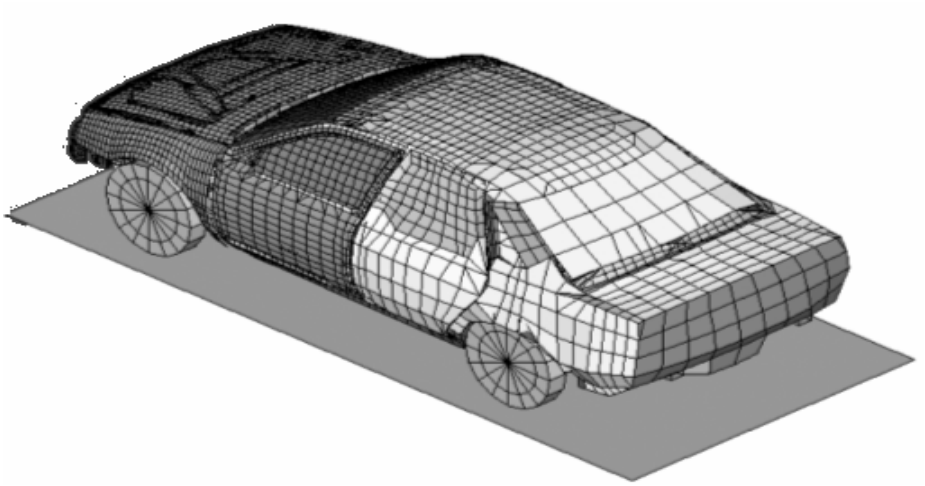

Figure 11. Vehicle system model

- **Excitations and responses**

Always, when dealing with NVH performances, we face the notion of excitations and responses.

Excitations are dynamic forces applied on some grid points and the responses are displacements (velocities, accelerations or pressures) assessed at some other grid points of the mechanical system. A grid point can be a point in the structure or a point in the fluid, in the case of fluid-structure coupling. We only take for grid points the translation degrees of freedom X, Y and Z. Rotational d.o.f Rx, Ry and Rz are neglected. Only pressures are not dependent on the chosen d.o.f, because they are scalar values calculated on response grid points.

The response grid points are distributed on the panels and their frames. Figure 12 illustrates an example of the distribution of response points on the windshield and its frame. The same procedure is applied to the rest of the main body panels. Figure 13 gives some of the main panels of a BiW.

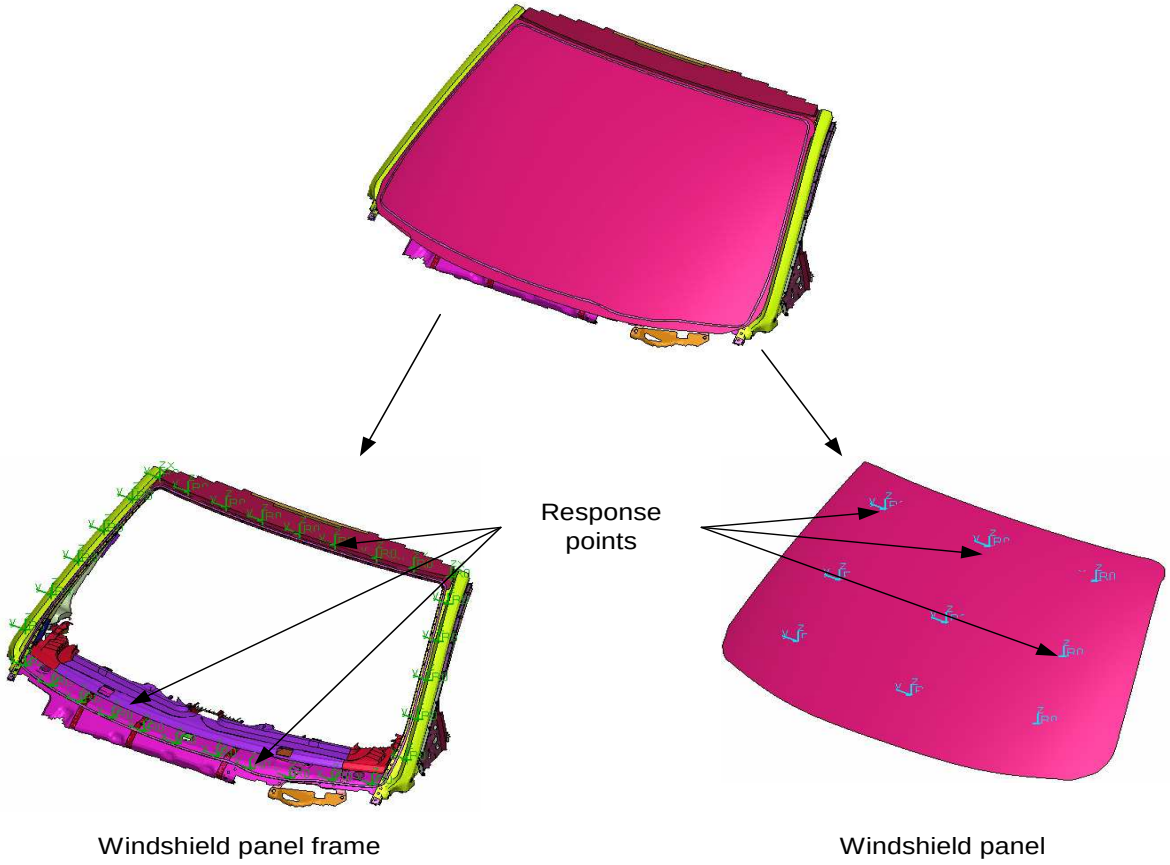

Figure 12. Example of vehicle panels and their frames: the windshield panel

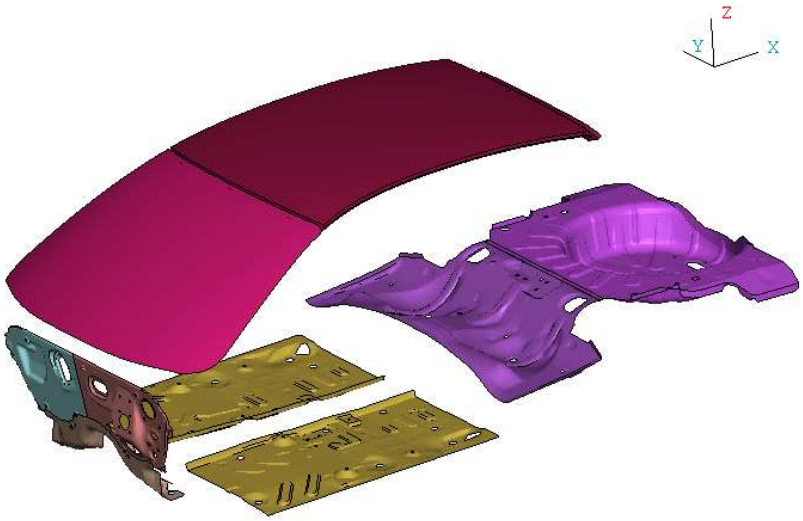

Figure 13. Main panel sets of a BiW

The excitations are forces that may be external or internal to the vehicle. Excitation grid points are located where the forces are applied to the car body. Main excitation points are located at:

- the engine mounts
- the shock absorber mounts
- the subframe mounts
- the fixing points of the exhaust line

Figure 14 illustrates some of the excitation points.

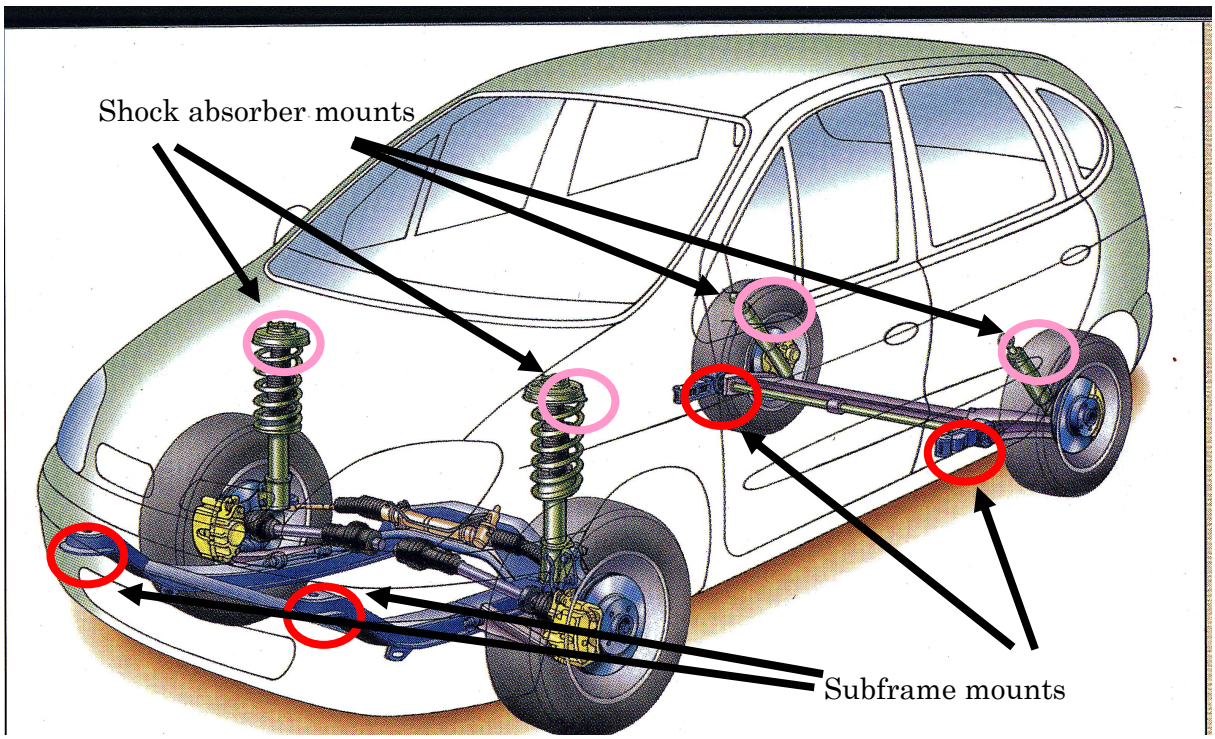

Figure 14. Example of excitation points of a car body

- **NVH performances**

All the NVH performances that we tackle in our work are calculated from the Frequency Response Functions (FRFs). FRFs are frequency dependent functions that express the mechanical system responses due to dynamic excitations. In section § 6.1 we give an extended definition of FRFs.

In the case of the BiW, The NVH performances that engineers assess are the **Inertances** and the **Vibration Transfer Functions** (VTF) of the panels and their frames.

Inertances are FRFs where the excitation Degree of Freedom (d.o.f) and the response d.o.f are the same. So inertances are assessed only at the excitation points where the responses are acceleration at the same points.

Figure 15 shows an example of an inertance that we have computed using NASTRAN (FEM software) for the purpose of an NVH study that we have achieved at Renault. It gives the inertance on the shock absorber mount due to an excitation in the Z d.o.f.

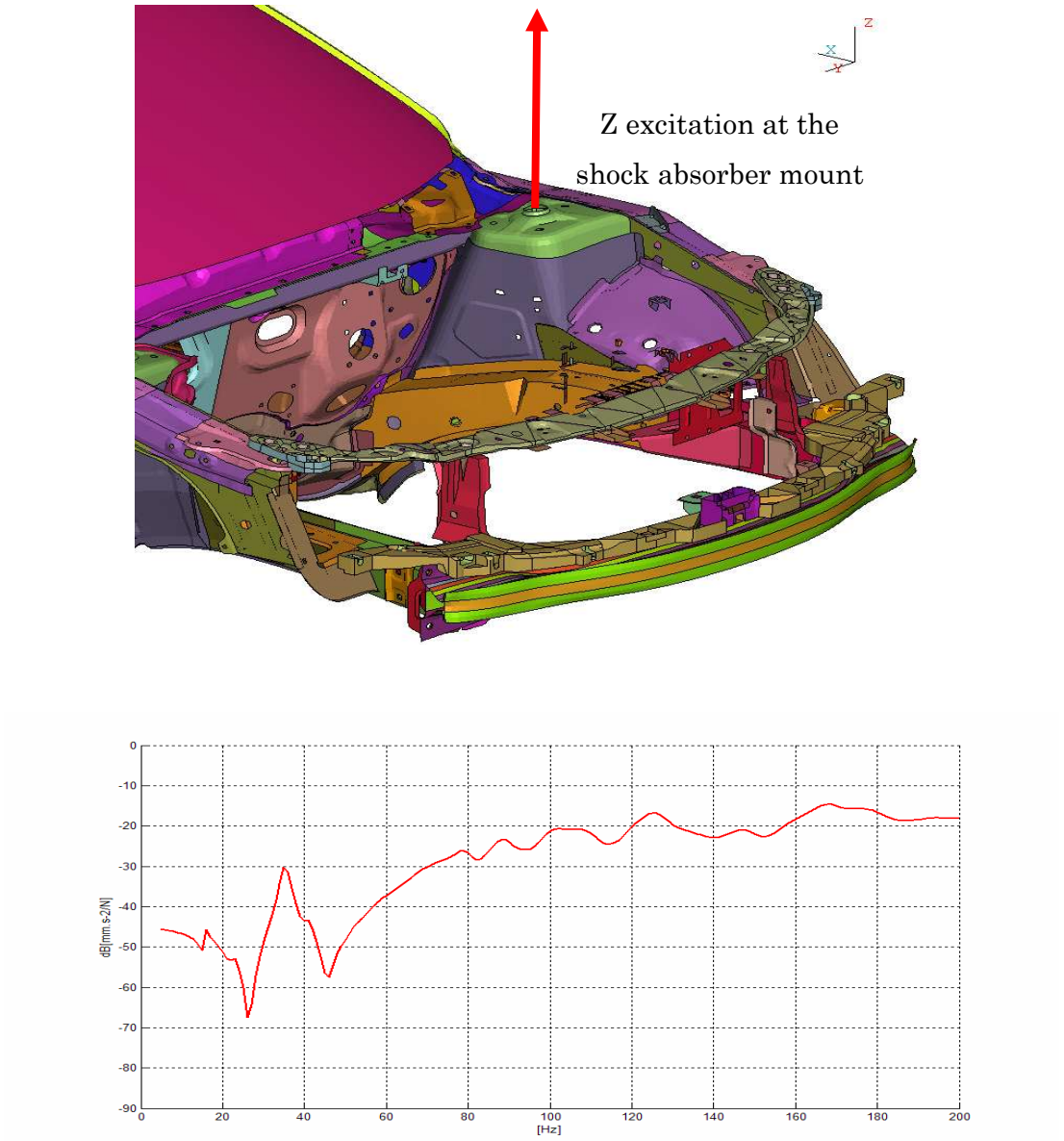

Figure 15. Inertance calculated at the shock absorber mount

Vibration Transfer Functions are frequency dependent functions calculated by averaging a number of FRFs that have the same excitation d.o.f.

Responses are displacements at distributed grid points on panels and on panel frames.

Figure 16 gives an example of the VTF that we have calculated for the same NVH study of a new sedan model. We computed the VTF at the windshield panel due an excitation at the shock absorber mount at Z d.o.f.

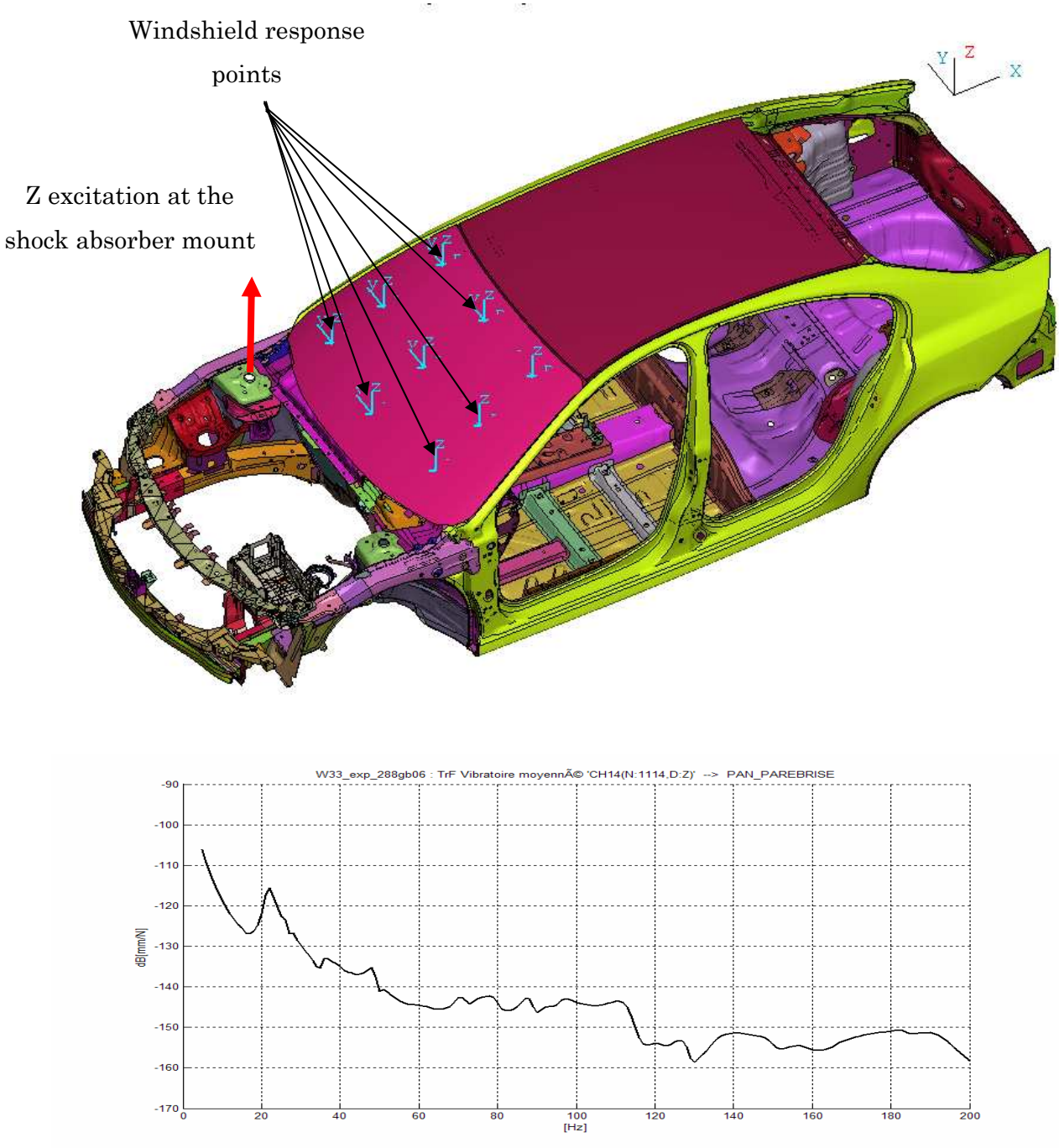

Figure 16. Vibration Transfer Function at the windshield panel due to an excitation at the shock absorber mount

In the case of the trimmed body, in addition to the same performances assessed for BiW, there are the Noise Transfer Functions (NTF).

Noise Transfer Functions are FRFs where excitation d.o.f are located at the structure side of the car body as it is described previously and the response points are located inside the interior acoustic cavity. Response points are located at the supposed positions of the driver and the passenger ears. In the interior acoustic cavity the responses are the fluid (the air) pressure variations in the low frequency range [20,200]Hz. Figure 17 illustrates an example of a calculated NTF from our NVH studies.

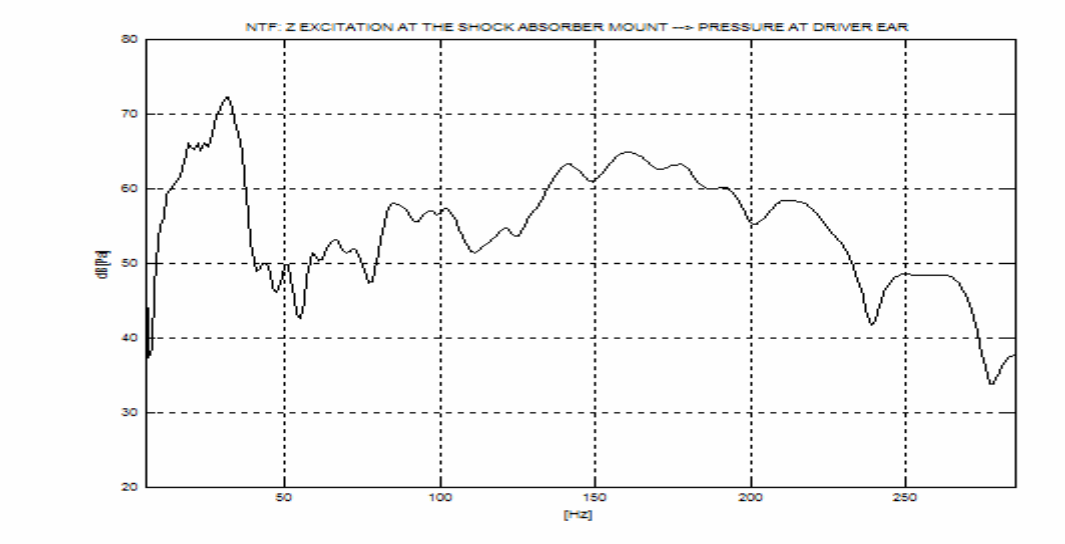

Figure 17. Noise Transfer Function at the driver ear due to an excitation at the shock absorber mount

Due to the structural components added to the BiW in order to obtain the trimmed body, the Intertances and the Vibration Transfer Functions are not exactly the same in comparison between the BiW and the trimmed body.

In the case of the vehicle system, we do not detail NVH performances because the study of the vehicle system is more concerned with detailed design stage. We mainly assess the same performances as the case of the trimmed body plus other Noise performances as well as the Sound Pressure Level (SPL) (e.g. total noise) which is a summation of all the NTFs.

3.3 The NVH Targets and Target Cascading in Car Body Design

As we can notice previously, the main NVH performances, which we deal with during our study in the preliminary design stage, are the inertances, the Vibration

Transfer Functions and the Noise Transfer Functions. In this section, we explain how the targets over these performances are set, we evoke the target cascading logic, and we give the targets that are set for these performances.

For NVH design, the vehicle level performance (see hierarchical decomposition within the V cycle design in §1.1.1) are the Sound Pressure Level inside the interior acoustic cavity of the vehicle system. The SPL-or the total noise-in the acoustic cavity is due to the excitations at the structure part of the system and the propagation of the induced vibration waves to the fluid part via coupling effects between the fluid and the structure. The lower the level of the SPL, the better the NVH performance of the vehicle. So targets –or Function Requirements- are set on the SPL performance as a curve which is called target level. Engineers work to have the SPL curve under the target level. Figure 18 gives an example for the SPL performance and the target level for vehicle system. We have computed this example using Renault software called VISA (VIrtual Synthesis of Acoustics).

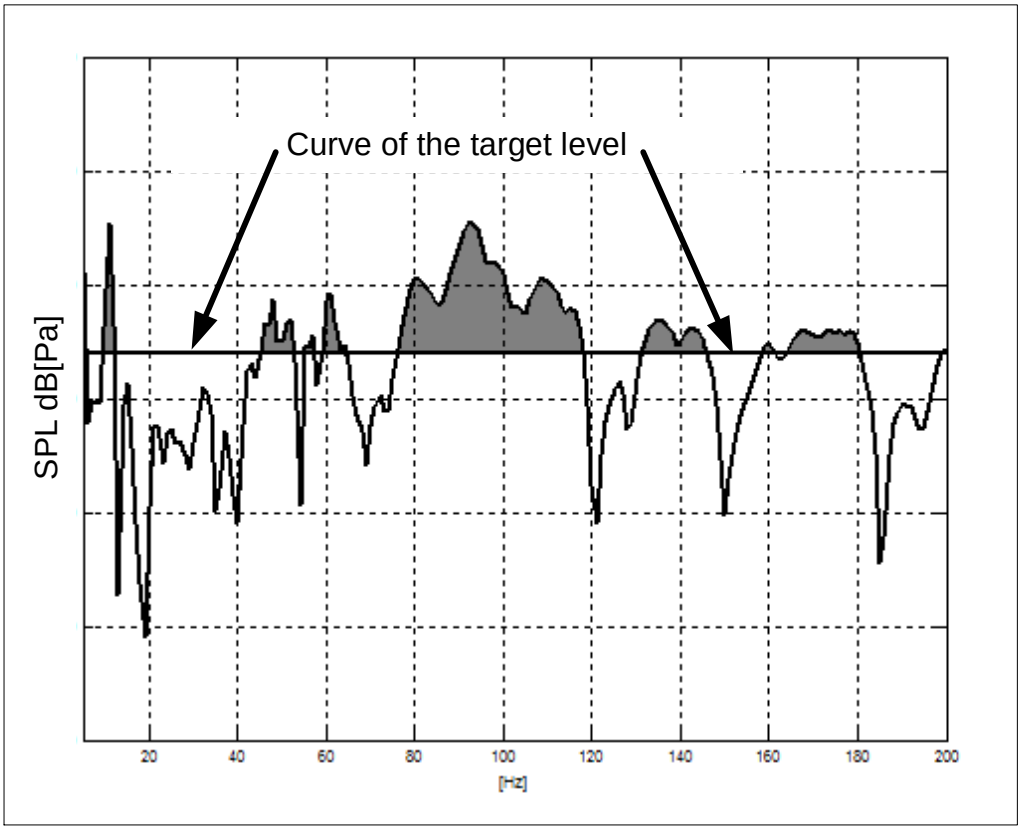

Figure 18. SPL at driver ear due to structural excitation at the vehicle mounts

As it is described in the V cycle design, hierarchical decomposition of the vehicle system induces that the target set for performances at the vehicle level are cascaded into targets at the lower levels.

For NVH design, the hierarchical decomposition from the vehicle level gives, in the up-down direction, the trimmed body then BiW.

To cascade the targets from the vehicle level to the trimmed body, we start from the fact that the SPL is a summation of the Noise Transfer Functions. Then, to have lower SPL at the vehicle level, it is necessary to set the NTFs at lower levels. So a curve of target level is set also on each of the NTFs. The target level on NTF is set in a way that if all the NTF are below that level, the SPL will be below its target level. Figure 19 illustrates an example of a target level set over a Noise Transfer Function.

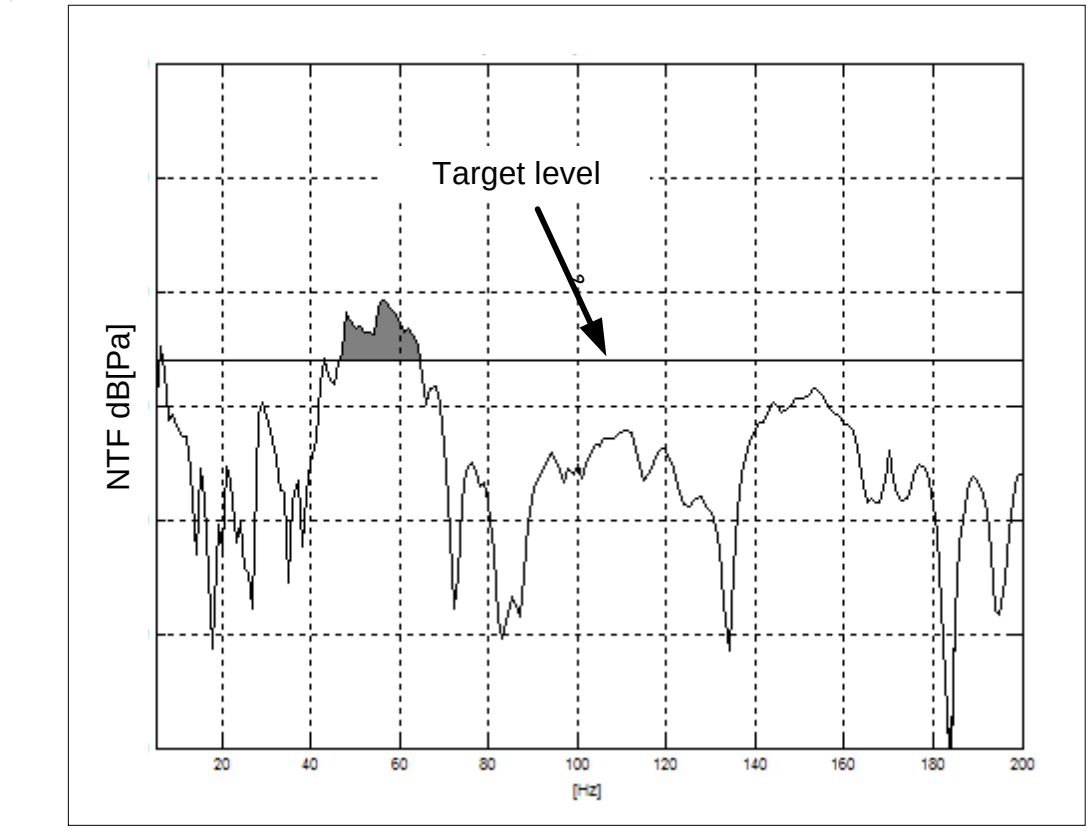

Figure 19. Noise Transfer Function target

But, for the trimmed body, there are also the Inertances and the Vibration Transfer Functions as performances to control.

The Inertances express, somehow, the stiffness of the structure at the excitation points. The lesser the level of the Inertances curves, the better the stiffness of the car body at the excitation points.

Vibration Transfer Functions express the displacements of the panels and their frames. As the panels and their frames are the structural part of the car body that are coupled with the fluid of the interior cavity, lesser the displacements of them means lesser excitations of the fluid and therefore lesser noise.

Moreover, the trimmed body represents a coupled structure-fluid system, so the three types of performances, that engineers assess, have a relationship between them. Figure 20, after [Calvel 2004] shows results which are of common use in Renault NVH studies : they are the possible relationships between the high level peaks of the displacements on the VTF at the windshield and the high levels of the NTF for the same excitation point at the engine mount for the same frequencies. The same figure illustrates also that some higher level peaks which are present on the Inertances can occur at the same frequencies for the VTF. The peaks on the Inertances and the VTF are called the main body structural modes.

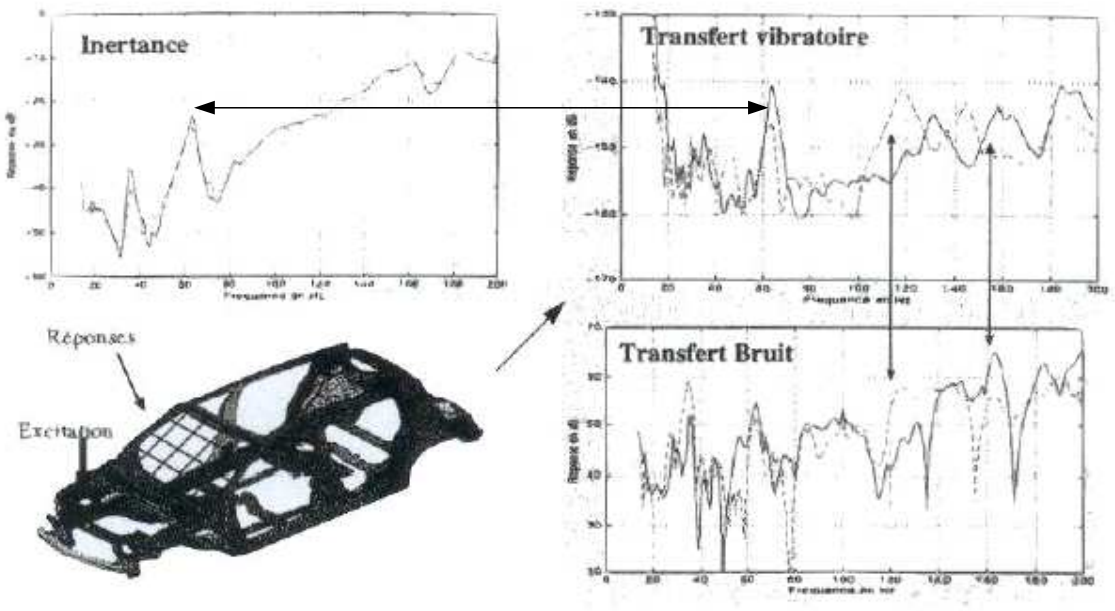

Figure 20. The Car body NVH performance at Renault, from [Calvel 2004]

Like the NTF case, curves of target levels are also set on the Vibration Transfer Functions and on the Inertances. We plot the Figure 21 and Figure 22 to give respectively the targets for an Inertance and for Vibration Transfer Function. The two performances, to be better, have to be under their target curves.

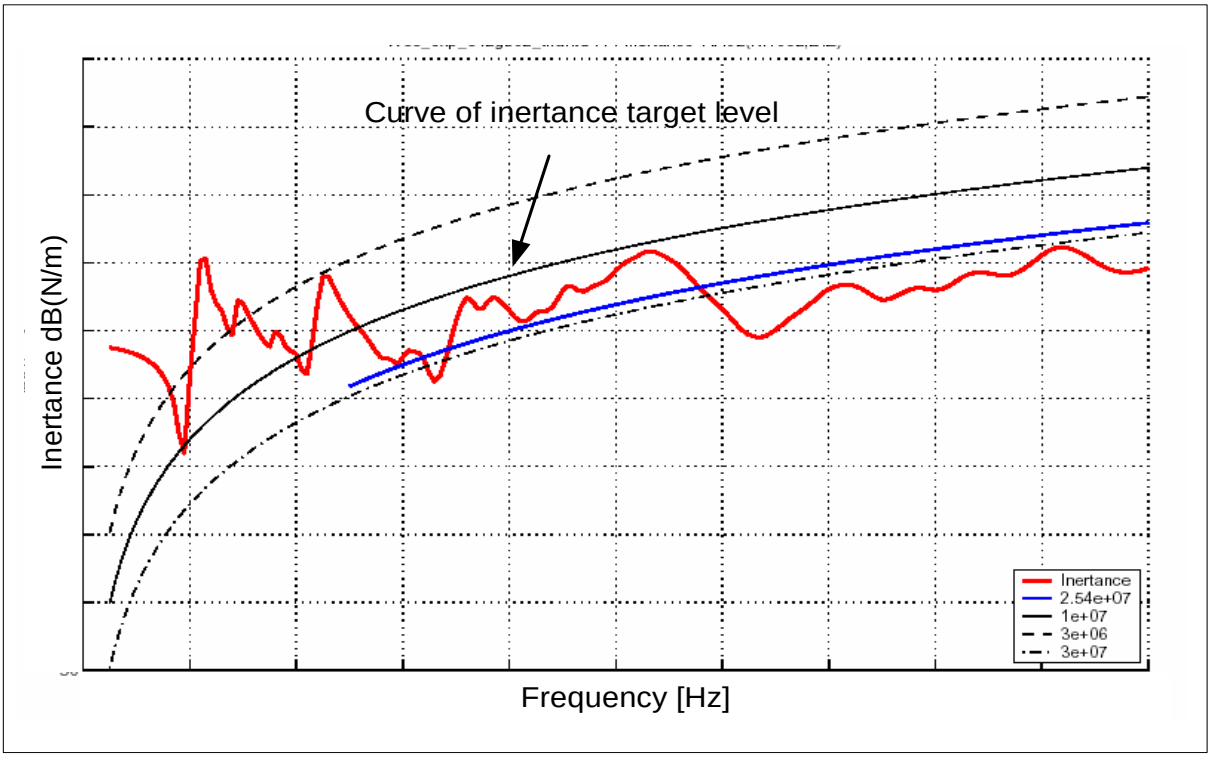

Figure 21. Inertance target

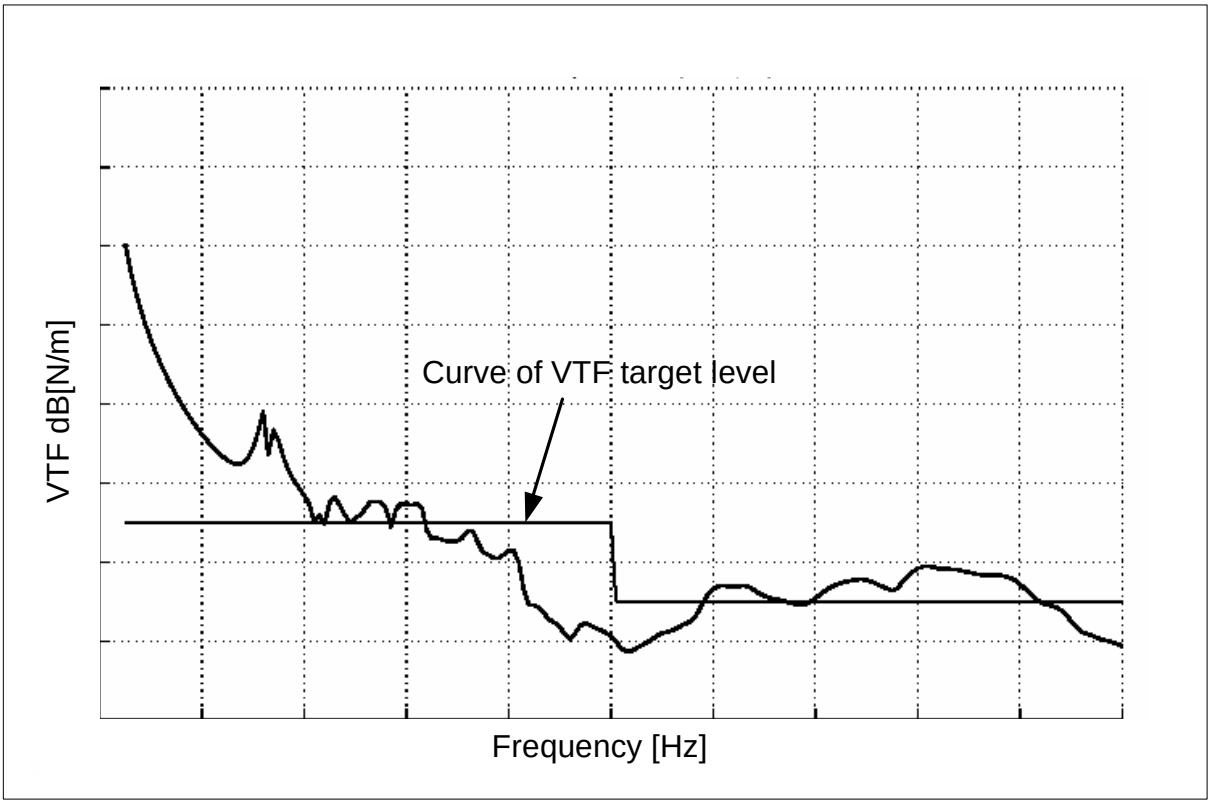

Figure 22. Vibration Transfer Function target

For the BiW case, while it comes from a hierarchical point of view under the trimmed body, the BiW model is available weeks before the trimmed body in respect to the chronological development stream. As the two later models are constructed on the base of the BiW model, there are strong relationships between the BiW NVH performances and the performances of later models. So, to prevent from the stage of the BiW to have high level on NTF, later on the trimmed body, and high level on SPL, more later on the vehicle system, engineers try to control the Inertances and the Vibration Transfer Functions of the BiW. Targets are set for BiW on the Inertances and on the VTF. They are like target curves for the trimmed body (see Figure 21 and Figure 22) but not necessary at the same levels because targets can evolve during the design process.

Chapter 4 Design Case Study

We take as a case study the BiW and the trimmed body of a low-size vehicle. Our study is intended to improve NVH performances of the BiW while respecting the tight architectural constraint from the volume envelope of the car powertrain.

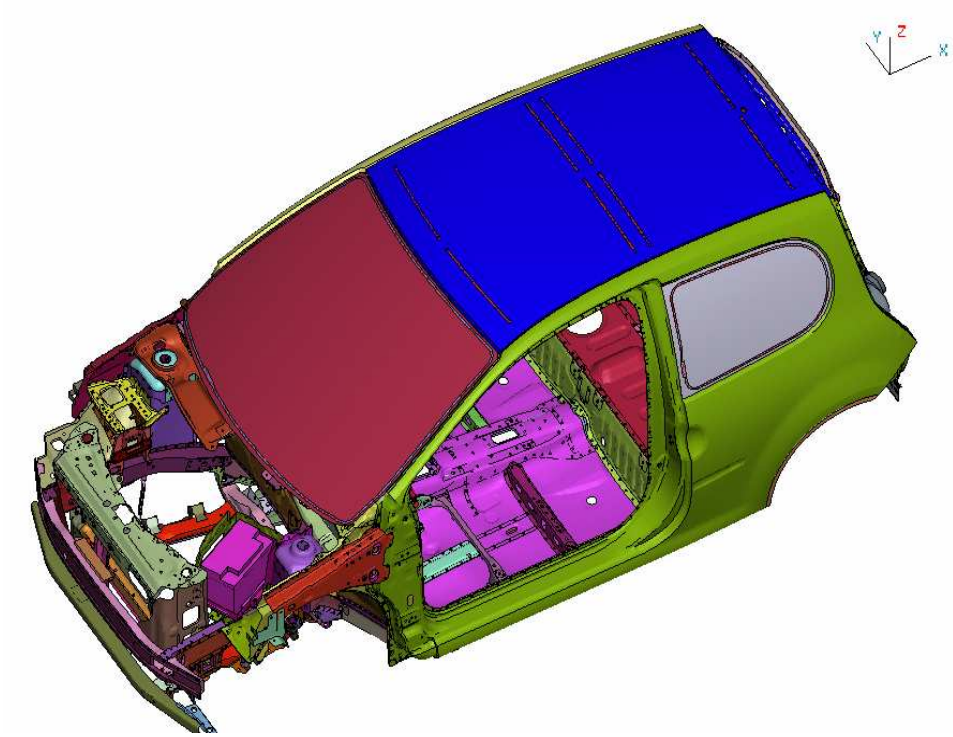

Figure 23. BiW of our vehicle case study

Part Synthesis

The objective of this first part has been to describe the preliminary design practices in the automotive industry through the case of Renault. The development processes are addressed and their two decomposition models are introduced: hierarchical decomposition through the V Cycle and chronological decomposition through the design workflow.

A special focus on the vehicle architecture versus the noise performance design has been addressed. It has been mentioned that the architecture of the vehicle influences many of the vehicle performances and, among them, the NVH performances. The stage of volume allocation in the preliminary design of automobiles has been described. Then the NVH performances have been defined.

Finally, the design case study that will be used further in our proposal has been presented.

Part II

Orientations: A Methodological Framework to Design Mechanical Structure with Architectural Constraints

In this part we introduce the proposed methodological framework to deal with the problem of the interaction between allocations of volume envelopes and the assessment of mechanical performances.

The framework consists of stages. Every stage is described briefly in order to have the overall idea of the framework. The framework is a proposal to answer the issue of the design of complex structures in early stages of the design process. The issue has been extensively described in the introduction and in Part I.

With the proposed method, we make possible to engage tradeoffs between architects and mechanical engineers about the non-respect of architectural constraint and the fulfillment of mechanical performance targets. The method consists of the incorporation of the stage of the volume envelope allocation from the CAD environment into the pre-processing environment of FEM simulation. More specifically, both the non-respect of the architectural constraints and the Noise Vibration and Harshness (NVH) performances are assessed within the same environment using the same FEM model.

Negotiations between architects and design engineers are no longer based on qualitative judgments but they are, now, based on quantitative criteria for both of the architectural constraints and the mechanical performances. The proposed methodological framework consists of, firstly, assessing NVH performances using an aggregate criterion and the non-respect of the architectural constraints by a maximal depth penetration criterion, secondly, encompassing the input-output simulation models into a metamodel [Barton 1992], then, using the metamodel to generate the Pareto frontier [Mattson et Messac 2002b; Pareto 1906], and finally, on the basis of the Pareto frontier, negotiations are engaged in order to find a compromise design. The application of the methodology to an automotive case study stresses the efficiency of the method to improve the NVH performances of a car BiW while respecting the tight architectural constraints in the neighborhood of the volume envelope allocated to the vehicle powertrain. The originalities of our approach lies in different points :

- metamodeling architecture (volume envelopes) constraint, or rather the performance which is the degree of respect of the architecture constraint,
- aggregating vibrational abilities of mechanical components into a limited number of scalar performances which guaranty an overall satisfactory system noise performance,

- exploring in a conjoint way the two previous performances.

- **A framework to design mechanical structure with architectural constraints**

We propose a framework that helps to manage the architectural constraints is a cascaded modeling methodology. We illustrate through Figure 24 the main ideas of the framework. The methodology can be described by the following process:

1. Modeling the design problem:
   a. FEM simulation modeling
   b. Architectural constraint modeling
2. Metamodeling the design problem
3. Using the design metamodel as a black box model to evaluate the functions of the Multi-Objective Optimization Problem
4. Generating the Pareto frontier using the Multi-Objective Optimization Problem
5. Leading Negotiations and tradeoffs based on the Pareto frontier representation in order to obtain a design compromise between architectural constraints and mechanical design performances.

In the following we briefly describe the content of each stage of the methodological framework.

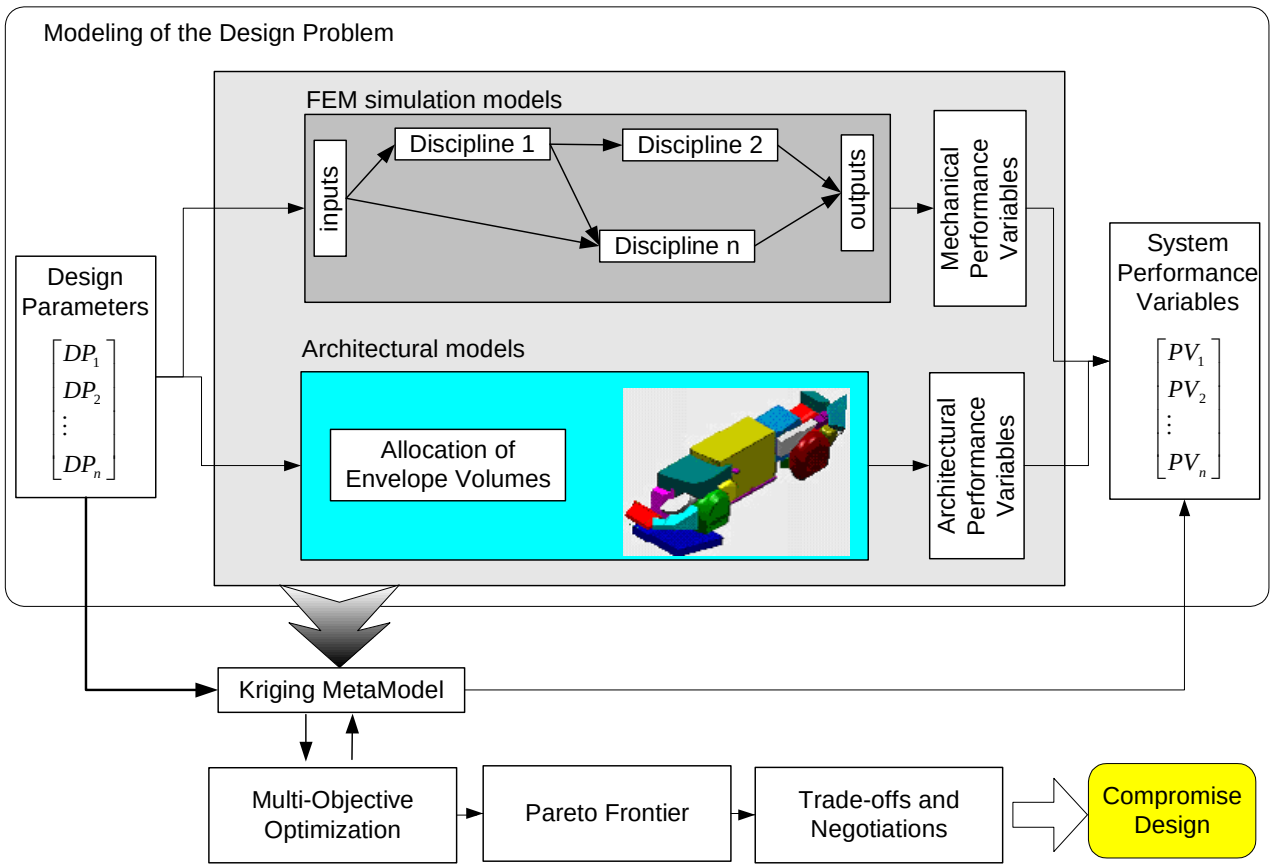

Figure 24. Methodological framework to design mechanical systems with architectural constraints

- **Modeling the design problem**

Hard mechanical performances usually need the use of FEM (Finite Element Method) simulations, for instance, the NVH performances of the car BiW.

We provide further the mechanical performance variables that are interesting for the NVH design of the BiW.

We are also interested in modeling architectural (geometrical) constraints between the subsystems and the components which are involved in the determining stage of volume allocation. Setting architectural constraints consists in allocating authorized volume envelopes to the different subsystems that constitute the overall system. These constraints are modeled as CAD parametric models for, theoretically, allowing later slight variations in case of future negotiations. Unfortunately, mechanical engineers use to assess the performances they are in charge of within CAE (Computer Aided Engineering) environments. Consequently, they directly make varying mesh models

instead of initial CAD models and they omit in practice to synchronize their current geometry to the permitted volume envelopes. Hence, there is no current assessment of a degree of compliance or non-respect of envelope constraints. This checking is made a posteriori in a non-automated way. We want instead to propose a tool for simultaneously assess their mechanical performance and the degree of compliance of the envelope constraints so as to always work with a consistent geometry and to instantaneously explore the tradeoff. Therefore, we propose here a measure –criterion- of this degree of compliance of the envelope constraints as well as the software implementation solutions.

We further detail both modeling aspects in following sections.

- **Metamodeling the design problem**

The FEM simulation models are computationally expensive. Furthermore in preliminary design, we aim to widely explore the design space. Therefore, surrogate models or metamodels [Simpson et al. 2001a; Simpson et al. 2001b] are used to rapidly and approximately assess the performance variables (also designated as design criteria) within a controlled precision.

Metamodeling consists of the building of an approximate mathematical model for straightforwardly assessing the design criteria (performance variables, PVs) from the influent Design Parameters (DPs). An appropriate design of experiments must preliminarily been carried out.

Five steps characterize the implementation of metamodel techniques. The first is to select the type of approximation function to be used. The second step is to perform the Design of Experiments (DOE) for efficiently sampling design points using the "true" engineering simulation model. The third step is the metamodel fitting from the experiments of the previous DOE. The fourth step is the metamodel validation for which various methods exist. The last step is the exploitation or prediction of the metamodel at untried inputs, for estimating the optimal design or for simulating tradeoffs.

The most popular approximation functions of metamodels are: Least Squares Polynomials, Neural Networks (NN) and Fuzzy Logic, Kriging, Response Surface Methodology (RSM), Radial Basis Functions (RBF), Wavelets, and Multivariate Adaptive

Regression Splines (MARS). For Lin et al [Lin et al. 1999], the kriging metamodel is more suitable to approximate Finite Elements simulations. This is why we use it in this work.

• Formulation of the Design Problem as a Multi-Objective Optimization Problem

Let us formalize the design problem into a multi-objective optimization problem as follows:

Problem P1

$$\min_x \{PV_1(x), PV_2(x), \ldots, PV_n(x)\} \qquad (n \geq 2) \tag{4.1}$$

$$g_j(x) \leq 0 \qquad (1 \leq j \leq r) \tag{4.2}$$

$$h_k(x) = 0 \qquad (1 \leq k \leq s) \tag{4.3}$$

$$x_{li} \leq x_i \leq x_{ui} \qquad (1 \leq i \leq n_x) \tag{4.4}$$

where $x = \{DP_1, DP_2, \ldots, DP_{n_x}\}$ is the vector of the design parameters and $\{PV_1(x), PV_2(x), \ldots, PV_n(x)\}$ is the vector of Performance variables. In Problem P1, g in equation (4.2) and h in equation (4.3) are inequality and equality constraint vectors, respectively; and equation (4.4) features the lower and upper bounds of the design parameters. As stated, Problem P1 generally does not yield a unique solution because of the conflicting nature of performances. This is why we further use the techniques that generate the Pareto frontier of the design space, a useful representation to engage negotiations.

• Generating the Pareto frontier

Engineering design problems commonly require consideration of more than one measure of performance, especially in multi-disciplinary design. The objectives in a multi-objective design problem are differently correlated. But, very often, a pair of objectives may be in competition, meaning that improvement of one typically comes at

the expense of the other. Tradeoffs must be considered when exploring a problem of this nature.

Pareto frontier contains all the Pareto optimal points. Pareto frontier is the complete set of Pareto optimal solutions [Mattson et Messac 2002a]. When multiple competing objectives exist, the optimum is no longer a design point but an entire set of non-dominated design points. Figure 25, from [Ferguson et Lewis 2004], gives an illustration in the case of two competing objectives. The set of non-dominated design points is commonly referred to as the **Pareto frontier** [Pareto 1906].

Many methods are available to generate the Pareto frontiers. Among them, three methods have proven to be effective in generating good representations of the Pareto frontiers. They are: Physical Programming (PP) Method [Messac et al. 1996] which is an extension of the Goal Programming (GP) Method [Ignizio 1976], Normal-Boundary Intersection (NBI) Method [Das et Dennis 1998], and the Normal Constraint (NC) Method [Ismail-Yahaya et Messac 2002b].

Improved NC method which is the Normalized Normal Constraint Method is presented in detail in Messac [Messac et al. 2003]. It provides advances over the other available methods. The method generates even (well) distributed points on the Pareto frontier. We use this method in our work.

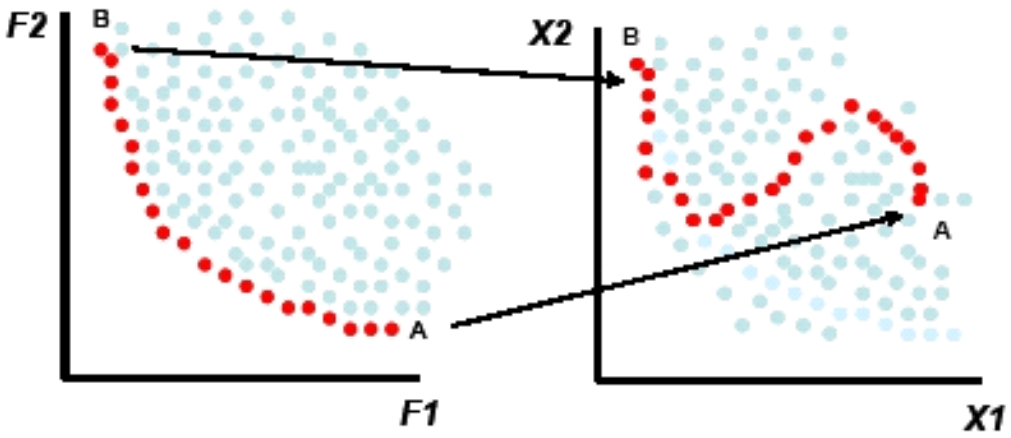

Figure 25. Representation of the Pareto frontier in the performance space (left) and in the design space (right) from [Ferguson et Lewis 2004]

- **Negotiating tradeoffs and obtaining compromise design**

On the basis of the representation of the Pareto frontier, design tradeoffs between design teams can be engaged. After negotiations, a compromise design can be set as a

best tradeoff between the conflicting design performances. Using the compromise design, the target attainment (achievement of design requirements) in the system level is a posteriori checked.

Part III Modeling the Design Problem in Preliminary Design

Part Presentation

In this part, we describe our design problem. We set up the modeling of the design problem which is concerned with the preliminary design of a large and complex mechanical system (e.g. an automobile).

We start by defining large and complex mechanical systems and how they are decomposed into subsystems and sub-design problems in order to enable concurrent engineering. The decomposition leads to an increasing number of targets, performances and design variables for each of the subsystems. After system decomposition we deal with the problem of convergence of the targets. The convergence (i.e. system synthesis) is that, after system decomposition, how to ensure that if the performances achieve the targets at the subsystem level, it induces that the targets over the system-level performances are also achievable. We evoke the three approaches to tackle with this problem: heuristic approach, design sensitivity approach, and target cascading methodology. While the last two approaches are likely to be appropriate, the one we use is the heuristic approach for reasons of availability and feasibility.

We focus later on the decomposition of our specific design problem with application to the car system regarding the NVH performances and the architecture constraints. From section §3.2, we see that the system level is the vehicle system model. Then down in hierarchy, we have on the same level the **trimmed body** model and the powertrain model. Next, at the lower level the trimmed body is decomposed into the acoustic cavity, the trimmings (seats, doors,…) and the **body in white** model. Our main studied subsystem is the body in white. We focus for that subsystem only on the decomposed NVH performances and on the architectural constraints.

For NVH, Section §3.3 gives us the performances that are assessed for that subsystem at that level of the decomposition. We give the theoretical background for that decomposition that leads us to consider the proposed performances and the assumptions that are made. The targets for the NVH BiW performances are also described at section

§3.3. We recall them. We see later that the decomposition of the NVH performance from the car system level to the trimmed body then to the body in white leads to an important number of performances and targets. We make a proposal to aggregate that important number of performances and the targets, at the BiW level, then at the trimmed body level, into one (real value) criterion.

For architecture constraints, they constitute the set of the constraints to which the design problem is subject to. We focus more on how to model the architecture constraints by expressing the relationships between the allocated volumes to components or subsystems and their geometries. Relationships are the possible interpenetrations between the geometrical configuration and the surrounding allocated volumes. Then, a criterion of maximal depth penetration is proposed. We achieve by the proposed criterion a transformation of the architecture constraints into a design problem performance.

To continue on the description of the design problem we provide the design problem parameters. Design parameters are considered, in our work, as the design variables. Design parameters are in great number and of different natures, when designing a complex system. In preliminary design, it is a question of how to manage the variability of the concept solutions. While optimization in the development-design-stage is a fine tuning toward the value of the design variables on a restricted area of their respective domains, in preliminary design we aim to have the largest extent of the variable domains. In preliminary design, we aim to explore largely the design space. When we are defining the design parameters for our design problem, we focus on two topics. The first topic is about the screening of the design parameters. In depth, what are the most important variables, to which the design performances are highly sensible? And, how much have we to set the extent of the domains of the parameters? The second topic is about the manner of how to make varying the structure of the mechanical system. Many ways can be adopted. Varying the geometry can be limited to local variations or can be carried out in a more global manner. To parameterize the mechanical structure, local variations of the geometry can be carried out by choosing major structural parameters available from the most CAD and/or CAE software. Or, a more global variation strategy corresponding to a design logic can be adopted like appropriate combinations of structural parameters, i.e. a kind of re-parameterization, or with *morphing techniques*.

Chapter 5

Modeling a Complex Mechanical System

5.1 What is a Complex Mechanical System?

Product system complexity results from a large number of parts in an assembly, complex geometry or multiple functions within the subsystems, and the combination of any different design disciplines within a single assembly. The individual components and functions are linked together in a network of relationships through which the design becomes more complex than the sum of the individual subsystems. An automotive vehicle is typically a large and complex system to design.

Often the term “system” is used in contrast to the term “component.” The context then is to address complexity derived from studying a collection of components that function jointly to perform an entire functioning system. A system can be composed of other systems that are often referred as “subsystems,” if one wants to emphasize the indivisible nature of a component. For example, a system can be an automobile—a collection of a great number of subsystems and components. This is one of the contexts for which the term “system” is used in the present work.

For concurrent engineering reasons, the industry proceeds to the decomposition of complex systems. In the next section, we deal with the issue of the decomposition of complex and large-scale systems.

5.2 Design of Complex and Large-Scale Systems by Decomposition and Coordination

Concurrent engineering and distributed design by means of model decomposition and coordination takes advantage of a decomposed design model by solving smaller design problems. The subproblems at the same level can be solved in parallel, using the optimization technique most suitable for the underlying submodel often linked to one or a limited number of disciplines.

In general, decomposition methods [Wagner 1993] are classified as object or **structural** decomposition (by physical components), aspect or **functional** decomposition (by knowledge domains or discipline), **sequential** decomposition (by directed flow of elements or information), and **model-based** decomposition.

Structural and functional decomposition are "natural" decompositions and typically large companies employ both types of decompositions simultaneously in a matrix organization. For example, an automotive manufacturer decomposes its organization in a structural manner into powertrain, body, chassis, or electronics divisions , but perform also decompositions in a functional manner with dedicated groups for durability, packaging, dynamics, safety, or noise-vibration-harshness [Michelena et al. 1999]

As said by Michelena et al [Michelena et al. 1999], "*However, drawing "boundaries" around physical components and subassemblies is very subjective, while division by specialties or disciplines (knowledge domains) may be dictated by management considerations that fail to account for disciplinary coupling. Sequential decomposition presumes unidirectionality of design information flow that contradicts the cooperative behavior desirable in concurrent engineering. Finally, computational resources often dictate in practice design strategies for large systems whose simulations may require days of computation on workstations or use of massively parallel machines - a requirement difficult to address in the decomposition strategies above.*"

Model-based decomposition methods are formal mathematical procedures that divide large models of a system into smaller, more manageable models [Krishnamachari et Papalambros 1997; Kusiak et Wang 1993]. After decomposition, design variables are categorized into linking variables, common to more than one subproblem, and local variables belonging only to one subproblem.

While it is not clearly formulated in sections §2.2, §3.2 and §3.3, our design problem decomposition from the viewpoint of NVH performance and architecture constraints is a model-based decomposition. In the next section we give one example of model-based decompositions we are using in the present work.

5.2.1 Example of the Application of Model-Based Decomposition to NVH Performances

Sections §3.2 and §3.3. give us a first approach to the model-based decomposition we are using for our automotive application.

Figure 26 illustrates an example of model-based decomposition with application to the design problem of road noise reduction inside the car. The interaction between the road and the vehicle wheel is modeled by excitation forces front to the wheels. The system level model is the transmission of the vibration excitations through the chassis (subsystem A) then through the shock absorber joints then through the structure of the body (subsystem B) which, due to structure/fluid coupling, generates noise in the passenger compartment (the cavity) near the passenger ears (response points r). We give the mathematical formulation of the system-level model in section 6.1.

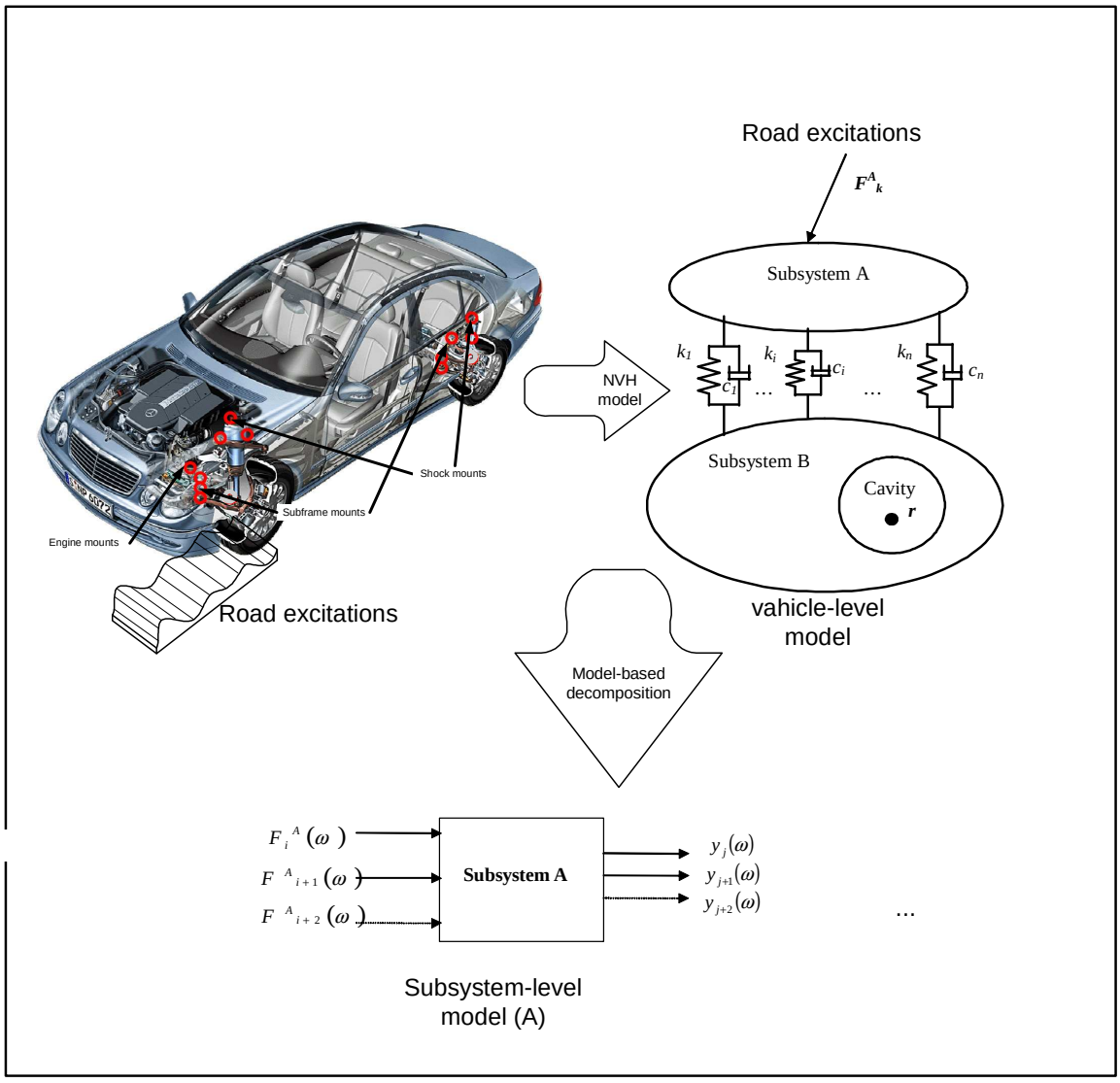

Figure 26. Example of model based-decomposition with NVH design problem of a car

Using model-based decomposition and based on a weak vibration coupling assumption between substructures, we obtain a modeling for each of the subsystems. For example, reducing the road noise inside the car turns, for the level of subsystem A, to reduce the responses at the interfaces with subsystem B. The model of the subsystem A can be studied (simulated and assessed) independently from the rest of the system.

5.3 The Problem of Convergence in the Design of Complex Systems

While the decomposition of a complex design problem certainly creates a series- of smaller, less complex problems, it also creates several challenging issues associated with the coordination of these less complex problems [Chanron et Lewis 2005]. The origin of these problems is the fact that the less complex subproblems are usually coupled and dependent upon information from other subproblems. The ideal case would be when a system could be broken up into subsystems without interdependence. Unfortunately, there are usually design variables and parameters that have an influence on several subproblems.

In engineering, convergence means to tend toward a common solution. The convergence is how to ensure, after system decomposition, that if the subsystem performances achieve the targets at the subsystem level, the system performances will systematically achieve the system-level targets. Convergence of design problem is, in our case, a kind of correlation between the achievement of targets for performances for all the subsystems and the achievement of targets by performances at the system level.

We focus on our work on the convergence properties of the solution for decentralized or distributed subsystems, where each subsystem has its own design problem, including objective(s), constraints, and design variables.

The challenging aspect of the convergence problem comes in the coupling of the subproblems upon each the subsystems, which creates complex research and implementation challenges in the modeling and in the solving.

The ideal scenario would certainly be when the subproblems are completely uncoupled, as recommended in the Axiomatic Design theory proposed by Suh [Suh 1990]. Unfortunately, a system with no coupling is typically difficult to achieve [Chanron et Lewis 2005]. The presence of the coupling generates a number of issues, including the allocation of the system design variables to the subproblems. For instance, if one variable has an influence on more than one subproblem, a first issue is the question of who should be in charge of having the control of this design variable; another issue is how the design variable can influence the convergence of the other subproblems. Previous work has been done on the allocation of the design variables by considering the strengths of the couplings [Bloebaum 1992] or by effectively propagating the desirable top-level design specifications to appropriate subsystems (Michelena 2002). Another

challenge in coupled systems is the communication barriers that exist between the design teams. The presence of non-local variables (design variables controlled by another design team or company) requires a certain level of communication in order to achieve a final optimal design. However, even within the same corporation, a perfect communication and cooperation is difficult to achieve due to several factors, including the complexity of the design, team specialization, geographic separation or information privacy.

For our design problem, we give three manners of how to deal with the convergence problem. The **first is a heuristic approach.** We explain later how we set up this heuristic approach. The **second is a design sensitivity approach** (see [Mahmoud et al. 2003]). The third one is the **target cascading methodology** ([Michelena et al. 2002]).

5.3.1 Heuristic Approach

The heuristic approach consists of a validation of the achievement of the target system afterward. It is an a posteriori validation at the system level of the achievement of the targets by the system performances. The approach is based, in part, on logic of performance cascading with simplifying hypotheses.

The method is the easiest one to use because that validation is only restricted to the achievement of targets by the system level performances.

Drawbacks are that the method is not applicable until an entire digital simulation model of the system is available. The heuristic approach takes advantage from the model-based decomposition without having to follow the entire approach of the target cascading. But the heuristic approach is based on a posteriori validation (i.e. late validation) that can leads to a poor achievement of the design performances or objectives at the vehicle level.

The advantages are the simplicity and the possibility to work independently on the submodel without having to model the entire system.

5.3.2 Design Sensitivity Approach

For Mahmoud [Mahmoud et al. 2003], the design sensitivity approach is an approach that is based not only on the assessment of the system-level and subsystem

level performances, but it assesses the sensitivity of the achievement of the subsystem targets by subsystem performances (the sensitivity) toward the system performances. Which are the most important improvements to do on the subsystem level that have grater influence to improve the system performances?

The approach quantifies the influence of changes in the different subsystem design targets on overall system performances. Calculating the sensitivities of system-level performance with respect to subsystem targets rather than design variables, as traditionally done in the design literature, is a key component of the approach. The approach is based on a procedure for ranking subsystem targets. The ranking enables to focus on the modification of the subsystem targets which are the most influencing for the improvement of the overall system performances.

5.3.3 The Target Cascading

Many techniques such as Multi Disciplinary Design techniques are developed to design complex mechanical systems. Among them the target cascading methodology seems to be effective in the design of complex mechanical systems as well as ground vehicles and aircrafts. Kim [Kim 2001] acquaints that designing a large mechanical system by distributing and synthesizing requirements to local levels in using optimization, has a greater chance of reaching optimum than optimization carried out at later stages, in detailed design, where only minor changes in thickness or shape are possible.

Target cascading assumes the existence of analytical models for systems, subsystems, and components. Computationally inexpensive models are essential for target cascading, given the large number of components and the number and complexity of interactions. Hence, high- fidelity, expensive models need to be replaced by simpler ones, referred to as “surrogate” models.

The target cascading methodology assumes that the supersystem (i.e. the top system-level) and associated models can be hierarchically partitioned into model-based subsystems and components, with as many levels as needed. Each entity at each level, which corresponds to a node of a tree structure, is called an “element”. Figure 27 illustrates a kind of hierarchical decomposition of an automotive vehicle.

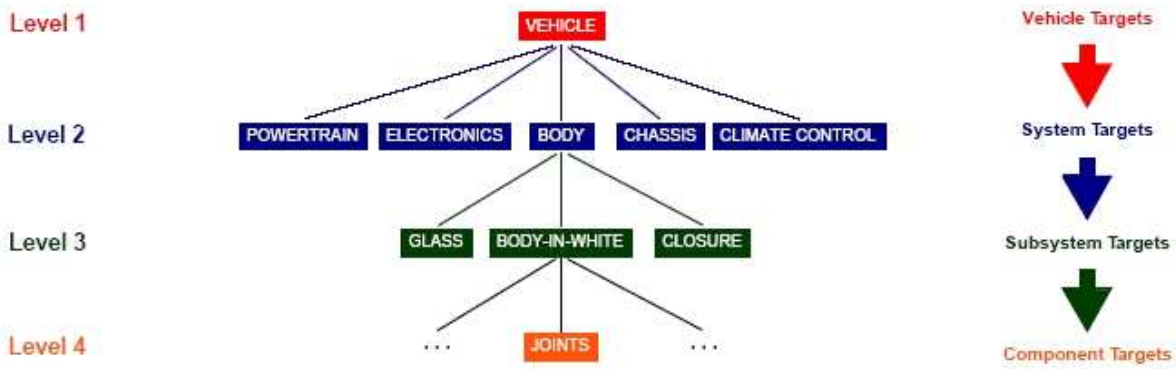

Figure 27. Vehicle Decomposition for Target Cascading, from [Michelena et al. 1999]

Target Cascading in vehicle design can be viewed as a four-step process [Rideout et al. 2001]: (i) specify overall vehicle mission targets, (ii) propagate vehicle targets to subsystem and component sub-targets, (iii) design vehicle systems, subsystems and components to achieve their respective sub-targets, and (iv) verify that the resulting design meets overall vehicle mission targets (see [Kim 2001]). To set up this Target Cascading process the vehicle system must be partitioned into subproblems, the subproblems ordered into a hierarchy and linked by a coordination strategy and, finally, models of appropriate complexity for each subproblem are established.

One advantage of the approach is that, under the assumption of the convexity of the design problem, the target cascading methodology is proven to be convergent [Michelena et al. 2002]. The convergence at the system level is achieved by assuring the convergence at the subsystem and component levels for each of the subproblems. The subproblems are solved iteratively until convergence criterion is achieved at that subsystem level.

Chapter 6 Noise Performances of an Automobile and its Subsystems: Model-Based Decomposition

As mentioned previously, our approach uses a model-based decomposition since we design a complex system. For our case of NVH design, the system-level design problem is concerned mainly with the reduction of the engine noise and the road noise inside the passenger compartment of the car. The noise that the passenger hears inside the car is the variation of the air pressure near his/her ear. The interior noise performances of an automobile are physically represented by the Sound Pressure Levels (SPL) inside the interior acoustic cavity of the vehicle system. The SPL-or the total noise-in the acoustic cavity is due to the excitations at the structure part of the system and the propagation of the induced vibration waves to the fluid part via coupling effects between the fluid and the structure. The lower the level of the SPL, the better the NVH performances of the vehicle. So targets –or Function Requirements- are set on the SPL performance as a curve which is called *target level*. Engineers work to get the SPL curve below the target level. Figure 18 gives an example for the SPL performance and the target level for the vehicle system.

6.1 NVH System-Level Model of the Automotive Vehicle

Our aim is to assess the Sound Pressure Level inside the automotive vehicle due to external and internal excitations, by considering the system as a model of a coupled structural-acoustic system.

In section §5.2.1 we give a description of how the system level model of the automotive vehicle is schematically modeled by a structural subsystem (A) for the chassis and by a subsystem (B) for the structure of the body. Subsystems (A) and (B) are linked by shock absorber joints modeled as spring and damper subsystems. Figure 28 shows the vibro-acoustic system model which has two substructures connected by spring and damper elements. Substructure B has a closed cavity modeling the air fluid, in which a point **r** is selected as a response point where the Sound Pressure Level is to be assessed. The powertrain excitations (considered as internal NVH excitations) and the road excitations (considered as external NVH excitations) constitute the external forces $[F_A]$ and $[F_B]$ that excite respectively the substructures (A) and (B). The variables $\mathbf{k_i}$ and $\mathbf{C_i}$ represent the stiffness and damping coefficients of the i*th* spring-damper element. There are n connection degrees-of-freedom (d.o.f.) along the interface boundary.

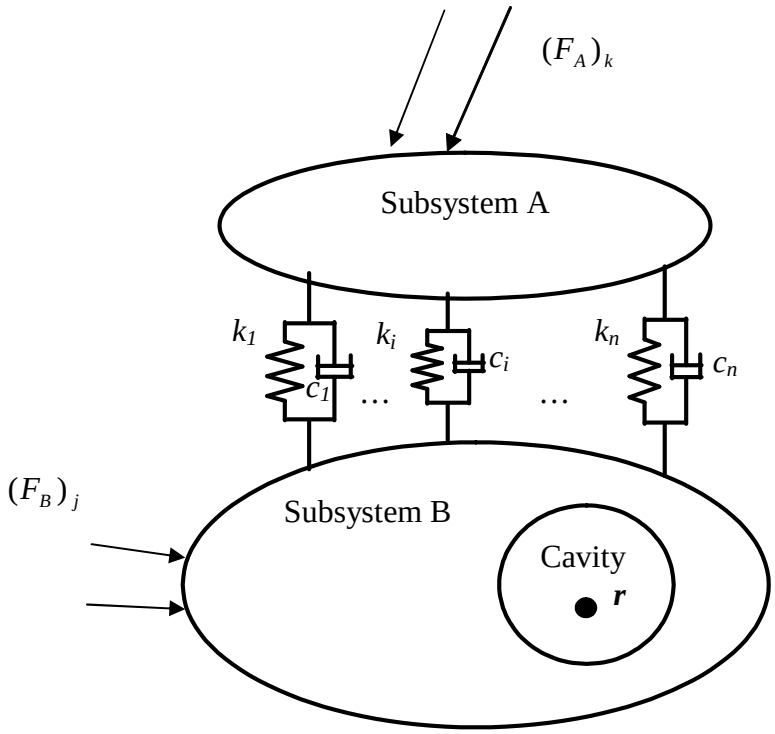

Figure 28. A structural-acoustic system consisting of two subsystems

Our structural-acoustic model has two aspects to deal with. The first one is the coupling between substructures (A) and (B) and the second one is the structure-fluid coupling between substructure (B) and the acoustic cavity.

The noise transfer function matrix of the coupled structures (A) and (B) with the acoustic cavity is denoted by $[NTF_{AB}]$

The noise transfer function matrix of the subsystem B coupled with the acoustic cavity is denoted by $[NTF_B]$.

Then the Sound pressure level is given by:

$$SPL_r = 20\log 10(\frac{[NTF_B]_r[F_B]+[NTF_{AB}]_r[F_A]}{2e^{-5}}) \text{ in dB[Pa]} \quad (6.1)$$

Numerous valuable commercial software packages exist to perform these calculations using the finite-element method (FEM). The reader can refer to [Meirovitch 1986] for a thorough discussion on structural dynamics.

6.2 Subsystem-Level Model

Based on the same schema of the Figure 28 and according to the model based decomposition approach, the structural subsystems (A) and (B) are the subsystem-level models. We assess the Vibration Transfer Functions of each of the subsystems. In this configuration subsystems are Multi-Input Multi-output vibration systems. This leads to a bunch of VTF to assess and to control toward the VTF targets. Figure 29 illustrates the form of a VTF matrix we obtained from our calculation, where in the column-wise are the grid point responses and in row-wise are the excitation d.o.f. Each component of the matrix is a Vibration Transfer Function which is a description of the displacement amplitude (y axis) function of the excitation frequency (x axis).

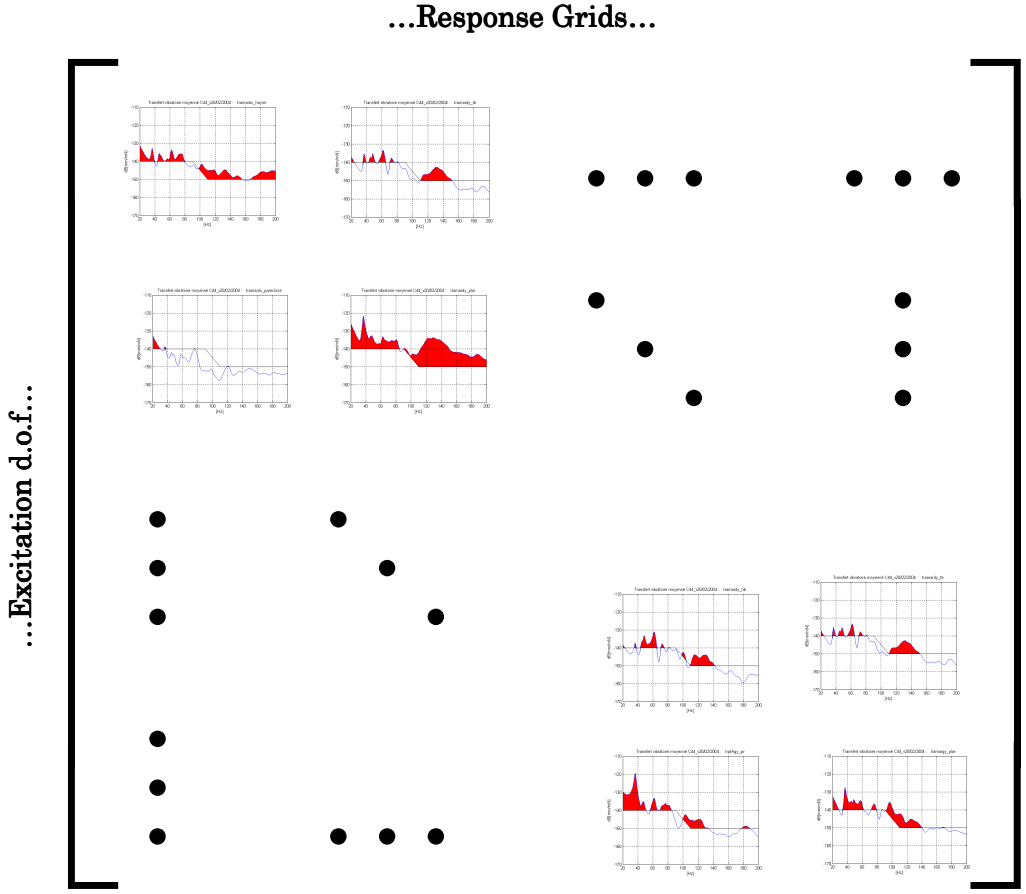

Figure 29. VTFs of a subsystem

In the next section, we describe how to proceed to deal with MIMO vibration subsystems.

6.3 Aggregating NVH Performances of an Automobile

In the automotive industry, one metric used to evaluate the NVH performances of the Body in White (BiW) is the root mean square (rms) of the transfer functions between output and input signals [Hamdi et al. 2004; Mahmoud et al. 2005; Yannou et al. 2004]. To assess the vibration performances, the automotive structure is assimilated to a Multi-Input-Mutli-Output (MIMO in terms of frequencies) vibrating system (see Figure 30). The inputs to the car BiW in this case are forces or displacements causing vibrations, and the outputs are displacements or velocities at locations of interest. Vibration transfer function in MIMO system between the output displacement signal at a given

location $u_i(f)$ and the input force signal at another given location $F_j(f)$ is known as the frequency response function (FRF). The FRF is then expressed as $H_{ij}(f)=\frac{u_i(f)}{F_j(f)}$. where f designates the frequency. The input signals are taken as white noise (unit) excitations. For a MIMO system with N inputs and M outputs, there is NxM FRFs. The FRFs are assembled into a NxM transfer matrix (see Figure 30).

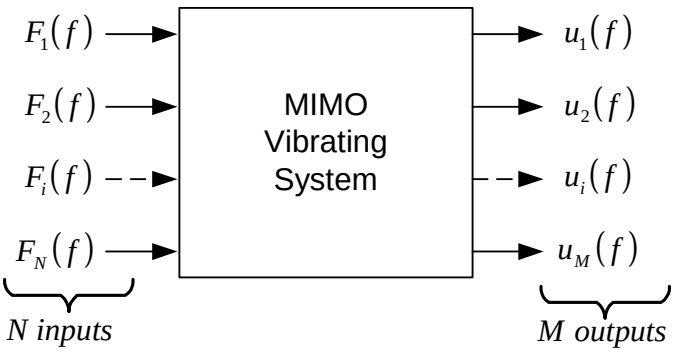

Figure 30. MIMO Vibrating System Model of the BiW

The fact to aggregate the whole transfer matrix into a single criterion by aggregating the NxM FRFs has the benefit of allowing the assessment of the overall vibration performances of the system, in the desired frequency range, without having to focus separately on each FRF. As an aggregate criterion, we propose the root mean square (rms) of the transfer matrix, denoted RMS_BiW criterion and expressed as follows:

$$RMS\_BiW(f_{\min}, f_{\max}) = \sqrt{\frac{1}{M \times N} \int_{f_{\min}}^{f_{\max}} \langle \frac{|H(f)|^2}{CDC(f)^2} \rangle df} \qquad (6.2)$$

The proposed RMS_BiW criterion is detailed and discussed in the Appendix A.

Chapter 7

Architecture Criterion and Subsystem Interface Constraints

We present the problem that has motivated this thesis. The problem consists in taking into account in an integrated manner the vibration performance criteria and criteria for the respect of geometric constraints in the preliminary design. We study first (1) the problem of volume allocation, a necessary stage to splitting the design tasks in a Concurrent Engineering process, then (2) we introduce a criterion for the respect of geometric constraints.

In this chapter we present design criteria that express the assembling and geometrical constraint between parts in the preliminary design stage. We already introduced the concept of ***volume allocation*** for mechanical components in**Part I**. We rather focus here on practical issues about the volume allocation. We introduce how to implement it in a CAE environment. We present how to use the allocated volumes in order to detect the possible collision between the subsystems. Then, if collisions occur we explain how to assess the maximum depth of penetration of one subsystem into the allocated volume of another subsystem. This value is considered as a geometric counter-performance that can be negotiated between engineers. During optimization, this performance may be kept below a minimal allowed limit so as to minimize the risk for two parts to really collide.

The criterion uses the penetration of the component into its neighbors.

7.1 Geometrical Preprocessing

Our approach must be as much independent from CAD software as possible. NVH engineers are more familiar with CAE tools where they can process the meshed models of the structure. Moreover, with recent available CAE software, we are able to create parametric, concept-level FEA models without waiting for geometry created in a CAD system. For that reason, we implemented our techniques of volume allocation only in mesh preprocessing software based on FE mesh. We use the ANSA software for this purpose. ANSA software is specialized in preprocessing and mesh preparation. It is easy to implement rapidly, in FE mesh format, the envelope volumes of mechanical subsystems.

Using FE meshes instead of a CAD format helps us, later, to make geometric computing. Compared to CAD databases that we can access only through their specific CAD software, there is an ease of access to the information in the files that describe FE models, using simple text parsing techniques. Extracting the grid positions of the FE meshes from the FE model files help us to set up in an easy way the geometric criteria. We describe the geometric criteria in the next section.

In a more practical way, volume allocation is based on a simplified envelope of the mechanical organs taking into account their possible 3D motion or displacement **(see Chapter 2)** For instance, for a powertrain we build a simple envelope based on mesh elements (see Figure 31). We take first into account a few sets of points from the powertrain mesh grids that represent the powertrain extent. Then, we translate the set points in the 3D space around the powertrain, in order to take into account the possible displacements of the powertrain. From the established set of points after taking into account the geometric dimensions and of the possible displacement of the mechanical components, we build up, in a simple geometry, a 3D mesh volume that represents the volume allocation.

Figure 31. Process of volume allocation within CAE software

7.2 Expressing the Criterion for the Non-Respect of Volume Allocation

The geometric criterion expresses the degree of interference between the subsystem or the mechanical structure in study with its environment. The environment is represented by a simple volume or surface representing the volume allocation for the other subsystems. The ideal is that the studied subsystems do not interfere with the allocated volume for the other subsystems. But, for the reason of improving the performances of the studied subsystem, we need to add mass or modify the dimensions and the geometry of the subsystem. That can lead to interference between the actual subsystem and the allocated volume. For some systems that have already their volume allocated, it is allowable to modify the geometry or dimension in order to improve the neighbor mechanical structure performance and in consequence the overall performance of the system. The amount accepted for the penetration of the structure into the allocated volume is a matter of negotiation between design teams. That is why the amount must be quantified into a metric. The metric expresses, if there is interference, the degree of the max depth of the penetration of the studied structure into the allocated volume for the subsystems in the neighborhood environment.

In the following paragraphs, we set first how we detect if there is collision or an intrusion of structure into one allocated volume. Then, we tell if an intrusion is detected, how we measure the max depth penetration of the structure. This measure is then considered as a metric used further for our design problem.

Maximal Penetration Depth

The maximal penetration depth, which is the architectural criterion, is a distance representing the maximal depth of penetrations of the structure grid points of the FEM mesh into the volume envelope of another system. Both the structure and the neighbor volume envelope are modeled as FEM meshes.

Penetration Depth

The penetration depth is the distance between a grid point of the structure, denoted as Pi, that is interior to the volume envelope and the nearest grid point on the surface of the volume envelope, denoted as Ps (see Figure 32).

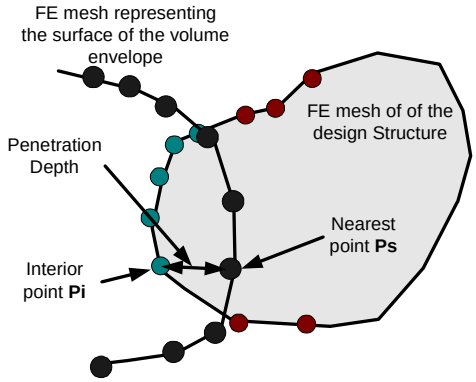

Figure 32. Penetration Depth of Grids of the Structure Mesh into the Volume Envelope

Condition of penetration

A grid point, Pi, from the FE mesh is said to be interior to the volume envelope only when it satisfies the following condition:

$$\mathbf{PiPs} \bullet \mathbf{Ns} = \|\mathbf{PiPs}\|.\|\mathbf{Ns}\|.\cos\alpha > 0$$

where:

- is the scalar product between two vectors

PiPs designates the vector between the interior point Pi and the nearest point from the envelope surface Ps, **Ns** is the external normal vector to the surface of the volume envelope and α is the angle between **PiPs** and **Ns**.

Implementation Consideration of the Architectural Criterion

We have implemented the architectural criterion in Matlab software. The FEM meshes of the design models and of the volume envelopes are loaded into Matlab. The maximal depth penetration criterion is calculated using the FEM meshes. Figure 33(b) illustrates, with a black point, the mesh grid that has the maximal depth penetration into a volume envelope represented in Figure 33(a).

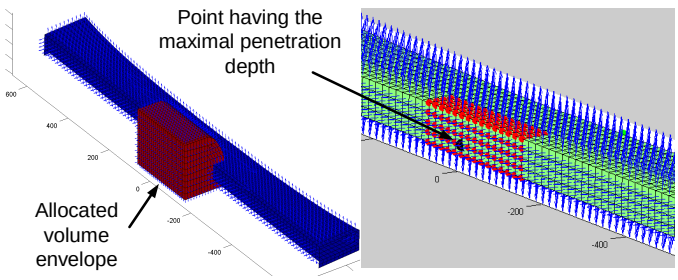

Figure 33. Implementation of Maximal Depth Penetration Criterion in Matlab Software

Chapter 8 Setting the Design Variables in Preliminary Design

8.1 Variable Screening

One approach, when we meet a design problem with a large number of variables, is to try to focus only on the most important variables and to reduce the problem dimensionality [Koch et al. 1999]. This technique is called variable screening. Therefore, screening is employed only if the problem includes a large number of variables. A number greater than 10, is considered as a large number [McCormick et Olds 2002]. Design experiences show that, in most case, some of the variables are important while others are not ([Myers et Montgomery 1995], [Kleijnen 1987]). The important variables can later be used to optimize the model or to build a surrogate model for the design problem [Stander et al. 2003].

First step to find the important independent variables in a simulation model is to conduct a screening experiment. These screening experiments can be expensive in terms of computation. Minimizing the number of experiments while maximizing the information about important variables is the ultimate goal of this stage[Trocine et Malone 2000]. Many techniques are available for variable screening. We discuss in the next section the criteria that evaluate their relevance.

.

8.1.1 Criteria for Screening Methods

After Trocine and Malone [Trocine et Malone 2001], in choosing a screening method there are three or four main criteria to consider. The criteria are efficiency, effectiveness, robustness, and ease of use.

Efficient screening methods are those that need limited number of experiments. Efficiency depends on the size of the problem.

Effectiveness is assessed by comparison to alternative methods. Effectiveness of screening is much like a heuristic criterion.

The third criterion is ***robustness***. Some methods require prerequisite conditions to be well applied. However, the conditions of the design problem are what they are So we need screening methods that work well without prior knowledge of the problem. "*For example, sequential bifurcation requires that the direction of the signs of all the effects in the problem are oriented in the same way. In general this is not the case"* [Trocine et Malone 2001].

The last criterion is the ***ease of use.*** Certain methods are easier for the experimenter but can perform less better with regard to effectiveness, efficiency, and robustness.

8.1.2 Variable Screening Methods

We start first by setting the used techniques for data sampling for methods of variables screening. Then we present some variety of the methods used for the purpose. We give application to our design problem for each of the methods. And we show how these methods help us to choose the most important variables for our design problem.

Sampling techniques for variable screening

Prior to using variable screening methods, it is important to choose the best sampling technique of data. Sampling data is more commonly known as Design of Experiments (DoE). The most suitable DoE technique for data sampling for the purpose of variable screening is the Plackett Burman Design [Montgomery 2001].

General Sensitivity Analysis

The General Sensitivity Analysis (see [Cundy 2003]) is a fast technique to determine which variable has a greater effects on which output parameter. A first order derivative of the output parameters with respect to each input variable is calculated using finite differencing. The derivative is calculated with setting the level of the selected variable to its extreme values, while the values of the remaining variables are set to their nominal values.

We obtain of the derivatives as follows:

$$\frac{\partial Out}{\partial In} \cong \frac{Out_{Hi} - Out_{Low}}{In_{Hi} - In_{Lows}} \tag{8.1}$$

where Out and In refer to output parameters and input variables respectively, and Hi and Low refer to the level at which the input variable of interest is set.

Significant Effects Variable Screening

Another method of variable screening is *significant effects variable screening*. It is to evaluate the contribution of an input variable (linear effects only) to the total model variance. The method of significant effects is based on the analysis of variance

For our study we make use of the General Sensitivity Analysis mainly for its ease of implementation then for its efficiency.

8.2 Varying the Shape Parameters by FE Parameterization and Mesh morphing

The incorporation of the architectural criterion in FEM pre-processing environment leads us to parameterize the FEM mesh model of the structure instead of the CAD model. The advantage of the FEM mesh parameterization is that it enables to assess architectural criterion and NVH criterion using the same FE mesh model. No need for FEM re-meshing and further pre-processing in order to prepare the design model for FEM simulation.

To parameterize a FEM mesh, two methods exist. Available commercial CAE tools for FEM pre-processing use one or the other type of the methods. The first type of the methods is based on parametric FEM elements. One of the available commercial tools is SFE CONCEPT [Zimmer 2000]. It permits fast-parameterized geometry development (see Figure 34) with the possibility of automatic re-meshing of the FEM model. But this type of parameterization does not allow wide variations of the structural parameters and includes the same difficulty of expressing a high level of parameterization from modeling element parameters as CAD models do. The Second type of FEM model parameterization is modifying the mesh model by the use of morphing tools. For instance, in ANSA software [ANSA] and LMS Virtual.Lab, the Morphing Tool can widely modify the shape of the FEM model with high level meaningful parameters (see Figure 35). The modification can be done without having to return to the CAD model and without losing the mesh that was already created. Distortion on elements that may be produced during morphing can be handled by the automatic reconstruction of the FEM mesh, so the morphing process is not limited by element quality criteria (e.g. distortion criteria of FEM elements).

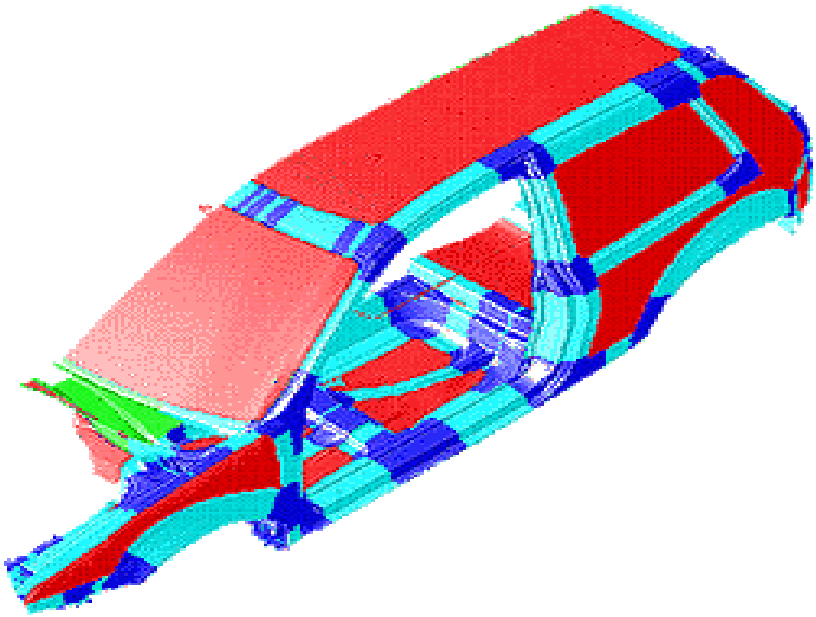

Figure 34. SFE CONCEPT Model of a BiW FE Mesh

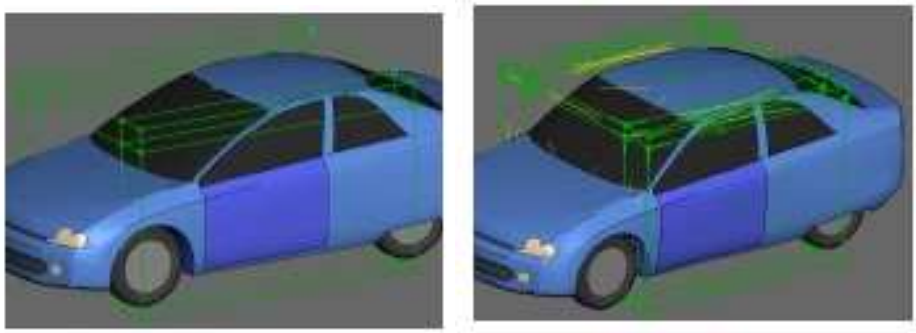

Figure 35. The morphing tool of ANSA meshing software [ANSA]

LMS Virtual.lab has also integrated a morphing tool (see Figure 36 and Figure 37).

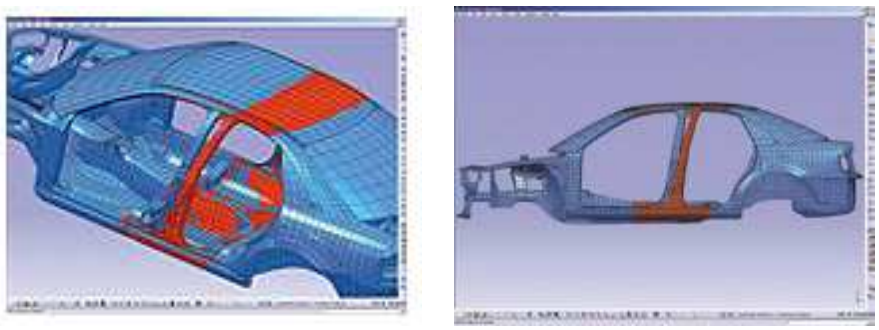

Figure 36. Changing the B-pillar styling using the LMS morphing tool

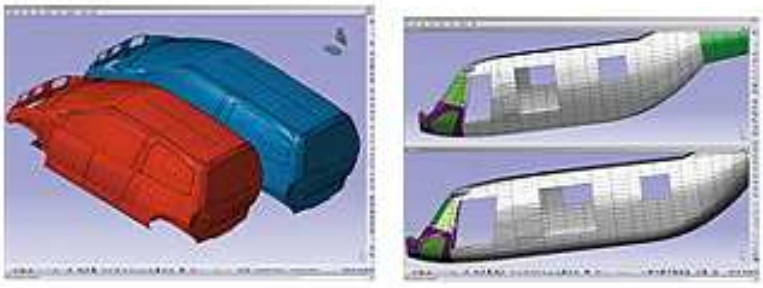

Figure 37. Stretching from predecessor models and quickly creating design variants using the LMS morphing tool

Part Synthesis

In this part we have presented the whole data streaming of the variables, the performance and the constraint of a typical mechanical design problem with application to the NVH design problem of automobiles. The Figure 38 synthesizes a full description of the design problem.

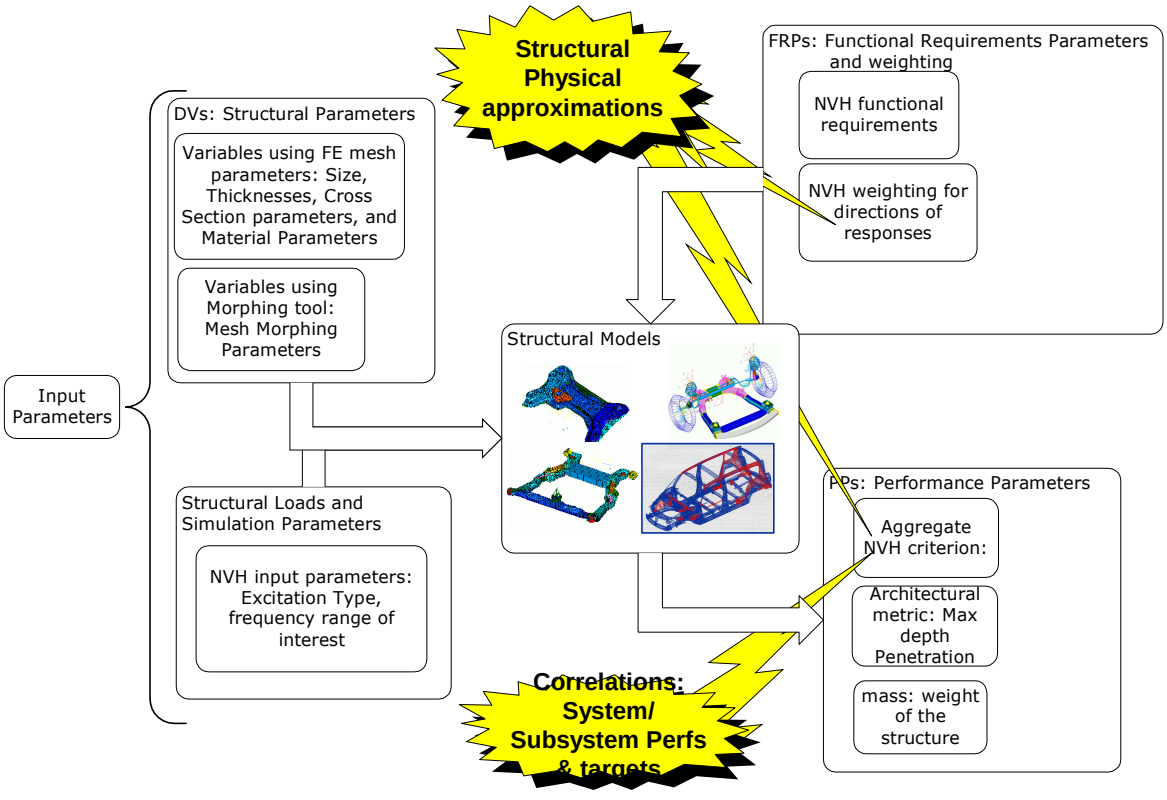

Figure 38. The whole data streaming for approximate design problem

Part IV
Tradeoff Exploration using Surrogate Models

Part Presentation

In this part we present our Strategy that consists of rapid assessment of mechanical performances to help design exploration and to enable dimensioning compromises for a multidisciplinary problem.

We present briefly in **Chapter 9** the advantages we get from the use of surrogate models (or metamodels) first for graphical deterministic exploration of the design space in Chapter 10and secondly for dimensioning with tradeoffs using Pareto frontier representation in Chapter 11.

Chapter 11 explains how to use the Pareto Frontier representation to deal with engineering design problems requiring the consideration of more than one measure of performance, especially in multi-disciplinary design. In such a case tradeoff situations occur when, for instance, a pair of objectives that are in competition, meaning that the improvement of one typically comes at the expense of the other.

Chapter 9 Metamodel Techniques

- **Metamodels**

There is several metamodels available from the literature [Chen et Simpson 2000]. The approximation function varies from one technique to another. The most popular techniques are: Least Squares Polynomials, Neural Networks (NN) and Fuzzy Logic, Kriging, Response Surface Methodologyn (RSM), Radial Basis Functions (RBF) and Wavelets, and Multivariate Adaptive Regression Splines (MARS). The reader can refer to the Appendix B for a literature review of these metamodeling techniques.

There are five main steps for implementation.. The first one is to **select the type of the metamodel** which the more adapted to the type of the design problem. . The second step is to perform the **Design of Experiments** (DOE). DOE serve to sample efficiently data points and to fill the design space using the "true" engineering simulation model. The third step is **metamodel fitting**. The parameters of the metamodel need to be estimated from the DOE sampled data. The fourth step is the **metamodel validation**. Various methods are available for the purpose. The last step is the **use of the metamodel** to predict responses at untried inputs and performing optimization runs, tradeoff studies, or further exploring the design space.

Neural networks as well as kriging metamodels are suitable but the neural networks demand greater effort and more training time to be implemented [Cundy 2003]

After Lin [Lin et al. 1999], the kriging metamodel is suitable to approximate Finite Elements simulations. Kriging metamodel has some variants. Some of them can better approximate FE simulation model than others. This is why we have used kriging

metamodels for our design problems. We provide more details hereafter on the kriging metamodel.

- **The kriging metamodel**

The kriging metamodels are a spatial correlation metamodels forming a class of techniques that enable to build global and accurate approximations of the design space [Meckesheimer 2001].

In a metamodel based on spatial correlation, the design variables are correlated as distance functions. These metamodels take advantages from being quite flexible in the sense that they can either making accurate interpolation of the data or smoothing data with lesser accurate interpolation. This is made possible with the choice of the spatial correlation function [Simpson et al. 1997].

- **Selecting kriging metamodel for our design problem.**

Lin et al [Lin et al. 1999] have made the demonstration that the kriging model with the cubic spatial correlation function performs a good accuracy and efficiency in the metamodel of Finite Elements simulations. We use the same technique for our design problem.

Chapter 10 Deterministic Exploration of Design Space

We present here up-to-date tools for design space explorations based on the use of surrogate models. Graphical representations of the design space give the designer a practical understanding of mechanical design problems from the viewpoints of performances, design parameters and their coupling. Graphical representations of the design space help designers to apprehend the regions of possible (acceptable or feasible, I.e. respecting the constraints) solutions for the design.

Exploring the design space helps to examine more candidate designs, and avoid inadequate or unfeasible solutions.

- **3D Projection of the hyper-dimensional Design Space**

Hyper dimensional design space is design space that has more than 3 dimensions. In order to visualize the hyper-dimensional design space, one utilizes a set of 3D views of the design space, each of which corresponding to three design performances. Therefore, an N-dimensional performance space can be substituted by number of N(N-1)(N-2)/6 of 3-dimensional spaces for viewing.

- **What is visualization?**

McCormick, DeFanti, and Brown [McDeBr87] define visualization as "the study of mechanisms in computers and in humans, which allow them in concert to perceive, use, and communicate visual information". Thus, visualization includes the study of both image synthesis and image understanding.

- **Data visualization**

Conventional visualizations techniques used by data analysis tools are pie charts, scatters plots, bar charts, histograms, volumetric rendering, Charnoff Faces etc. but most of them have limitations in handling the analysis of multidimensional data effectively. Thus, there has been a long-standing need for better methods of visualizing the collected information.

The graphic displays show patterns in the data more clearly than plain numbers, leading to better descriptive and explanatory models of the data.

- **Multivariate Visualization with Parallel Coordinates Method**

Multivariate visualization is a technique that represents the N dimension in parallel coordinates with polygons. The advantage of this method is the possibility to visualize, quickly and without confusions, the positive, the negative or the absence of correlation between design performances. This technique is found to be useful for the further developments in our work when speaking about Pareto Frontier.

Inselberg [Inselberg 1985] in 1985 and Wegman 1990 [Wegman 1990] are the first to introduce the Parallel Coordinate Method.

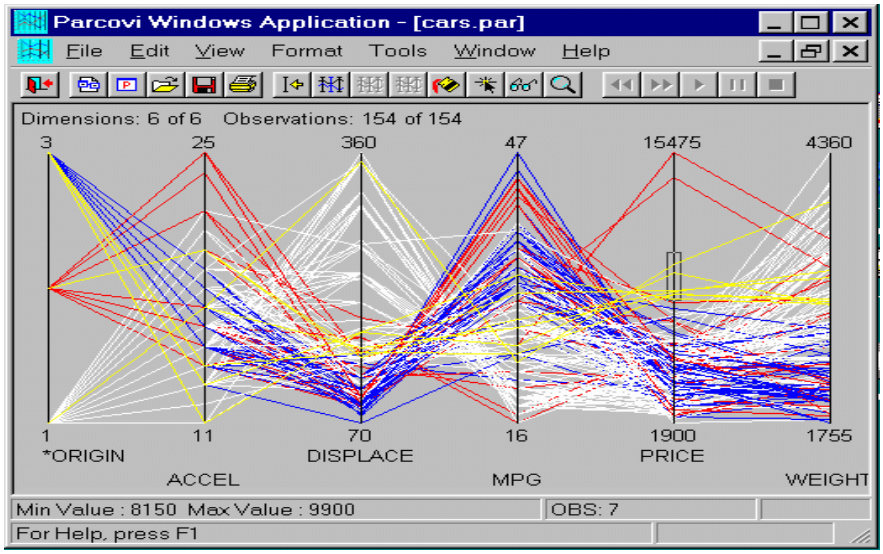

Figure 39. Parallel coordinate representation of 6 dimensional data

Chapter 11 Design Tradeoff

"*As the complexity of multidisciplinary system design has substantially increased, so too has the need for incorporating tradeoffs into the design process*" [Ferguson et Lewis 2004]. By incorporating such tradeoffs, the optimal system performance of each objective is sacrificed to increase the overall range of the system's functionality.

In our methodology and in order to enable design tradeoffs, we use the Pareto frontier representations. And for the generation of the Pareto frontier, we make the use of the surrogate models (i.e. metamodels), the techniques described in chapter 6. Combining surrogate models and Pareto frontier can be of a great benefit for preliminary design of mechanical structure. Not only the design performances are rapidly assessed, but with the Pareto frontier a designer or decision maker can make tradeoffs between disparate and conflicting design performances. Then, on the basis of these choices, tradeoffs between design teams about the design sizing and performances can be found.

The Pareto frontier provides the designer with information regarding the maximum performance of the system.

First a Pareto frontier must be built as the subset of feasible design points which are not completely dominated by any of the others feasible design points (i.e., dominated on every performance). Feasible design points are design points that comply to the design constraints and specifications [Yannou et al. 2005].

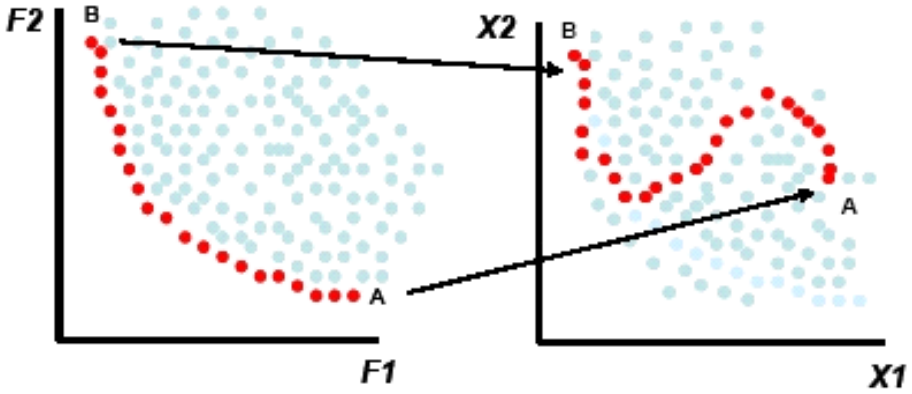

Figure 40 Representation of the Pareto Frontier in the Performance Space (left) and in the Design Space (right), from [Ferguson et Lewis 2004]

Second, The Pareto frontier (dark points in Figure 40) in the performance space can be inversely mapped to the design space, which is obviously useful for making final decisions on design parameters.

In the following, we properly define the Pareto frontier. Then, we give a description of the selected method, the *normal constraint method*, that we use to generate the Pareto frontier. In addition, some illustrative examples are provided, in the end of the part, for a better understanding of the methodology.

11.1 Pareto Frontier

11.1.1 Definition of Pareto Optimality

In the following, we mean by ***objective***, which is an optimization term, the *design criterion* or the *design performance* of our design problem. We start by setting the definitions of Pareto optimality, Pareto frontier, and Pareto set.

- **Pareto optimality**

A design point is a ***Pareto optimal*** point if there is no feasible point that would reduce one criterion of the performance space without increasing the value of one or more of the other criteria. According to Messac [Messac et al. 2003] a ***Pareto solution*** is one where any improvement in one objective can only occur through the worsening of at

least one other objective. This class of solutions is central to multiobjective optimization ([Pareto 1906], [Steuer 1986]).

- **Pareto Frontier**

Pareto frontier contains all the Pareto optimal points. Pareto frontier is the complete set of Pareto optimal solutions [Mattson et Messac 2002a]. When multiple competing objectives exist, the optimum is no longer a design point but an entire set of non-dominated design points. This set is commonly referred to as the **Pareto frontier** [Pareto 1906].

- **Pareto Set**

The *Pareto set* is a discrete representation of the Pareto frontier. The Pareto set is composed of Pareto optimal solutions [Mattson et Messac 2002a]. In our dissertation we confound the term Pareto set with Pareto frontier. The latter term designates, in the following,the two definitions (Pareto frontier and Pareto set).

11.1.2 Drawbacks of Classical Weighted Sum Optimization

Optimization methods based on sums of weighted criteria have been outwardly criticized in the multiobjective optimization community [Koski 1985; Messac et Ismail-Yahaya 2001]. The main limitation of weighted sum methods is that they do not yield solutions that lie in non-convex regions of the feasible performance space. These methods succeed in getting points from all parts of the Pareto set only when the Pareto curve is convex [Steuer 1986]. And it is a frequent observation [Das et Dennis 1997] that, even for convex Pareto curves, an evenly distributed set of weights fails to produce an even distribution of points from all parts of the Pareto set.

Another important drawback is that it is sometimes very artificial to attempt to straightforwardly capture preference models as the minds of designers, customers or decision makers are not clear at that time. This is why providing them a mean to graphically explore Pareto sets has been proved to be a valuable way to understand the correlation between design parameter and performance variable on the one side and between performance variables themselves on the other side.

11.1.3 For which Design Problems Pareto Frontier is Better Used?

Engineering design problems commonly require consideration of more than one measure of performance, especially in multi-disciplinary design. The objectives in a multi-objective design problem may relate differently to one another. Two objectives may be in competition, meaning that improvement of one typically comes at the expense of the other. Tradeoffs must be considered when exploring a problem of this nature.

Objectives may also be in cooperation with each other, meaning that improvement of one typically accompanies improvement of the other. In this case, there is a single superior design and tradeoffs do not occur. The third possibility is that there is no relationship, as is the case if the objectives have no parameters in common. The latter two cases are less interesting than the first one and are therefore not considered further in our work.

Practically, when we are in the case of a design problem with multiple performances, we use the technique of parallel coordinates to separate the conflicting performances from the complete set of the performances. The technique is described in section (**Chapter Deterministic exploration of design space**). The technique helps us to determine the positive, the negative or the absence of correlation between performances. The negative correlation means that the performances are somehow conflicting and there is a need to establish a tradeoff between them using Pareto Frontier. This method holds approximations because we evaluate a limited number of design points and the negative correlation can not be captured for some cases. The technique is better used when there is a large number of performances (more than five performances) in order to focus rapidly and only on conflicting performances.

11.1.4 Pareto Frontier Population Methods

Many methods are available to generate the Pareto frontiers. Among them, three methods have been proved effective in generating good representations of the Pareto frontiers. They are: ***Physical Programming*** Method [Messac et al. 1996] which is an extension of the Goal Programming Method [Ignizio 1976], ***Normal-Boundary Intersection*** (NBI) Method [Das 1997; Das et Dennis 1998], and the ***Normal Constraint*** Method [Ismail-Yahaya et Messac 2002a, 2002b; Messac et al. 2003].

We give here an overview description of Normal Boundary Intersection and of Physical Programming. Then, we describe the assessment criteria of the methods that generate the Pareto frontier. These criteria help us to make the choice of the method we use in our work.

Normal-Boundary Intersection (NBI)

The NBI generates evenly spaced Pareto points for an even spread of weights, and the spacing of the points is independent of the relative scaling of the objectives. NBI is not limited to bi-objective problems.

Physical programming

Messac and Sundararaj [Messac et Sundararaj 2000] employ Physical Programming to generate a distribution of points along the Pareto frontier. Physical Programming is an optimization method that does not rely on weights, but uses designer preferences in the form of metric classes in the optimization process.

Normal constraint Method

In the Appendix C we present in detail the Normalized Normal Constraint Method. Messac [Messac et al. 2003] proved the advantages of this method over the other available methods. We use this method to generate the Pareto frontiers for the design problems presented in our work. Based on the literature, we have implemented this method in Matlab software.

11.2 Tradeoffs in Preliminary Mechanical Design

In this section we show how we use the Pareto frontier developed in the previous section in order to obtain tradeoffs between conflicting performances in the preliminary design.

- **How negotiation can be held between experts?**

In the preliminary design stage of large mechanical system important choices are to be made. The exploration of the design space can lead to identify conflicting situations, where, for a number of design candidates, if we want to improve some of the performances it leads to worsen other ones. The negotiation is used as a mean of clarifying these conflicts [Scott 1999]. And because of the lack of information and of the high level of uncertainty, in this stage of design, decision-takers hold negotiation with their different perceptions based on their sets of performance requirements and design specifications. But the use of the Pareto Frontier as a tool for tradeoff negotiation offers a way to reach a consensus in quantifying the optimality of one performance relatively to other conflicting performances.

Part V　Example: NVH Car Body Design of Automobile

Chapter 12 Case Study Presentation

In the present case study we apply our methodological framework in order to find a compromise design of a crossmember that is intended to improve NVH performances of the BiW while respecting the tight architectural constraint from the volume envelope of the car powertrain.

The original design of the car BiW suffers from a high level of vibration on a frequency range of particular interest for NVH performances between 90 and 110Hz. The frequency response functions representing the vibration transfers from excitation points of road noise and powertrain noise to response points on the body car remain high in that frequency range (see Figure 43). The high level of transfer functions for the initial design in the targeted frequency range implies that there is a high risk that the overall acoustic performance (expressed by the Sound Pressure Level on the driver ears) will be high within the same frequency range. After multiple sensitivity analyses by increasing the stiffness of some components to see how it influences the vibration transfers and by studying the shape modes of the BiW components along the frequency range of interest, the design team has concluded that the weakness comes from the fact that a crossmember in the top of the powertrain compartment has a reduced cross section in its middle (see Figure 41). The reduced cross section weakens the overall stiffness of the front of the BiW.

The reduced cross section of the original design of the crossmember is the consequence of architectural constraints of the overall dimensions of the powertrain.

To overcome the problem, a rough design proposal is submitted by the NVH design team. The BiW is re-analyzed in order to see how the new design improves the NVH performance of the BiW. The proposal consists of an additional crossmember with a rectangular cross section that is located under the original crossmember (See Figure 42).

After a one loop analysis, the design team has been convinced that this design proposal significantly improves the NVH performance (see Figure 43).

But the proposed design fails to fit in the allocated envelope volumes of the powertrain. Besides, the proposed crossmember interpenetrates with components of the powertrain (see Figure 42).

The design case has been a challenging one between the NVH design team and the architects of the vehicle. In the one side, the powertrain design is so advanced in the project timetable that only minor changes are tolerated and, in the other side, the proposed design significantly improves the NVH performance of the BiW.

A tradeoff has then to be found between the NVH performance and the architectural constraints. This tradeoff consists of how much necessary to reduce the interpenetration of the crossmember (1) to affect only components that can be cheaply redesigned (without major change on powertrain performance or design) and (2) to maintain a significant improvement in the NVH performance in order to justify the costs of the added crossmember (costs = cost of the mass of the crossmember + manufacturing costs).

To help the NVH design team to found a tradeoff with the architects, we propose to apply the presented methodology.

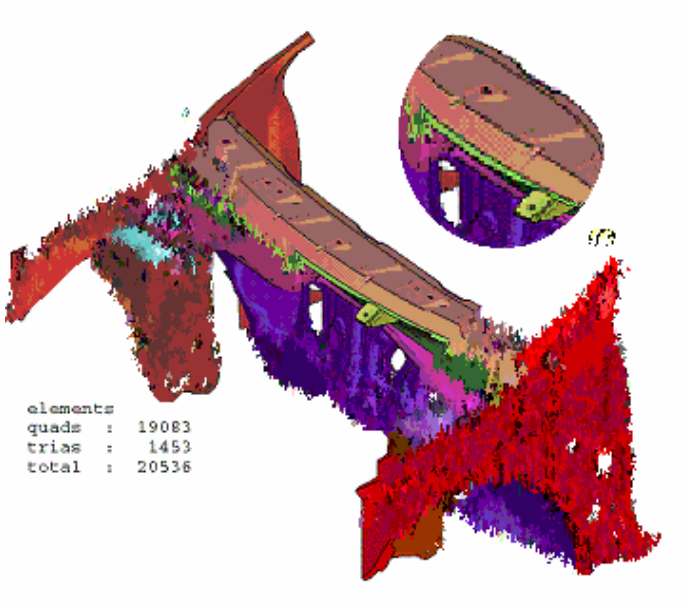

Figure 41. Original Design with Reduced Cross Sections in the Middle of the Designate Part (the drawing has been voluntarily fuzzyfied for confidentiality reasons)

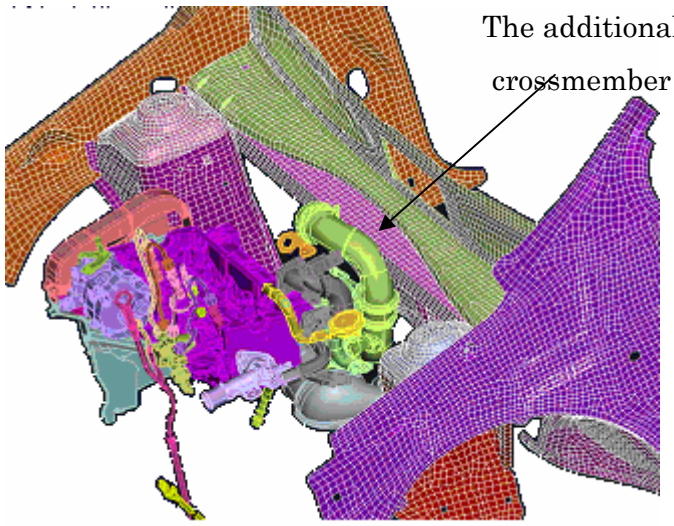

Figure 42. The Additional Crossmember Proposal for Improvement of NVH Performance of the BiW

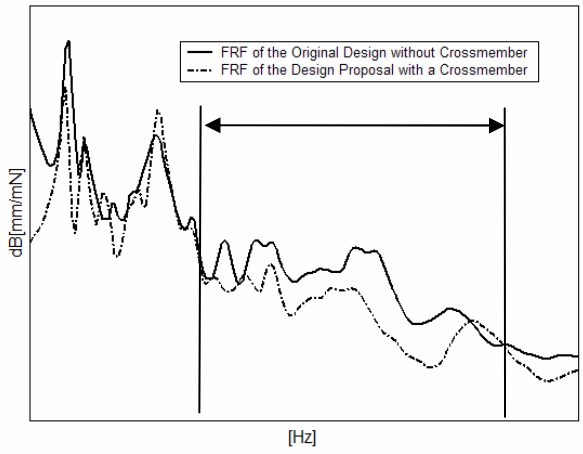

Figure 43. Improvement of the Vibration Transfer in the Targeted Frequency Range

Chapter 13 Formulation of the Design Problem

13.1 Output Performance Variables

The NVH performance is aggregated over the targeted frequency range as it is mentioned in the above section of NVH performance criterion.

The RMS_BiW is used as the NVH performance criterion. The frequency range is restricted to the targeted range of frequencies.

The non-respect of architectural constraints due to the overall dimension of the powertrain is expressed by the maximal penetration depth criterion. As suggested in the formulation, the overall dimension of the powertrain and its possible displacement is represented by an allocated volume. The annotated box in Figure 44 illustrates the allocated volume to the powertrain.

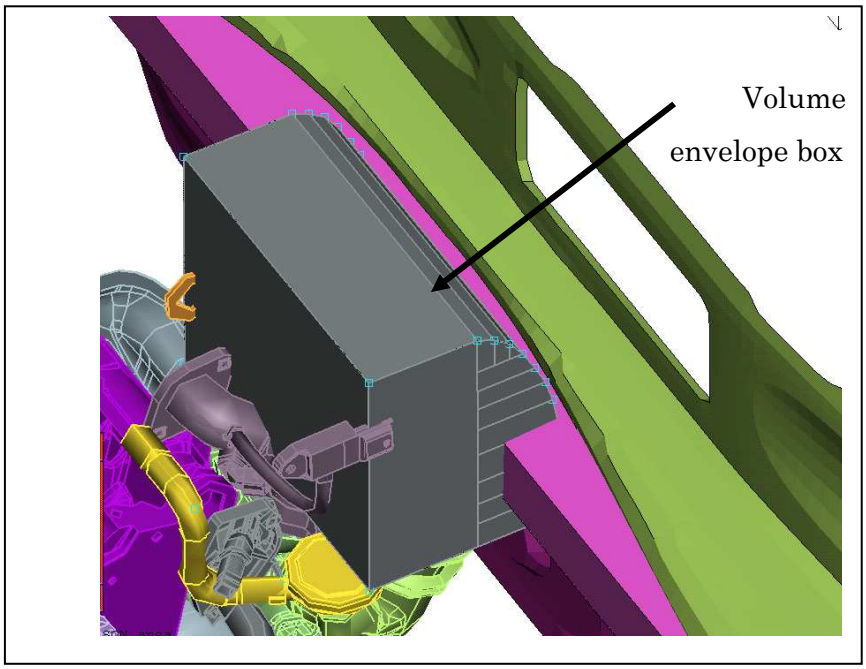

Figure 44. Volume Envelope Box Corresponding to the Overall Dimension and the Possible Displacement of the Powertrain

As the non-respect of architectural constraints comes from the interpenetration of the middle cross sections of the crossmember into some components of the powertrain, one way to parameterize the crossmember is to reduce the middle cross sections. Using the morphing techniques, we have parameterized the crossmember structure with only two global parameters (see Figure 45), namely the height H and the width (W) of the middle cross section of the crossmember.

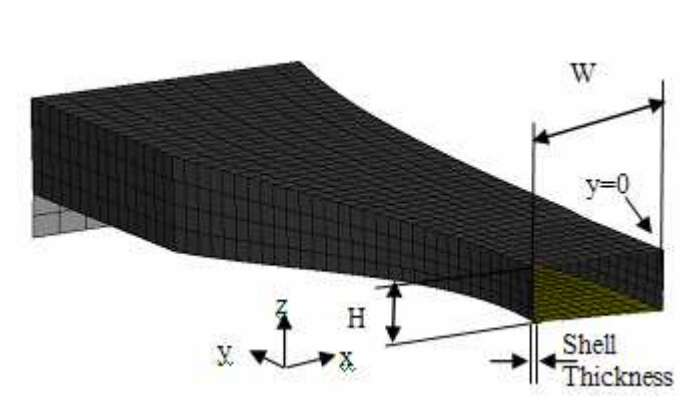

Figure 45. The Height and Width Morphing Parameters for Middle Cross Sections

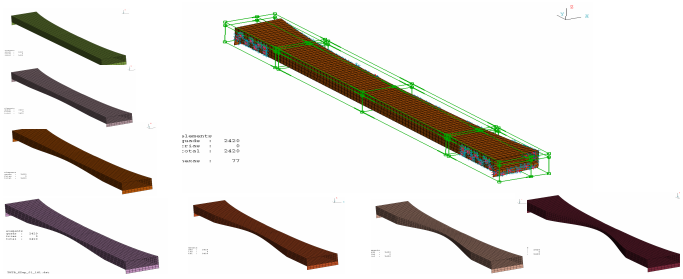

Figure 46. Using Morphing Techniques to Modify the Shape of the Crossmember

The two parameters of the current crossmember section smoothly evolve when moving from the middle cross section to both extremities. Figure 46 displays a set of possible shapes addressed by such a parameterization using the morphing tool. A third design parameter is the thickness of the crossmember shell.

13.2 Simulation Model

The simulation model is mainly based on the metamodeling techniques as it is explained in methodological framework section.

To obtain a metamodel we establish first a Design of Experiment (DOE). The height (H) and the width (W) parameters are split into 4 levels. As we have a small number of factors (2 parameters) we adopted a full-factorial DOE.

W=[43.2, 63.1, 81. , 99.7] mm

H=[15.7, 26.3, 36.9, 47.7] mm

Thickness = [0.8, 0.9, 1, 1.1] mm

We have chosen the kriging metamodel type as it is well adapted to approximate FE simulation. To validate the metamodel we use the cross validation technique. The kriging model built after the DOE provides after validation a Root Mean Square Error (RMSE) of [2mm; 0.4; 0.07 Kg]. respectively for the architectural criterion, the RMS_BiW criterion and the mass of the BiW.

The present metamodel is used to rapidly construct a representation of the performance space (see Figure 47). In a second stage, the Pareto frontier is generated from the Normalized Normal Constraint Method [Messac et al. 2003].

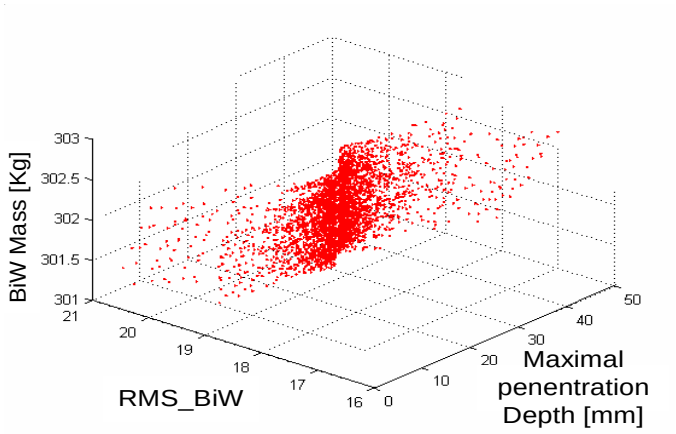

Figure 47. Design Performance Space Evaluated using the Kriging Metamodel

Chapter 14 Case Study Design Tradeoff

A compromise is found after having plot the Pareto frontier between the vibration criterion and the architectural criterion (see Figure 48). The coordinates of this compromise are (W=94.1877 H=43.3206 Thickness= 0.8000) (see Figure 48).

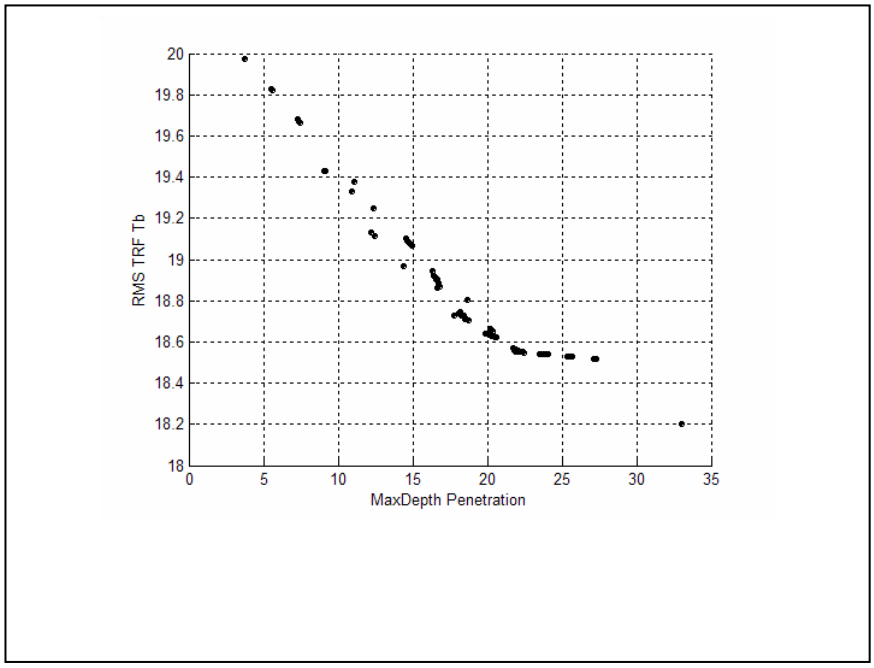

Figure 48. Pareto Frontier for Architectural and NVH Criteria

The tradeoff consists of the acceptance of the proposed design by the architects. The proposed design is different from the original proposal by a reduction of 10% in height and 6 % in width for the middle cross section. The compromise solution corresponds to a small interpenetration of the crossmember into the volume allocated to

the powertrain. But, after the architects, this is an acceptable agreement since this small penetration only corresponds to a part of a plastic cover. This plastic cover is an acoustic insulator to reduce medium and high frequency noise of the powertrain. The change of the plastic component does not engage high costs, because the mold is not yet manufactured and the redesign of the cover does not affect any functional components of the powertrain.

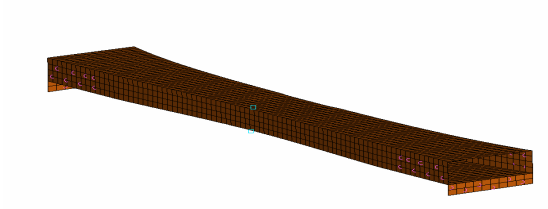

Figure 49. The Compromise Design of the Crossmember (W=94 ; H=43mm ;Shell Thickness=0.8 mm)

In parallel, the design that is being to be accepted by the vehicle architects gives satisfying improvements in NVH performances (RMS_BiW=16.7). We have rebuilt a structural design of the crossmember that corresponds to the design parameters of the compromise found using metamodel. After running the FE simulation model of the BiW, we have obtained the RMS_BiW criterion that differs from the metamodel's by only 4%. The obtained value of the RMS_BiW criterion has plainly met the NVH team expectations for the NVH performance improvement. Moreover the added mass with the compromise crossmember is about 1.5 kg. This amount of the added mass is in accordance with the allowable expected shift of costs regarding the benefits of the NVH performance improvement.

To complete the analysis we have focused on the vibration transfer functions for the compromise design. A significant improvement is obtained for the desired frequency range with the compromise design (see Figure 50).

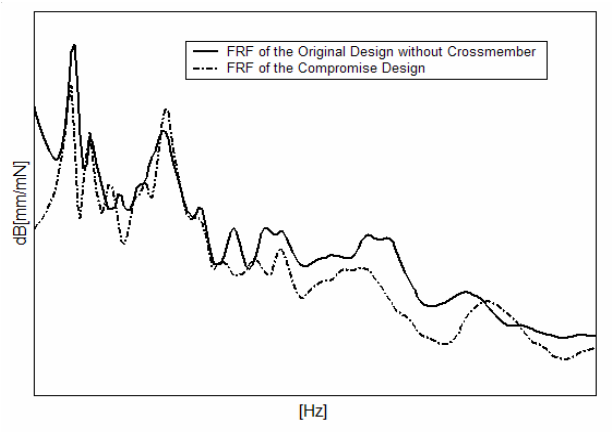

Figure 50. Improvement of Vibration Transfer in the Targeted Frequency Range with the Compromise Design

Conclusion and Discussion

- **Thesis Synthesis**

We presented, in this thesis, a framework of design methodology that is dedicated to the preliminary design of automotive vehicles. The methodology enables the exploration of tradeoffs between automotive architectural constraints and noise performances.

We presented first the industrial motivations. We described the actual practices in the preliminary design of automotive vehicle in Renault Company. We made obvious through that description that there was a real need to tools enabling to tackle concurrently with the noise performances and the allocated volumes. The subject seemed to be a matter of conflicts for the almost design cases. The source of the conflicts consisted in the fact that improving noise performances by adding mass or attributing more volumes to integrate structural solutions on the vehicle body is a difficult problem in today compact vehicles, because of the high number of geometrical constraints and because of the interior architecture complexity of the car body.

We established a holistic approach to help resolve this intractable problem. We presented a methodology with five main stages:

- **Stage 1:** Modeling the design problem
    a. Noise performance modeling
    b. Architectural constraint modeling
    c. Design variable setting
- **Stage 2:** Metamodeling the design problem
- **Stage 3:** Using the design metamodel as a black box model to evaluate the functions of the Multi-Objective Optimization Problem
- **Stage 4:** Generating the Pareto frontier using the Multi-Objective Optimization Problem
- **Stage 5:** Leading negotiations and tradeoffs based on the Pareto frontier representation in order to obtain a design compromise between architectural constraints and mechanical design performances

While presenting the modeling of the design problem, we introduced a method of aggregating noise performances into single real value criterion the RMS_BiW. The method we introduced, was efficient to reduce the dimensionality of the design problem and thus to deal with mechanical subsystem with multiple noise performances.

Then, we dealt with the problem of volume allocation in the preliminary design stage by introducing an architecture criterion that expresses the respect or the non-respect of the geometrical constraints. The originality of the method consisted in shifting the incorporation of the stage of the volume envelope allocation from the CAD environment (CATIA software) to CAE environment (ANSA software: pre-processing software of the FEM models).

We made possible to manage the architectural constraints and the noise performances within the same CAE environment. Now, it takes to the engineers to use the same FEM model for the assessment of the criteria.

One other interesting part of our methodology was the use of metamodels as fast tools for the assessment of the performance parameters. The kriging metamodel of our design problem enabled us to make a large exploration of the design space. The engineers and the architects were positively responsive to the technique because it was time effective.

Then, we presented our design problem in the formalism of a Multi-Objective Optimization problem. As it was formulated, our Multi-Objective Optimization problem did not yield to a unique solution because of the possible conflicting nature of the objectives (design performances). We presented then, when multiple competing objectives exist, that the optimum is no longer a design point but an entire set of non-dominated design points. The set of non-dominated design points is commonly referred to as the **Pareto frontier** [Pareto 1906].

To populate the Pareto frontier, we made the choice of the Normalized Normal Constraint method [Messac et al. 2003]. We gave a tiny improvement to this technique by introducing the use of global optimization technique in order to find the Anchor points (see Appendix C). Finding the good Anchor points is an important step to construct an accurate Pareto frontier with the Normalized Normal Constraint method.

We presented then how using the Pareto frontier representation made possible to initiate negotiation about design tradeoffs. After negotiations, a compromise design can be set as a best tradeoff between the conflicting design performances.

The negotiation is facilitated by the fact that each actor of the mechanical design (the architect or the engineer) figures out how much he/she is able to improve or worsen his/her performances in regards to the other performances. Using Pareto frontier, the negotiation is now based on quantitative metrics and no longer on qualitative a priori approximations. This work opens new perspectives in terms of more systematic tools for preliminary explorations of potential design concepts of subsystems.

We applied the methodology to a real case study consisting of a little compact vehicle. There were substantial shifts in quality of the NVH design of subsystems leading to the respect of design requirements. For instance, we achieved the structural solution that improves significantly the Vibration Transfer Function by lowering it over the frequency range of interest. The solution was with limited impact to the architecture constraints around the proposed structural component.

By the use of our methodology, conflicting situations with architects are well managed by finding trade-offs between architecture constraint and NVH design requirements.

One other benefit is that the process time allowed to choose between candidate subsystems, during the preliminary design stage, is reduced by 10 to 20% with a larger exploration of the design space. The negotiations between performance engineers and architects become to be fruitful and objectively carried out. For instance (see Figure 51), the time for the front subframe preliminary studies is reduced to 3 or 4 weeks compared with an initial process time of at least 5 weeks. The compromise trade-off of the front subframe configuration is largely optimized in shape and thickness with no architecture conflicts with other subsystems. The detailed design stage starts then on robust configuration basis.

The proposed methodology constitutes a new way to deal with the design of complex mechanical systems as automotive or airplanes for finding a compromise between architectural design constraints and mechanical performance.

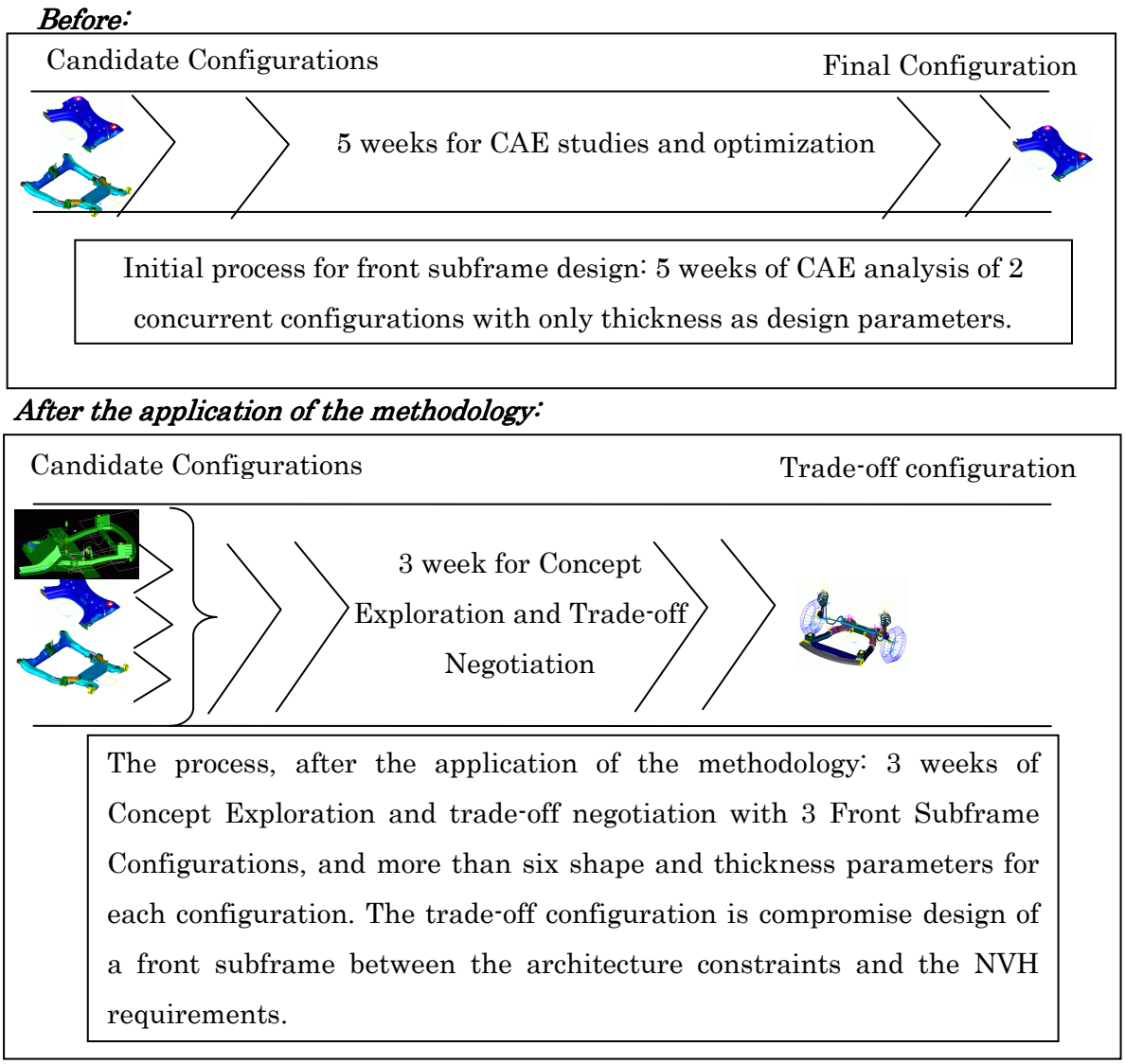

Figure 51. Benefits from the application of the proposed methodology in the case of front subframe design

- **Limits and future work**

A first experience of the application of the methodology to a real case study revealed that a great effort of preparation and explanation has to be done with engineers who are interested with. The cascade of techniques used within the methodology can somehow increase the natural fear of change for the engineers. The methodology is still progressing on the way of being largely accepted by engineers and integrated as a way of working in the preliminary design stage in an industrial context. Future work is to propose Design Rationale software that supports the user to achieve the different steps of the methodology and to keep his/her records and decisions during the whole process.

References

- **Bibliography**

ANSA, Ver 11.3. 5, User's Guide of v11.3.5. Beta CAE Systems SA.

Azarm, S., Reynolds, B. J. and Narayanan, S. (1999). *Comparison of Two Multiobjective Optimization Techniques with and within Genetic Algorithms*. DETC'99: ASME 1999 Design Engineering Technical Conference. Las Vegas, USA, DETC99/DAC-8584.

Barton, R. R. (1992). *Metamodels for Simulation Input-Output Relations*. Proceedings of the 1992 Winter Simulation Conference, edited by J. J. Swain, Goldsman, D., et al., eds. Arlington, VA, December 13-16.

Barton, R. R. (1994). *Metamodeling: A State of the Art Review*. Proceedings of the 1994 Winter Simulation Conference, edited by J. D. Tew, Manivannan, S., et al., eds. Lake Beuna Vista, FL, December 11-14, IEEE.

Barton, R. R., Limayem, F., Meckesheimer, M. and Yannou, B. (1999). *Using Metamodels for Modelling Propagation of Design Uncertainties*. 5th International Conference on Concurrent Engineering (ICE'99), edited by N. Wogum, Thoben, K.-D., et al., eds. The Hague, Netherlands, Centre for Concurrent Enterprising, March 15-17.

Bloebaum, C. L. (1992). *An Intelligent Decomposition Approach for Coupled Engineering Systems*. 4th AIAA/USA/NASA/OAI symposium on multidisciplinary analysis and optimization. Cleveland, OH, USA, September, AIAA-92-4821.

Bourgault, F., (2000). Modal Uncertainty and performance Analysis for Precesion Controlled Space Structures. MS Thesis. MIT. Department of Aeronautics and Astronautics.

Calvel, S., (2004). Conception d'organes automobiles par optimisation topologique. PhD Thesis. UNIVERSITE PAUL SABATIER - TOULOUSE III. Laboratoire MIP (Mathématiques pour l'Industrie et la Physique), Toulouse.

Chanron, V. and Lewis, K. (2005). A Study of Convergence in Decentralized Design Processes. Research in Engineering Design **16**: pp 133-145.

Chen, W., Allen, J. K., Mavris, D. N. and Mistree, F. (1996). A Concept Exploration Method for Determining Robust Top-Level Specifications. Engineering Optimization **26**: pp 137-158.

Chen, W. and Simpson, T. W. (2000). Comparative Studies of Metamodeling Techniques Under Multiple Modeling Criteria. AIAA-2000-4801.

Cundy, A. L., (2003). Use of Response Surface Metamodels in Damage Identification of Dynamic Structures. Ms. Virginia Polytechnic Institute and State University, Blacksburg, Virginia.

Das, I., (1997). Nonlinear Multicriteria Optimization and Robust Optimality. PhD thesis. Rice University. Department of Computational & Applied Mathematics, Houston, Texas.

Das, I. and Dennis, J. E. (1997). A Closer Look at Drawbacks of Minimizing Weighted Sums of Objectives for Pareto Set Generation in Multicriteria Optimization Problems. Structural Optimization **14**(1): pp 63-69.

Das, I. and Dennis, J. E. (1998). Normal-Boundary Intersection: A new Method for Generating the Pareto Surface in Nonlinear Multicriteria Optimization Problems. SIAM Journal on Optimization **8**(3): pp 631-657.

Davenport, A., Barbela, M. and Leedom, J. (1999). *An Integrated Approach to Random Analysis Using MSC/PATRAN with MSC/NASTRAN*. Proceedings of MSC Aerospace Users'Conference, April 15, The MacNeal Schwendler Corporation.

Dyn, N., Levin, D. and Rippa, S. (1986). Numirical Procedures for Surface Fitting of Scattered Data by Radial Functions. SIAM Journal of Scientefic and Statistical Computing **7**(2): pp 639-659.

Eddy, J. and Lewis, K. (2001). *Effective Generation of Pareto Sets Using Genetic Programming*. Proceedings of the 2001 ASME DETC,27th Design Automation Conference. Pittsburgh, Pennsylvania, USA, September 9-12.

Ellacott, S. W., Mason, J. C. and Anderson, I. J. (1997). Mathematics of Neural Networks: models algorithms, and applications, Kluver Academics Publishers, Boston, MA.

Engelund, W. C., Douglas, O. S., Lepsch, R. A., McMillian, M. M. and Unal, R. (1993). *Aerodynamic Configuration Design Using Response Surface Methodolgy Analysis*. Aircraft Design Sys. & Oper. Mngmnt., edited by AIAA. Monterey, CA, Paper 93-3967.

Ferguson, S. and Lewis, K. (2004). *Effective Development of Flexible Systems in Multidisciplinary Optimization*. 10th AIAA/USAF/NASA/ISSMO Symposium on Multidisciplinary Analysis and Optimization, AIAA-2004-4309.

Friedman, J. H. (1991). Multivariate Adaptive Regression Splines. The Annals of Statistics **19(1)**: pp 1-141.

Gawronski, K. W. (1998). Dynmaics and Control of Structures: A Modal Appoach, *Mechanical Engineering Series*, Springer-Verlag.

Giunta, A. A., Dudley, J.M., Narducci, R., Grossman, B., Haftka, R.T., Mason, W.H., Watson, L.T. (1994). *Noisy Aerodynamics Response and Smooth Approximation in HSCT Desing*. Proceedings Analysis and Optimization (Panama City, FL). Panama City, FL, AIAA, Washignton, DC.

Hamdi, A., Yannou, B. and Landel, E. (2004). *Design Target Cascading for Vibro-Acoustic Conceptual Design of An Automobile Subframe*. 8th International Design Conference DESIGN 2004, edited by D. Society. Dubrovnik, Croatia, May 18-21.

Hardy, R. L. (1971). Multiquadratic Equations of Topography and Other Irregular Surfaces. J. Geophys. Res. **76**: pp 1905-1915.

Ignizio, J. P. (1976). Goal Programming and Extensions, Lexington Books, Massachusetts, Toronto, London.

Inselberg, A. (1985). The plane with Parallel Coordinates. Special Issue on Computational Geometry, The Visual Computer **1**: pp 69-97.

Ismail-Yahaya, A. and Messac, A. (2002a). *Effective Generation of the Pareto Frontier using the Normal Constraint Method*. AIAA 40th Aerospace Sciences Meeting and Exhibit.

Ismail-Yahaya, A. and Messac, A. (2002b). *Effective Generation of the Pareto Frontier: the Normalized Normal Constraint Method*. 43rd AIAA/ASME/ASCE/AHS Structures, Structural Dynamics, and Materials Conference. Denver, CO, April.

Kalagnanam (1997). An Efficient Sampling techniques for Off-Line Quality Control. Technometrics **39**(3): pp 308-319.

Kim, H. M., (2001). Target Cascading in Optimal System Design. PhD thesis. University of Michigan.

Kleijnen, J. P. C. (1987). Statistical Tools for Simulation Practitioners, Marcel Dekker, New York.

Koch, P. N., Simpson, T. W., Allen, J. K. and Mistree, F. (1999). Statistical approximations for Multidisciplinary Design Optimization- The Problem of Size. Special Multidisciplinary Design Optimization Issue of Journal of Aircraft **36**(1): pp 275-286.

Koehler, J. R. and Owen, A. B. (1996). Computer Experiments, *Handbook of Statistics*, Elsevier Science, New York, pp. 261-308.

Koski, J. (1985). Defectivness of Weighting Methods in Multicriterion Optimization of Structures. Communications in Applied Numerical Methods **1**: pp 333-337.

Krishnamachari, R. S. and Papalambros, P. (1997). Hierarchical Decomposition Synthesis in Optimal Systems Design. Journal of Mechanical Design **119**(4): pp 448-457.

Kusiak, A. and Wang, J. (1993). Decomposition of the Design Process. Transactions of the ASME, Journal of Mechanical Design **115**(4): pp 687-695.

Lin, Y., Krishnapur, K., Allen, J. K. and Mistree, F. (1999). *Robust Design: Goal Formulations and A Comparison of Metamodeling Methods*. 1999 ASME Design Automation Conference. Las Vegas, NV, DETC99/DAC-8608.

Lin, Y., Krishnapur, K., Allen, J. K. and Mistree, F. (2000). *Robust Concept Exploration in Engineering Design: Metamodeling Techniques and Goal Formulations*. 2000 ASME Design Engineering Technical Conferences, edited by P. o. DETC'00. Baltimore, Maryland, USA, September 10-14, DETC2000/DAC-14283.

Mahmoud, H., Kabamba, P., Ulsoy, A. G. and Brusher, G. (2005). Target Management in Complex System Design Using System Norms. Journal of Mechanical Design **127**(4): pp 536-544.

Mahmoud, H., Kabamba, P. T., Ulsoy, A. G. and Brusher, G. (2003). *Ranking Subsystem Targets According to Their Influence on System Performance*. Proc American Control Conference. Denver, Colorado, USA, June.

Mattson, C. A. and Messac, A. (2002a). *Concept Selection in n-Dimension Using s-Pareto Frontiers and Visualization*. 9th AIAA/ISSMO Symposium on Multidisciplinary Analysis and Optimization. Atlanta, GA, USA, September 4-6.

Mattson, C. A. and Messac, A. (2002b). *Development of a Pareto-Based Concept Selection Method*. 43 rd AIAA/ASME/ASCE/AHS Structures, Structural Dynamics, and Materials Conference. Denver, CO, USA, April 22-25, AIAA 2002-1231.

Mattson, C. A., Mullur, A. A. and Messac, A. (2002). *Minimal Representation of Multiobjective Design Space Using a Smart Pareto filter*. 9 th AIAA/ISSMO Symposium on Multidisciplinary Analysis and Optimization. Atlanta, GA, USA, September 4-6, AIAA 2002-5458.

Mavris, D. N., Bandte, O. and Schrage, D. P. (1996). *Application of Probabilistic Methods for the Determination of an Economically Robust HSCT Configuration*. 6th AIAA/USAF/NASA/ISSMO Multidisciplinary Analysis and Optimization Conference. Bellevue, WA,, AIAA-96-4090.

McCormick, D. J. and Olds, J. R. (2002). *A Design of Experiments- Based Method for Point Selection in approximating Output Distributions*. 2002 AIAA/ISSMO

Symposium on Multidisciplinary Analysis and Design Optimization. Atlanta, GA, USA, September 4-6, AIAA 2002-5535.

Mckay, M. D., Beckman, R. J. and Conover, W. J. (1979). A comparison of three methods for selecting values of input variables in the analysis of the ouput from a computer code. Technometrics **21**(2): pp 239-245.

Meckesheimer, M., (2001). A Framework for Metamodel-Based Design: Subsystem Metamodel Assessment and Implementation Issues. PhD Thesis. The Pennsylvania State University. The Graduate School Harold and Inge Marcus Department of Industrial and Manufacturing Engineering.

Meckesheimer, M., Barton, R. R., Simpson, T. W., Limayem, F. and Yannou, B. (2001). Metamodeling of Combined Discrete/Continuous Responses. to be published in the AIAA.

Meirovitch, L. (1986). Elements of Vibration Analysis. 2nd edition, McGraw-Hill.

Messac, A., Gupta, S. and Akbulut, B. (1996). Linear Physical Programming: A New Approach to Multiple Objective Optimization. Transactions on Operational Research **8**: pp 39-59.

Messac, A. and Ismail-Yahaya, A. (2001). Required Relationship between Objective Function and Pareto Frontier Orders: Practical Implications. AIAA Journal **39**(11): pp 2168-2174.

Messac, A., Ismail-Yahaya, A. and Mattson, C. A. (2003). The Normalized Normal Constraint Method for Generating the Pareto Frontier. Structural and Multidisciplinary Optimization, Journal of the International Society of Structural and Multidisciplinary Optimization (ISSMO) **25**(2): pp 86-98.

Messac, A. and Mattson, C. A. (2004). *Normal Constraint Method with Guarantee of Even Representation of Complete Pareto Frontier*. 45th AIAA/ASME/ASCE/AHS/ASC Structures, Structural Dynamics and Materials Conference. Palm Springs, California, April 19-22, AIAA-2004-1679.

Messac, A. and Sundararaj, J. G. (2000). *Physical Programming's Ability to Generate a Well-Distributed Set of Pareto Points*. 41st AIAA/ASME/ASCE/AHS/ASC Structures, Structural Dynamics and Materials Conference, Paper No. AIAA 2000-1666.

Michelena, N., Kim, H. M. and Papalambros, P. (1999). *A System Partitioning and Optimization Approach to Target Cascading*. Proceedings of the 12th International Conference on Engineering Design ICED 99. Munich, Germany, August 24-26.

Michelena, N., Park, H. and Papalambros, P. (2002). *Convergence Properties of Analytical Target Cascading*. 9th AIAA/ISSMO Symposium on Multidisciplinary Analysis and Optimization. Atlanta, Georgia, 4-6 September.

Misra, H., Komzsik, L. and Johnson, E. (1999). *NVH Optimization on NEC Supercomputers Using MSC/NASTRAN*. 1999 MSC Worldwide Automotive Conference. Munich, September 20-22.

Mitchell, T. J. and Morris, M. D. (1992). *The Spatial Correlation Function Approach to Response Surface Estimation*. 1992 Winter Simulation Conference. Arlington, VA.

Montgomery, D. C. (2001). Design and Analysis of Experiments, Fifth Edition, John Wiley & Sons, New York.

Myers, R. H. and Montgomery, D. C. (1995). Response Surface Methodology: Process and Product Optimzation Using Designed Experiments, J. Wiley & Sons, New York.

Owen, A. B. (1992). Orthogonal Arrays for Computer Experiments, Integration and Visualization. Statistica Sinica **2**: pp 439-452.

Pareto, V. (1906). Manuale di Econòmica Polìttica, Società Editrice Libràia, Milan, Italy; translated into English by A. S. Schwier, as Manual of Political Economy, Macmillan, New York, 1971.

Powell, M. J. D. (1987). Radial Basis Functions for Multivariable Interpolation: a Review, *Algorithms for Approximation*, Oxford University Press, London.

Renaud, J. E. and Gabriele, G. A. (1991). *Sequential Global Approximation in Non-Hierarchic System Decomposition and Optimization*. Advances in Design Automation - Design Automation and Design Optimization, edited by G. Gabriele, ed. Miami, FL.

Rideout, D. G., Stein, J. L. and Ferris, J. B. (2001). *Target Cascading: a Design Process for Achieving Vehicle Ride and Handling Targets*. Proceedings of IMECE 2001 Symposium on Advanced Automotive Technologies. New York, USA, November 11-16.

Ross, T. J. (1995). Fuzzy Logic with Engineering Apllications, McGraw-Hill, New York.

Sacks, J., Welch, W. J., Mitchell, T. J. and Wynn, H. P. (1989). Design and Analysis of Computer Experiments. Statistical Science **24**(4): pp 453-473.

Sasena, M. J., (1998). Optimization of Computer Simulations via Smoothing Splines and Kriging Metamodels. Master Thesis. University of Michigan. Mechanical Engineering.

Schimerling, P., Sisson, J. C. and Zaïdi, A. (1998). Pratique des Plans d'Expériences, Technique & Documentation, Paris.

Scott, M. J., (1999). Formalizing Negotiation in Engineering Design. PhD Thesis. California Institute of Technology, Pasadena, California, USA.

Simpson, T. W., Mauery, T. M., Korte, J. J. and Mistree, F. (1998). *Comparison of Response Surface and Kriging Models for Multidisciplinary Design Optimization*. 7th Symposium on Multidisciplinary Analysis and Optimization. St. Louis, MO, September 2-4, AIAA-98-4755.

Simpson, T. W., Mauery, T. M., Korte, J. J. and Mistree, F. (2001a). Kriging Metamodels for Global Approximation in Simulation-Based Multidisciplinary Design Optimization. AIAA Journal **39**(12): pp 2233-2241.

Simpson, T. W., Peplinski, J., Koch, P. N. and Allen, J. K. (1997). *On the Use of Statistics in Design and the Implications for Deterministic Computer Experiments*. DETC '97 - Design Theory and Methodology. Sacramento, CA, DETC97/DTM-3881.

Simpson, T. W., Peplinski, J. D., P.N., K. and Allen, J. K. (2001b). Metamodels for Computer-based Engineering Design: Survey and recommendations. Engineering with Computers **17**: pp 129-150.

Stander, N., Roux, W., Giger, M., Redhe, M., Fedorova, N. and Haarhoff, J. (2003). *Crashworthiness Optimization in LS-OPT – Case Studies in Metamodeling and Random Search Techniques*. 4th European LS-DYNA Users Conference. ULM, Germany, May 22-23.

Steuer, R. (1986). Mutiple Criteria Optimization: Theory, Computation, and Applications, John Wiley & Sons, New York.

Suh, N. P. (1990). The Principle of Design, *Oxford Series on Advanced Manufacturing*, Oxford Unversity Press, New York.

Trocine, L. and Malone, L. C. (2000). *Finding Important independent Variables through Screening Designs: a Comparison of Methods*. Proceedings of the 2000 Winter Simulation Conference . edited by J. A. Joines, R. R. Barton, K. Kang and P. A. Fishwick. Orlando, Florida, USA, Society for Computer Simulation International.

Trocine, L. and Malone, L. C. (2001). *An Overview of Newer, Advanced Screening Methods for The initial Hase in an Experimental Design*. Proceedings of the 2001 Winter Simulation Conference, edited by B. A. Peters, J. S. Smith, D. J. Medeiros and M. W. Rohrer. Arlington, Virginia, USA.

Tu, C. H. and Barton, R. R. (1997). *Production Yield Estimation by the Metamodel Method with a boundary-focused Expirement Design*. Design Theory and Methodology Conference, DETC97/DTM3870.

Unal, R., Lepsch, R. A., Engelund, W. and Stanley, D. O. (1996). *Aproximation Model Building and Multidisciplinary Design Optimization Using Response Surface Methods*. 6th AIAA/USAF/NASA/ISSMO Symposium on Multidisciplinary Analysis and Optimization, edited by AIAA. Bellevue, WA.

Venter, G., Haftka, R. T. and Starnes, J. H. J. (1998). Construction of Response Surface Approximation for Design Optimization. AIAA Journal **36**(12): pp 2242-249.

Wagner, T. C., (1993). A General Decomposition Methodology For Optimal System Design. PhD Thesis. University of Mechigan.

Wamsler, M. and Rose, T. (1998). *Improved Identification of Contributing Modes in Superelement Modal Frequency Response Analysis, V70*. 1998 MSC Americas User's Conference. Universal City, CA, USA.

Wang, X., Liu, Y. and Antonnson, E. K. (1999). *Fitting Functuions to Data in High Dimentional Design Sapces*. Advances in Design Automation. Las Vegas, NV, September 12-15, DETC'99/DAC-8622.

Wegman, E. J. (1990). Hyperdimensional Data Analysis Using Parallel Coordinates. Journal of the American Statistical Association **85**(411): pp 664-675.

Wilson, B., Cappelleri, D. J., Simpson, T. W. and Frecker, M. I. (2000). *Efficient Pareto Frontier Exploration Using Surrogate Approximations*. 8th AIAA/USAF/NASA/ISSMO Symposium on Multidisciplinary Analysis and Optimization. Long Beach, CA, September 6-8, AIAA-2000-4895.

Wolf, W. L. (1997). *Applications in Automotive NVH Analysis and Optimization*. Proceedings of the 3rd International Conference on High Performance Computing in the Automotive Industry, edited by M. Sheh.

Yannou, B., Hamdi, A. and Landel, E. (2004). *A Framework for an Enhanced Mechanical Concept Exploration: Application to the vibro-acoustic behavior of a car subframe*. 14th International CIRP Design Seminar. Cairo, Egypt, May 16 - 18.

Yannou, B., Moreno, F., Thevenot, H. J. and Simpson, T. W. (2005). *Faster Generation of Feasible Design Points*. Proceedings of DETC'05 ASME 2005 International Design Engineering Technical Conferences & Computers and Information in Engineering Conference. Long Beach, California USA, September 24-28.

Zimmer, H. (2000). *Use of SFE CONCEPT in Developing FEA Models without CAD*. International Body Engineering Conference Detroit. Michigan, USA, October 3-5, SAE technical paper 2000-01-2706.

- **The author papers and contributions**

Hamdi A., Modèles conceptuels d'évaluation de performance acoustique dans la phase de préconception de liaison au sol des véhicules Renault, Mémoire de DEA, Ecole Centrale Paris, 2001.

Hamdi A., Yannou B., Landel E., Stratégie de construction de modèles conceptuels pour l'évaluation des performances mécaniques en préconception - Application à la conception vibro-acoustique d'un berceau automobile, *Proc. 16ème Congrès français de Mécanique*, Nice, France, 1-5 septembre 2003, 2003.

Hamdi A., Yannou B., Design Target Cascading for vibro-acoustical conceptual design of an automobile subframe, *Proc. International Design Conference*, Dubrovnik, Croatia, May 18-20, 2004.

Hamdi A., Yannou B., Landel E., Exploration in the preliminary mechanical design of trade-offs between automotive architecture constraints and aggregate noise performances, *Proc. IDETC/DAC: ASME International Design Engineering Technical Conferences & Computers and Information in Engineering Conferences / Design Automation Conference*, Philadelphia, PA, USA, Sept. 10-13, 2006.

Yannou B., Hamdi A., Landel E., Une stratégie de modélisation conceptuelle pour la prise en compte de performances vibro-acoustiques en préconception d'un berceau automobile, *Mécanique et Industries* vol. 4, 2003, p. 365-376.

Yannou B., Hamdi A., Truss dimensioning with an uncertainty reduction paradigm, *Proc. International Design Conference*, Dubrovnik, Croatia, May 18-20, 2004a.

Yannou B., Hamdi A., Landel E., A framework for an enhanced mechanical concept exploration - Application to the vibro-acoustic behavior of a car subframe, *Proc. International CIRP Design Seminar*, Cairo, Egypt, May 16-18, 2004, 2004b.

Yannou B., Hamdi A., Landel E., A Four-Stage Approximation Strategy for the Exploration of a Mechanical Concept, in *Advances in Design*, ElMaraghy H., ElMaraghy W. Editors, Springer, 2005, p. chapter 16.

Appendix A

Structural Dynamics Modeling and Performance aggregation

A.1 Introduction

Dans cette annexe, il s'agit d'aborder la question de l'agrégation des performances vibratoires d'une structure dynamique.

Les performances vibratoires qu'on traite sont des fonctions fréquentielles de transfert vibratoire. On rappelle qu'une fonction de transfert vibratoire est, tout simplement, les vibrations (en déplacements, en vitesses ou en accélérations) d'un nœud de la structure appelé noeud réponse suite à une excitation impulsionnelle par une force dynamique unitaire à un nœud d'excitation. La fonction de transfert vibratoire est exprimée dans le domaine fréquentiel. Sa représentation la plus usuelle est celle par deux courbes : une première exprimant l'amplitude en fonction de la fréquence et une deuxième exprimant sa phase en fonction de la fréquence. Durant l'annexe on fera usage que du premier type de courbe (Fréquence, Amplitude).

Durant notre thèse, afin de réduire la dimension du problème de conception, on eu a besoin de ramener les performances vibratoires d'une structure, qui consistaient à plusieurs fonctions de transferts, où chacune d'elle est exprimée en fonction de la fréquence, à une seule valeur réelle servant de critère (i.e indicateur) de performance vibratoire. Pour le faire, on a identifié deux niveaux d'agrégation possibles. Le premier niveau d'agrégation consiste à ramener les valeurs de l'amplitude de la fonction de transfert qui est dépendante de la fréquence à une seule valeur réelle par une simple intégration de ses valeurs quadratiques sur le domaine fréquentiel d'intérêt. Le deuxième niveau d'agrégation consiste à sommer quadratiquement l'ensemble des

fonctions de transfert vibratoire de toutes les réponses et toutes les excitations qu'on devait contrôler sur la structure. Ainsi on se ramène de nouveau à une seule valeur réelle faisant office de critère de performance vibratoire pour l'ensemble de la structure. On appelle ce critère agrégé, comme étant le critère RMS.

Le Lecteur qui se souci de trouver l'équivalence à la notion du critère **RMS_BiW** qui est exprimé dans le corps de thèse, trouvera sa réponse au niveau de la définition du critère RMS_CDC dans cette annexe.

D'autres notions sont présentées comme par exemple le critère de RMS cumulé et le facteur de participation d'un mode. Ces notions sont présentées qu'à titre extensif du sujet.

A.2 Critères de performance vibratoire d'une structure dynamique

On commence par donner la définition des critères vibratoires RMS et RMS cumulée au niveau d'un système SISO (Single Input Single Output). On prend comme exemple d'application à un simple système SISO de 3ddl. Puis, on donne la définition du critère pour un système MIMO (Multi Input Multi Output). Ce dernier est le plus proche d'une application à une large structure tel que l'automobile (Caisse ; trains ;…). On fait, alors, une application du système MIMO à un système de structure en 2D d'un treuil. On montre, à travers les calculs du critère, qu'on a la possibilité de détecter les modes qui dépassent les cahier de charge et qui sont en forte surtension. Ces modes sont les plus contributeur dans l'évolution de la courbe de RMS cumulative. L'application du critère RMS à chaque courbe de transfert et le tri suivant un ordre croissant permettent de détecter les voies de passage les plus contributrices en terme de niveaux vibratoires.

A.3 Modèles SISO(Single Input Single Output)

A.3.1 La norme H_2

Soit $H(f)=\frac{u(f)}{F(f)}$, la fonction de transfert du système **A** constitué d'une structure dynamique (où f est la fréquence en [Hz]). $F(f)$ est un signal d'entrée au système. $u(f)$ est le signal de sortie. La structure composant le système **A** est supposée ***flexible***, à ***faible amortissement*** et présente ***des modes distincts*** (en fréquences).

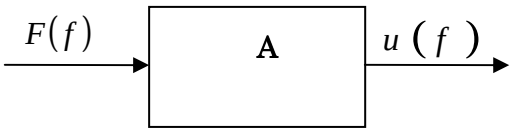

Figure 52 Schéma d'un système SISO

la norme H_2 du système **A** [Gawronski 1998] est définie comme suit :

$$\|H(f)\|_2 = \sqrt{\int_{-\infty}^{+\infty} H^*(f)H(f)df} \tag{A.1}$$

$$= \sqrt{2\int_{0}^{+\infty} H^*(f)H(f)df} = \sqrt{2\int_{0}^{+\infty} |H(f)|^2 df} \tag{A.2}$$

A.3.2 Le critère RMS

Le critère RMS (Root-Mean-Square) de la fonction de transfert du système **A** est une adaptation de la norme H_2 à une plage fréquentielle [$f_{\min}$, f_{max}] Hz.

$$RMS(A) = \sqrt{\int_{f_{\min}}^{f_{\max}} H^*(f)H(f)df} = \sqrt{\int_{f_{\min}}^{f_{\max}} |H(f)|^2 df} \tag{A.3}$$

La valeur RMS est une évaluation de la performance du comportement dynamique du système **A** dans la plage [f_{min}, f_{max}] Hz. Une interprétation de la valeur RMS est la racine carrée de l'aire au carré sous la courbe de l'amplitude de la fonction de transfert.

- **Exemple :**

On prend dans la suite l'exemple d'une structure simple à 3ddl (voir Figure 53). Les masses sont m_1=11 kg, m_2=5 kg et m_3=10 kg et les valeurs des éléments de raideur sont k_1=10 N/m, k_2=50 N/m, k_3=55 N/m et k_4=10 N/m. Les coefficients d'amortissement sont proportionnels aux éléments de raideurs : d_i=0.01*k_i .

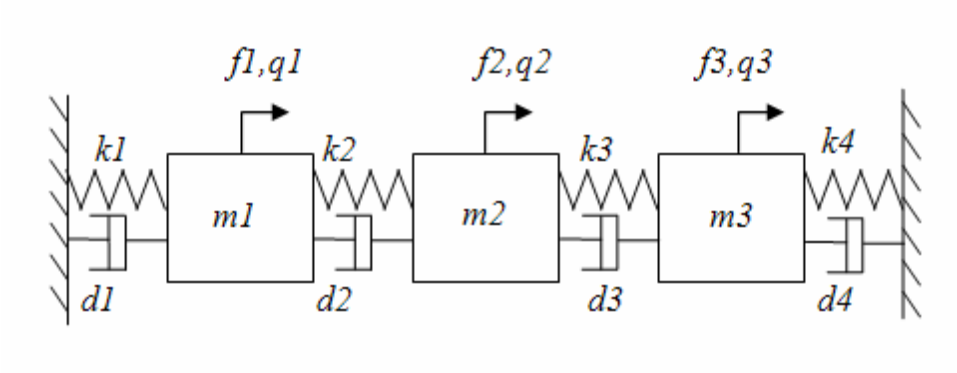

Figure 53 Système simple à 3 ddl

L'ensemble de la structure constitue un système SISO. L'unique signal d'entrée au système est un signal unitaire arbitraire $F(f)$ qui gouverne simultanément et linéairement les trois excitations (f_1, f_2 et f_3) au niveau de la structure tel que $f_1 = F(f)$, $f_2 = 2F(f)$ et $f_3 = -5F(f)$. Et l'unique sortie est : $u(f)$ qui est une composition -linéaire- des déplacements des 3 ddls (q_1, q_2 et q_3) de la structure tel que $u(f) = 2q_1 - 2q_2 + 3q_3$.

La Figure 54 illustre la fonction de transfert $H(f) = \frac{u(f)}{F(f)}$ du système SISO.

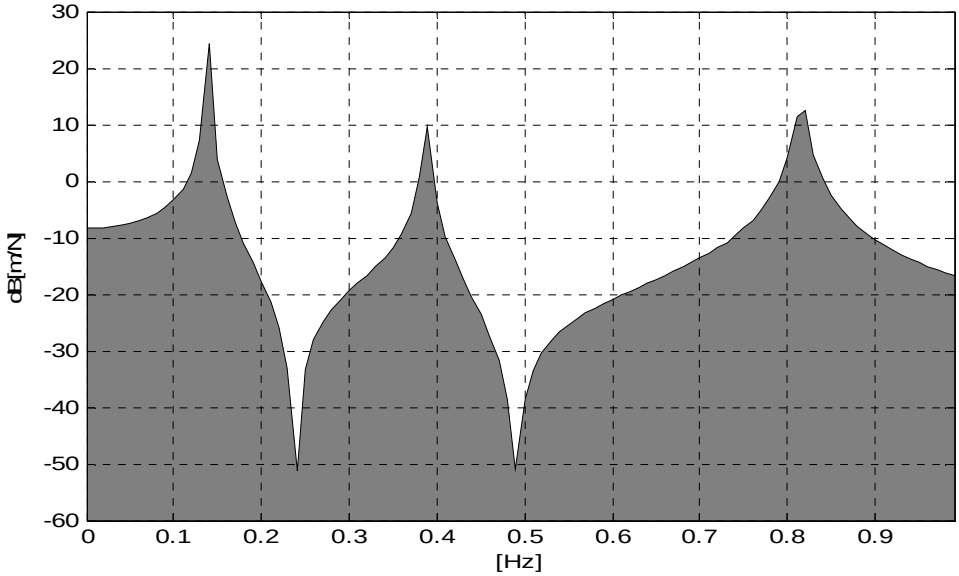

Figure 54 La fonction de transfert du système SISO

La valeur RMS du système SISO pour la plage fréquentielle [0, 0.99] Hz est : RMS=1.8277 [N/m rms]

A.3.3 La courbe de RMS cumulée

La RMS cumulée, qu'on note *RMScum*(*f*), est une fonction cumulative par rapport aux fréquences des valeurs du critère RMS. On formule la RMS cumulée comme suit :

$$RMScum(f) = \sqrt{\int_{f_{\min}}^{f} |H(f)|^2 df} \tag{A.4}$$

L'évolution de la courbe de RMS cumulée permet de voir l'importance de la contribution d'un mode à la valeur du critère RMS [Davenport et al. 1999].

- **Exemple :**

La Figure 55 illustre la courbe RMS cumulée pour le cas en cours du système SISO.

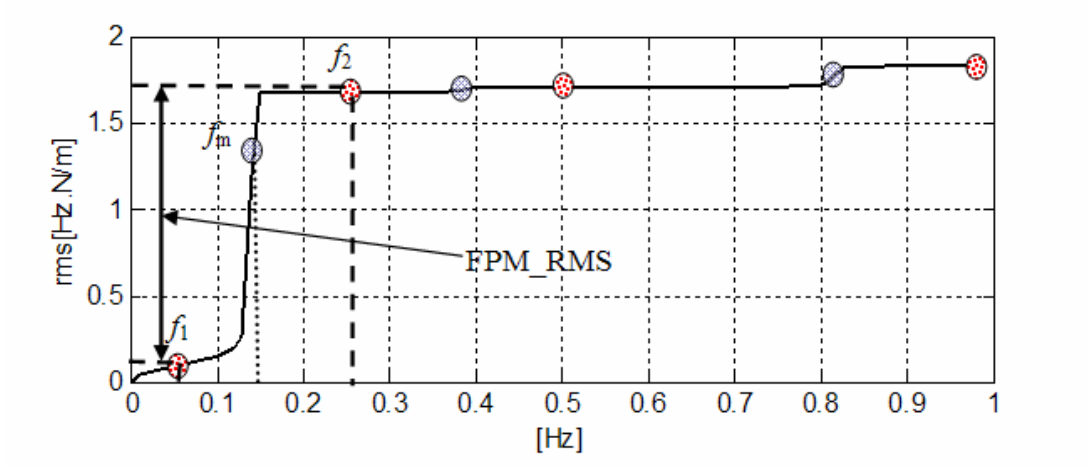

Figure 55 Courbe de RMS cumulée du système SISO

On remarque déjà sur cette courbe que le premier mode (à 0.14 Hz) de la structure est fortement contributeur dans l'évolution de la valeur de RMS cumulée, d'où une contribution assez importante au niveau de la valeur totale du critère RMS du système.

A.3.4 Facteur de participation modale (FPM_RMS)

Chaque mode, dans la plage fréquentielle en considération, contribue à la valeur totale du critère RMS. Pour savoir l'importance relative de chaque contribution dans l'évolution de la courbe de RMS cumulée et par rapport à la valeur totale du critère, on définit un facteur de participation modale qu'on note FPM_RMS.

L'étude de la fonction de RMS cumulée montre qu'il y a sur la courbe une succession de points d'inflexion, de convexe à concave et vis versa (voir Figure 55). La courbe est convexe avant le passage par un mode, puis elle devient concave.

Le *facteur de participation modale* est la contribution à la valeur du critère RMS sur la partie « convexe et concave » de la courbe au passage d'un mode.

Soit f_m fréquence du mode m, on cherche f_1 et f_2 tel que :

La dérivée seconde $RMScum''(f_{1,2}) = 0$ et la dérivé $RMScum'(f)$ devient croissante : c'est le passage par un point d'inflexion (voir Figure 55) où la courbe passe de concave à convexe, avec $f_1 < f_m < f_2$.

On peut alors exprimer le FPM_RMS comme suit :

$$FPM\_RMS(f_m) = RMScum(f_1) - RMScum(f_2) = \sqrt{\int_{f_{min}}^{f_2} |H(f)|^2 df} - \sqrt{\int_{f_{min}}^{f_1} |H(f)|^2 df} \quad \text{(A.5)}$$

Note : la définition qu'on donne au FPM_RMS est différente de la définition, dans la littérature, du MPF (Modal Participation Factor).

Pour montrer l'importance relative de la valeur du facteur de participation modale par rapport au critère, on le devise par la valeur totale du critère RMS et on exprime le résultat en pourcentage.

$$\%FPM\_RMS(f_m) = \frac{FPM\_RMS(f_m)}{RMS(A)} \times 100 \quad \text{(A.6)}$$

En comparant les %FPM_RMS, on s'intéresse aux modes qui ont le plus de contribution dans l'évolution de la courbe RMS cumulative [Bourgault 2000]. Les modes les plus contributeurs sont les modes qui mérite d'être vus plus en détail afin d'apporter des modifications sur la structure et de réduire les niveaux des réponses au niveau de ces modes. En appliquant ça, la valeur du critère RMS sera aussi réduite [Wamsler et Rose 1998].

- **Exemple :**

La Figure 56 illustre le %FPM_RMS pour un système à structure de 3ddl.

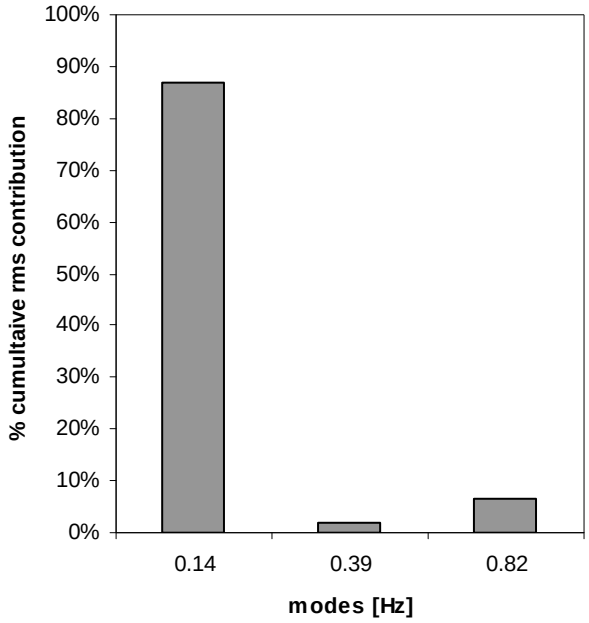

Figure 56 Facteur de participation modale %FPM_RMS

Le premier mode à 0.14Hz est le mode le plus contributeur dans l'évolution de la courbe de RMS cumulée. A lui seul, il participe presque à 90% dans la valeur totale du RMS. C'est souvent le cas des premiers modes d'une structure, car ils ont une dynamique forte. Les amplitudes des déplacements, au niveau des premiers modes, sont souvent assez importantes par rapport à celles des modes qui viennent après (de fréquences plus élevées).

A.3.5 Le critère RMS par rapport à une référence « CDC »

Pour limiter l'amplitude de la fonction de transfert à un certain niveau, on applique une « référence » sous forme d'un cahier des charges (CDC). La référence CDC est appliquée dans le domaine des amplitudes en dB. Grâce à la normalisation des niveaux par rapport à un niveau de référence, on peut contrôler au même temps (1) les amplitudes à fort niveau, là où la dynamique est forte et (2) les amplitudes de plus faibles niveaux mais qui peuvent être gênantes (voir Figure 57).

A l'aide du tracé de la référence CDC, on peut faire de l'allocation modale. Car avec la référence CDC, on peut pénaliser des zones fréquentielles là où on veut que la structure n'ait pas des modes et autoriser d'autres où on tolère la présence de modes.

Dans le cas des sous-systèmes dynamiques assemblés et qui présentent un couplage dynamique faible et une densité modale réduite, on peut optimiser (modifier), pour chaque sous-structure et au moyen de la référence CDC, les positions des modes et leur niveau afin d'avoir, au niveau de la structure totale des fonctions transfert peu amplifiées ou qui ne dépassent pas la référence CDC.

On note la courbe de la référence CDC : CDC(*f*), *f* fréquence en Hz.

On exprime le critère RMS_CDC comme suit :

$$RMS\_CDC(A) = \sqrt{\int_{f_{\min}}^{f_{\max}} \langle \frac{|H(f)|^2}{CDC(f)^2} \rangle df} \qquad \text{(A.7)}$$

avec $\langle \bullet \rangle$ désigne la fonction définie comme suit :

$$\begin{cases} \langle \frac{|H(f)|^2}{CDC(f)^2} \rangle = \frac{|H(f)|^2}{CDC(f)^2}, & \text{si} \quad 20Log10(|H(f)|) - 20Log10(CDC(f)) \geq 0 \\ = 0 & \text{si non} \end{cases} \qquad \text{(A.8)}$$

- **Exemple :**

La Figure 57 montre un cas d'application de la référence CDC sur la courbe de la fonction de transfert du système SISO.

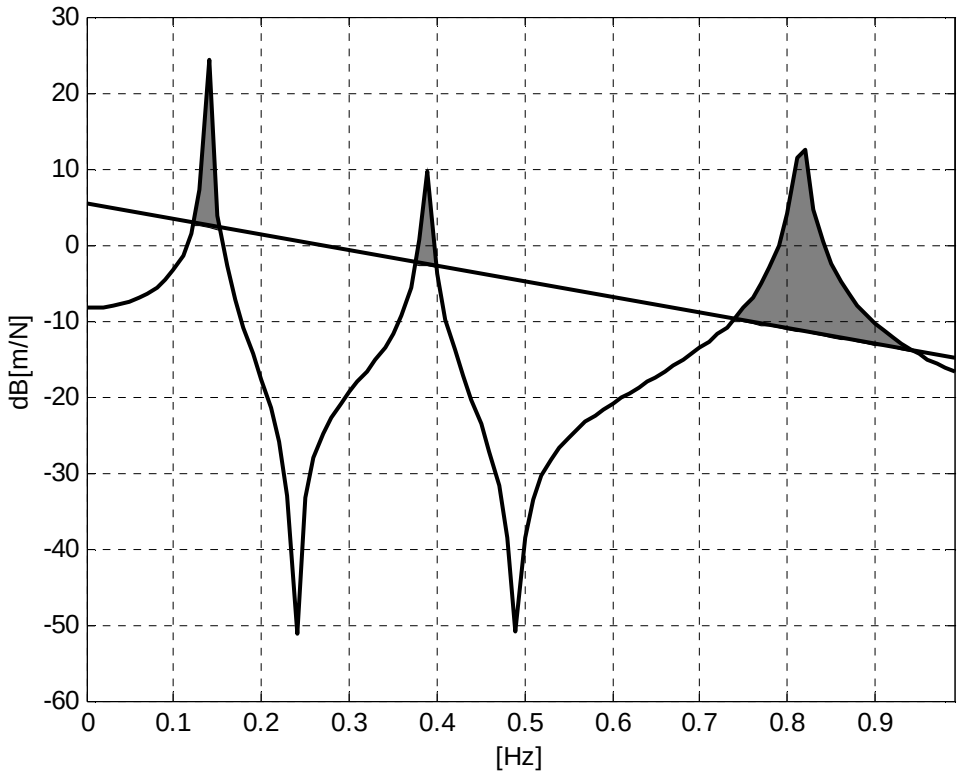

Figure 57 Référence CDC appliqué au système SISO

On trouve alors une valeur RMS_CDC(A) = 2.7969 rms.

A.3.6 La courbe de RMS cumulée : cas d'une référence « CDC »

La courbe de RMS cumulée en cas d'application d'une référence CDC, montre les contributions des dépassements par rapport au CDC à la valeur totale du RMS_CDC. L'expression de la fonction cumul devient dans ce cas comme suit :

$$RMScum\_CDC(f) = \sqrt{\int_{f_{\min}}^{f} \langle \frac{|H(f)|^2}{CDC(f)^2} \rangle df} \qquad (A.9)$$

- **Exemple :**

La Figure 58 illustre la courbe de RMS cumulée en cas d'application d'une référence CDC.

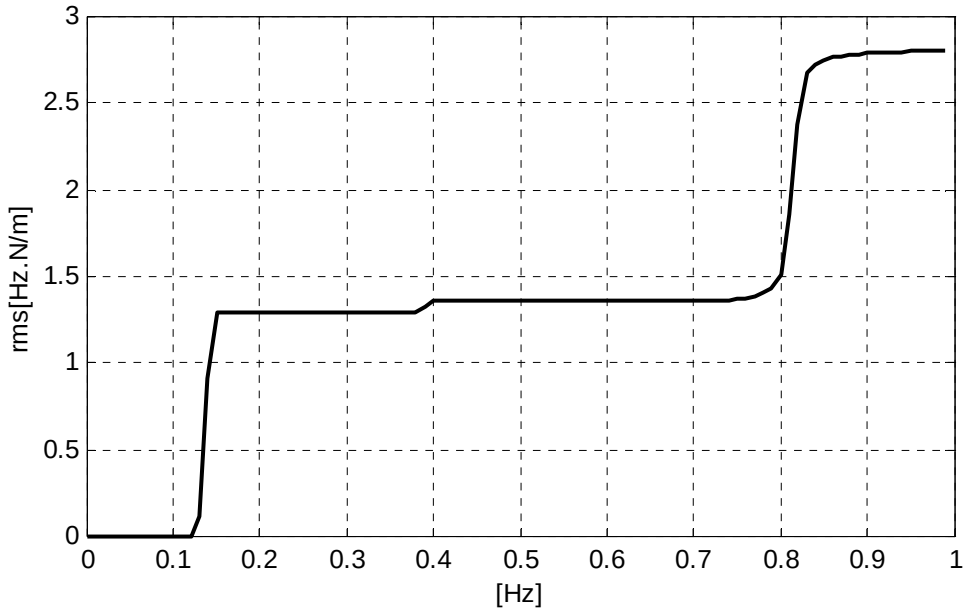

Figure 58 Courbe de RMS cumulée du système SISO : cas d'un filtre CDC

L'évolution de la courbe montre que les contributions des modes à la valeur totale du critère ne sont plus pareilles avec ou sans la référence. Sur cette courbe on voit que le troisième mode devient aussi contributeur que le premier mode, bien qu'il y ait approximativement une différence de 10 dB[m/N] entre leurs niveaux. L'effet de la forte dynamique du premier mode est gommé par l'application du filtre CDC. Le facteur de participation modale relatif à la RMS_CDC, illustré par la Figure 59, conforte ces constatations.

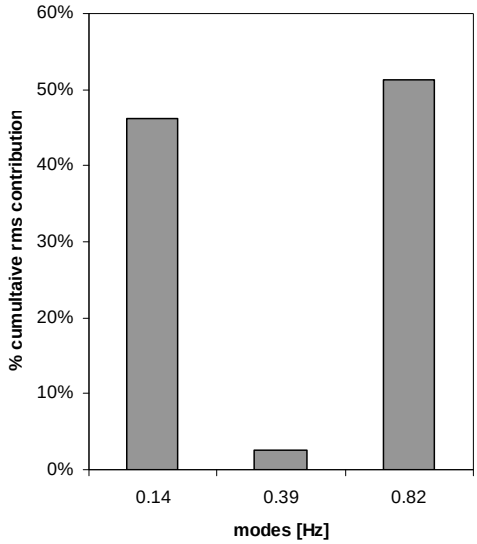

Figure 59 Facteur de participation modale %FPM_RMS_CDC

Dans la suite, on applique deux références CDC sur le même exemple en étude.

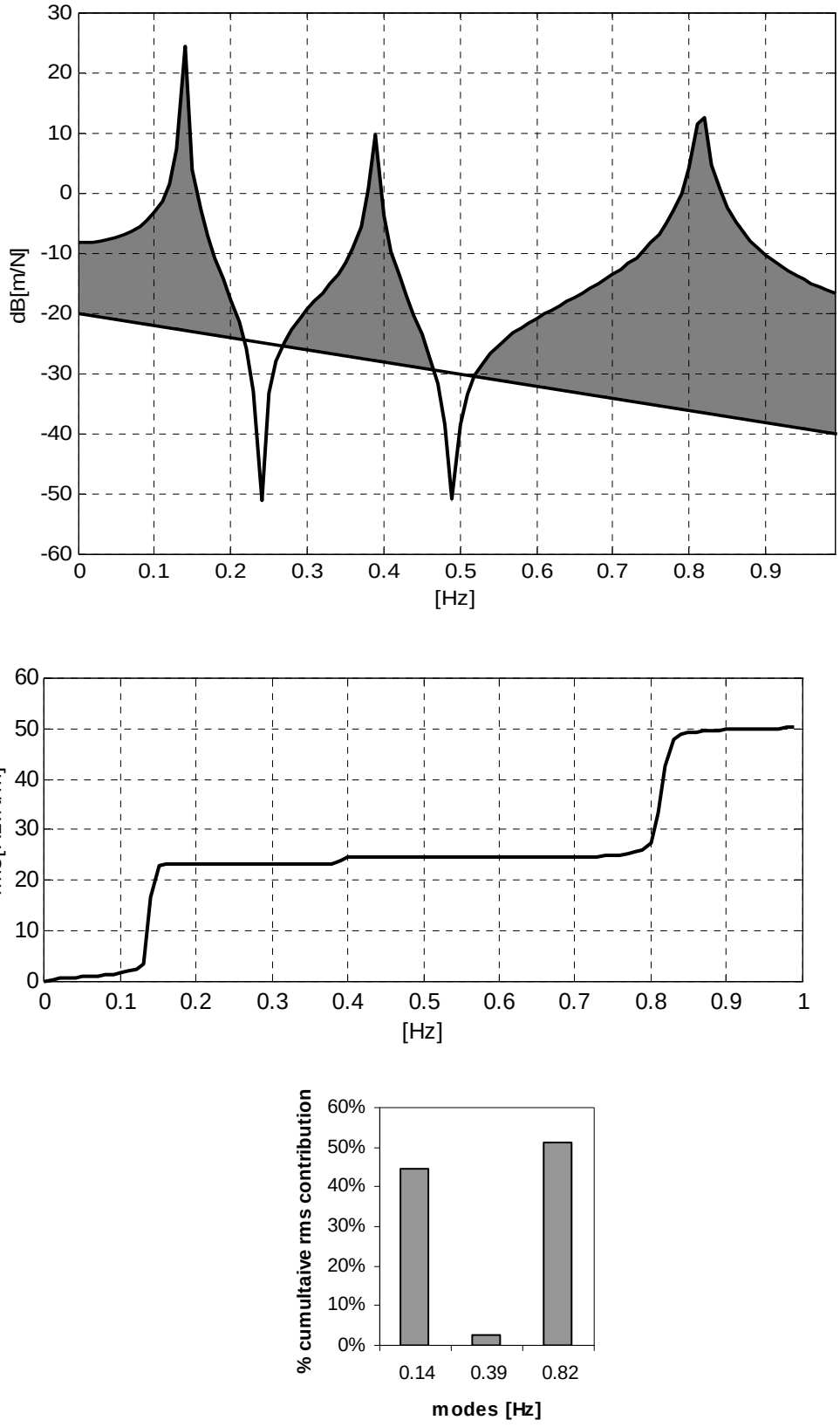

Figure 60 cas d'une référence CDC Pénalisante, RMS_CDC=50.123 rms

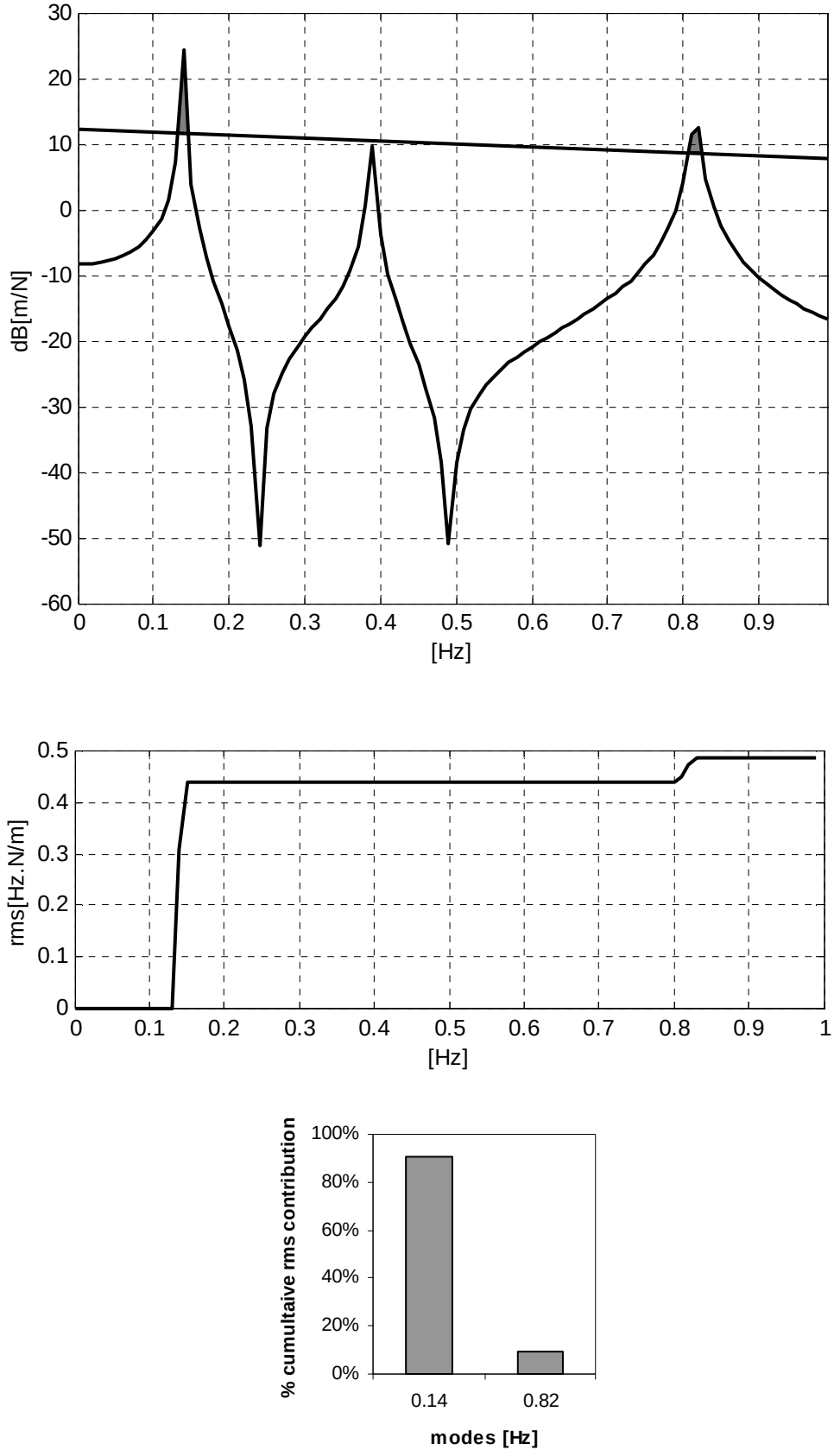

Figure 61 cas d'une référence CDC non Pénalisante, RMS_CDC=0.4844 rms

En essayant de varier les niveaux du filtre CDC (voir Figure 60 et Figure 61), on peut remarquer que plus on "sévérise" le CDC plus la valeur du RMS_CDC devient plus importante et on peut remarquer aussi qu'un mode de structure qui a son amplitude au dessous de la référence CDC ne contribue plus à la valeur totale du RMS_CDC.

A.4 Modèles MIMO (Multi Input Multi Output)

Soit $H_{ij}(f)=\frac{u_i(f)}{F_j(f)}$ la fonction de transfert entre l'entrée *j* et la sortie *i* pour un système MIMO (multi entrées multi sorties) représenté par le système **B** (voir Figure 62). *M* est le nombre total des entrées et *N* est le nombre total des sorties. Pour ce système il y a $M \times N$ fonctions de transferts avec $i=1,\ldots,N$ et $j=1,\ldots,M$.

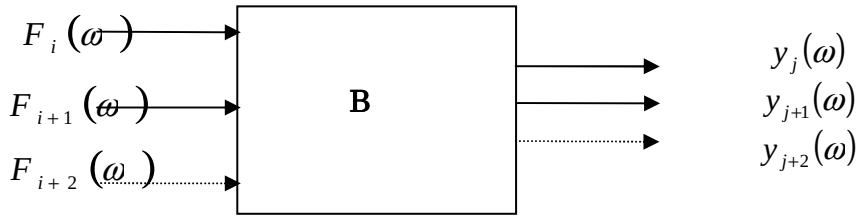

Figure 62 Schéma d'un système MIMO

La structure composant le système **B** est supposée flexible, à faible amortissement et présente des modes distincts (en fréquences).

A.4.1 Le critère RMS_{ij}

Le critère RMS_{ij} d'une fonction de transfert H_{ij} du système **B** sur une plage fréquentielle $[f_{min}, f_{max}]$ Hz est défini comme suit :

$$RMS_{ij}(B)=\sqrt{\int_{f_{min}}^{f_{max}} H_{ij}^{*}(f)H_{ij}(f)df}=\sqrt{\int_{f_{min}}^{f_{max}} \left|H_{ij}(f)\right|^2 df} \qquad \text{(A.10)}$$

Les propriétés qui s'ensuivent à cette définition du critère RMS_{ij} tel que ça était fait pour le système SISO (la courbe de RMS_{ij} cumulée, le facteur de participation modale et l'application de filtre CDC) s'appliquent de la même façon.

- **Exemple :**

On prend pour exemple un treuil plan (2D) (voir Figure 63) avec h = 150 mm et l = 200 mm. Il est constitué d'un assemblage de poutre en rond de mêmes caractéristiques.

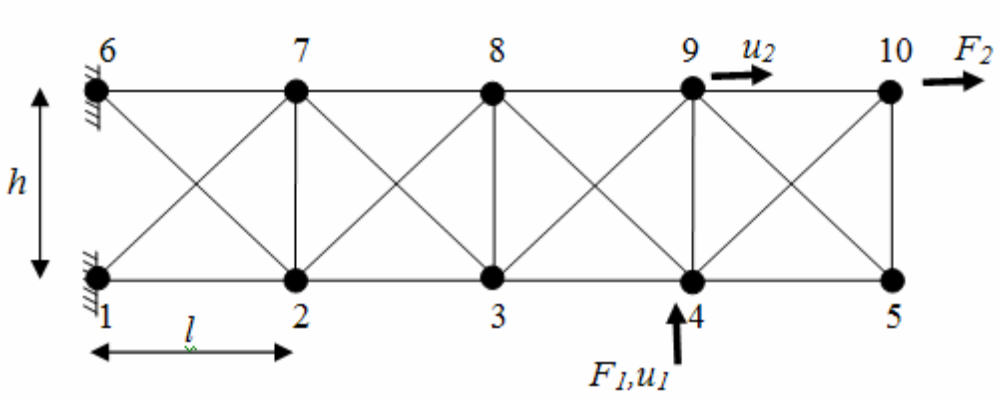

Figure 63 Système de treuil en 2D

Chaque élément possède une masse volumique de 7.8 10^{E-6} Kg/mm^3, un module d'élasticité de 2. 10^{E8} mN/mm² et une section d'une aire de 100 mm². En tout, la structure a 16 ddl (16 modes). On applique deux entrées :

- verticalement au nœud 4, $F_1(f)$ multipliée par un facteur de 90
- et horizontalement au nœuds 10, $F_2(f)$ excitation unitaire

Le système à deux sorties :

- verticalement au nœud 4, $u_1(f)$
- et horizontalement au nœuds 9, $u_2(f)$

On a en tout, quatre fonctions de transfert : $H_{11}(f)=\frac{u_1(f)}{F_1(f)}$, $H_{12}(f)=\frac{u_1(f)}{F_2(f)}$, $H_{21}(f)=\frac{u_1(f)}{F_1(f)}$ et $H_{22}(f)=\frac{u_2(f)}{F_2(f)}$

On applique un CDC en courbe linéaire (de -120 dB [m/N] à 0 Hz jusqu'à -130 dB [m/N] à 10000 Hz)

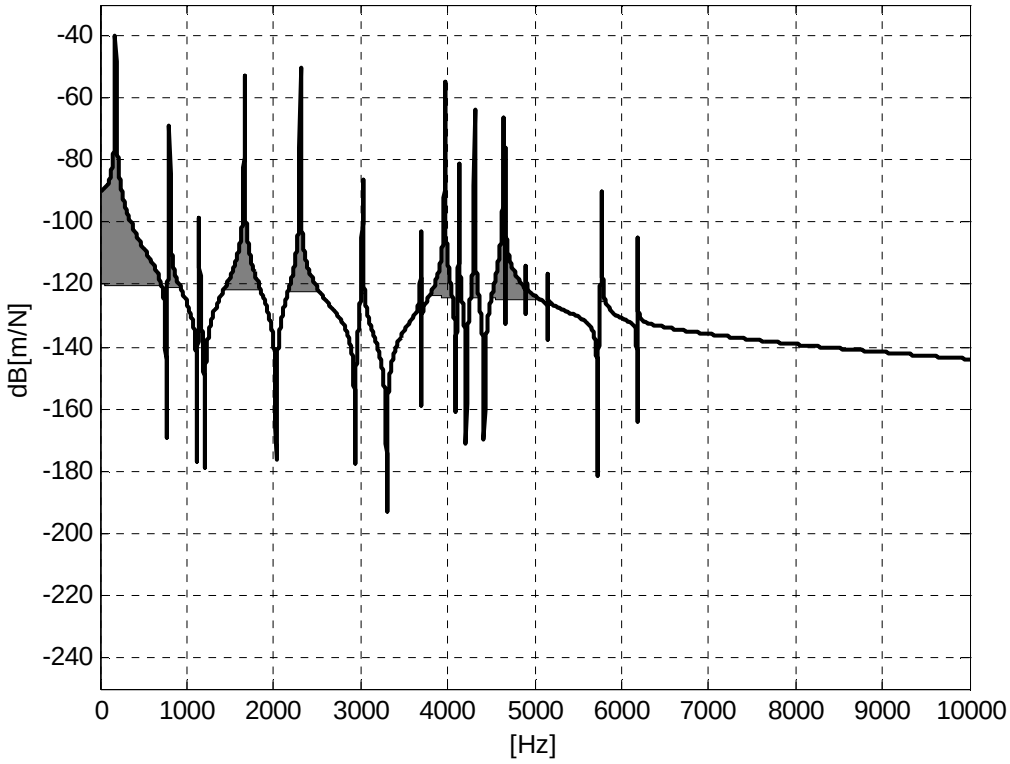

Figure 64 Treuil 2D, courbe H_{11} (f), RMS_CDC$_{11}$ = 12890. rms

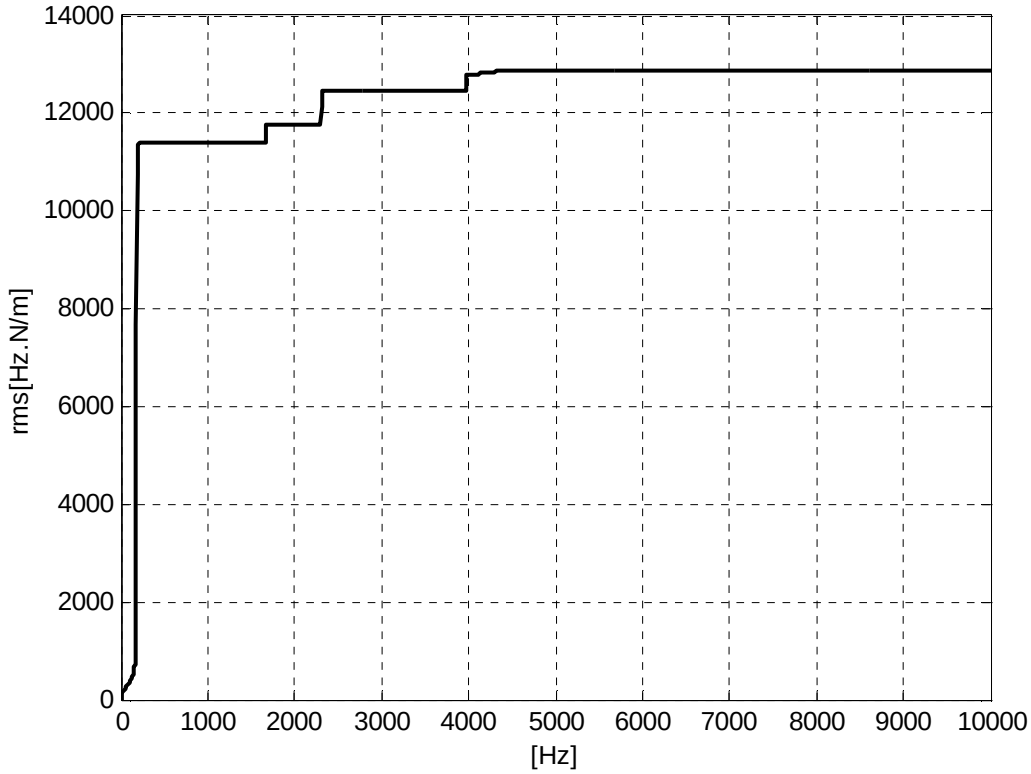

Figure 65 Treuil 2D, courbe *RMScum_CDC$_{11}$*

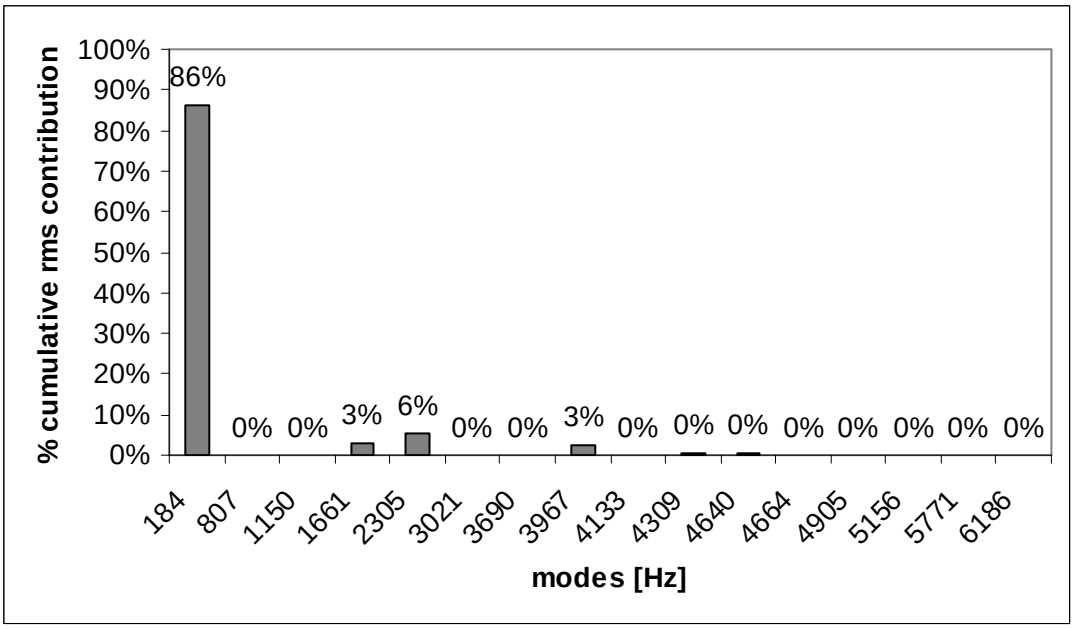

Figure 66 Treuil 2D, Facteur de participation modale %FPM_RMS_CDC$_{11}$

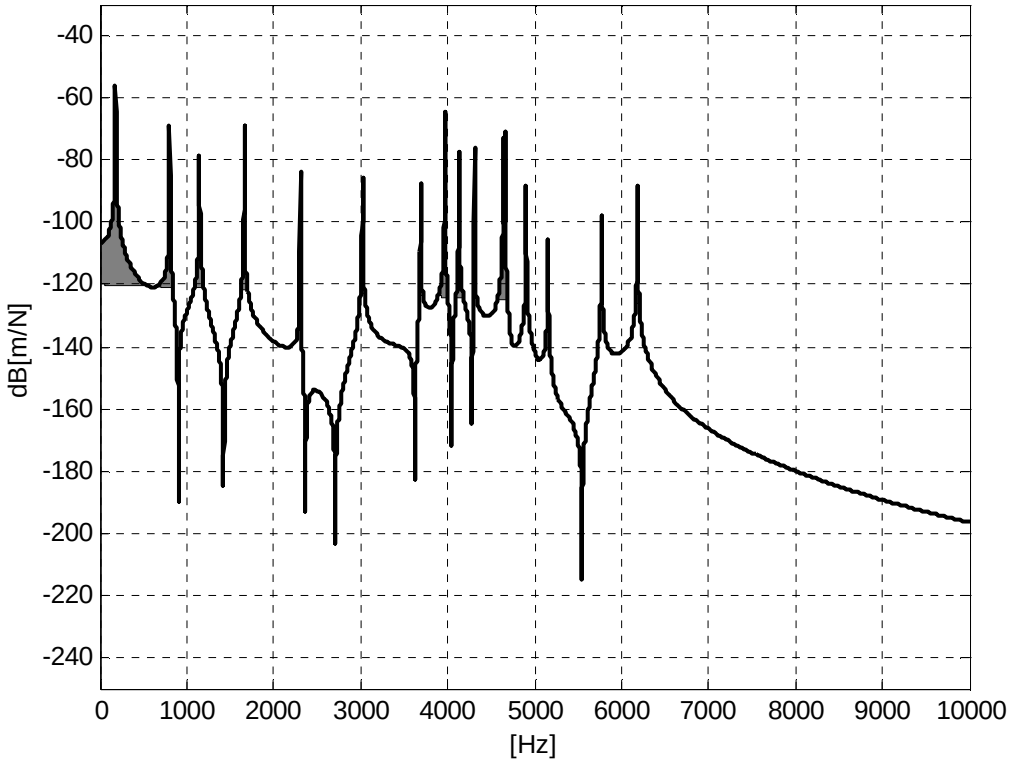

Figure 67 Treuil 2D, courbe H_{21} (f), RMS_CDC$_{21}$= 2271. rms.

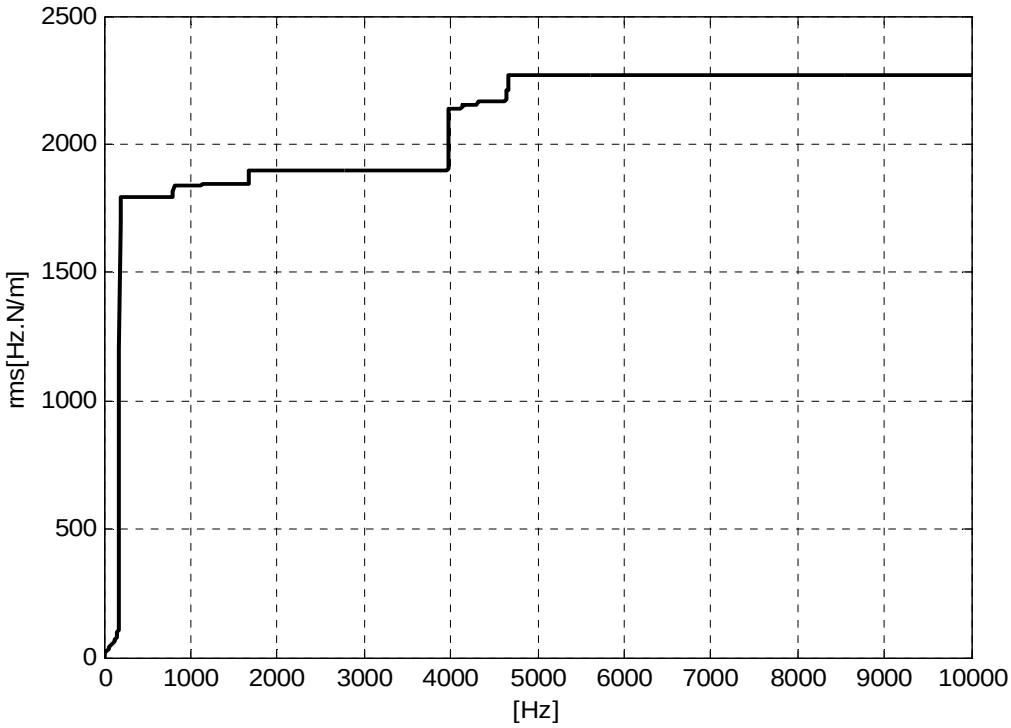

Figure 68 Treuil 2D, courbe *RMScum_CDC*$_{21}$

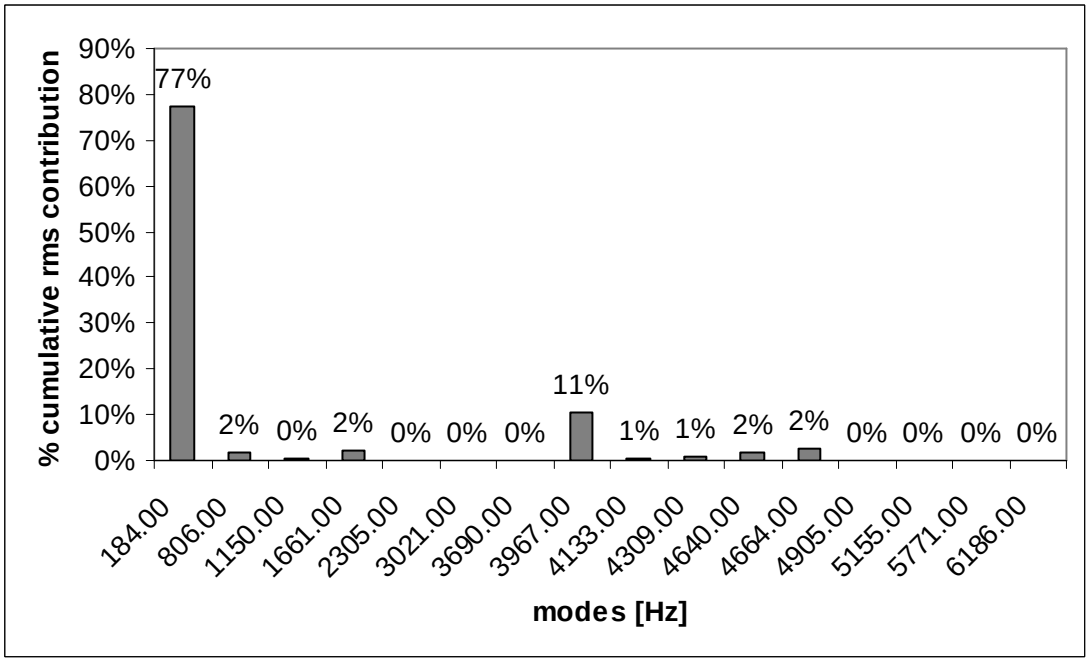

Figure 69 Treuil 2D, Facteur de participation modale %FPM_RMS_CDC$_{21}$

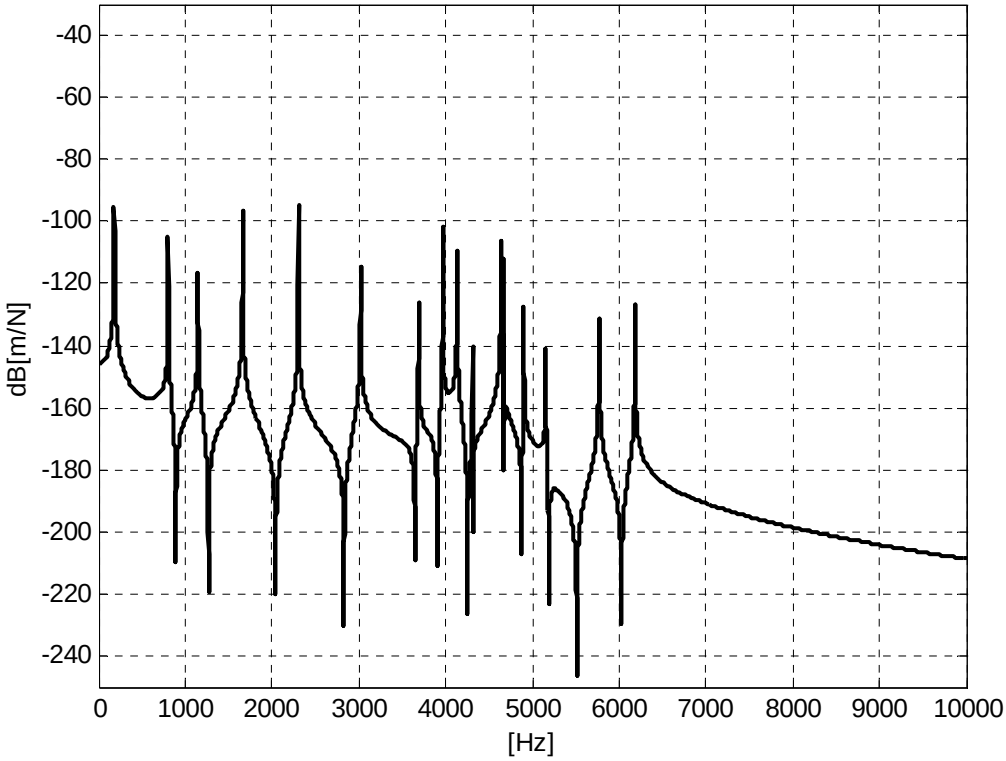

Figure 70 Treuil 2D, courbe H_{12} (f), RMS_CDC$_{12}$= 41. rms

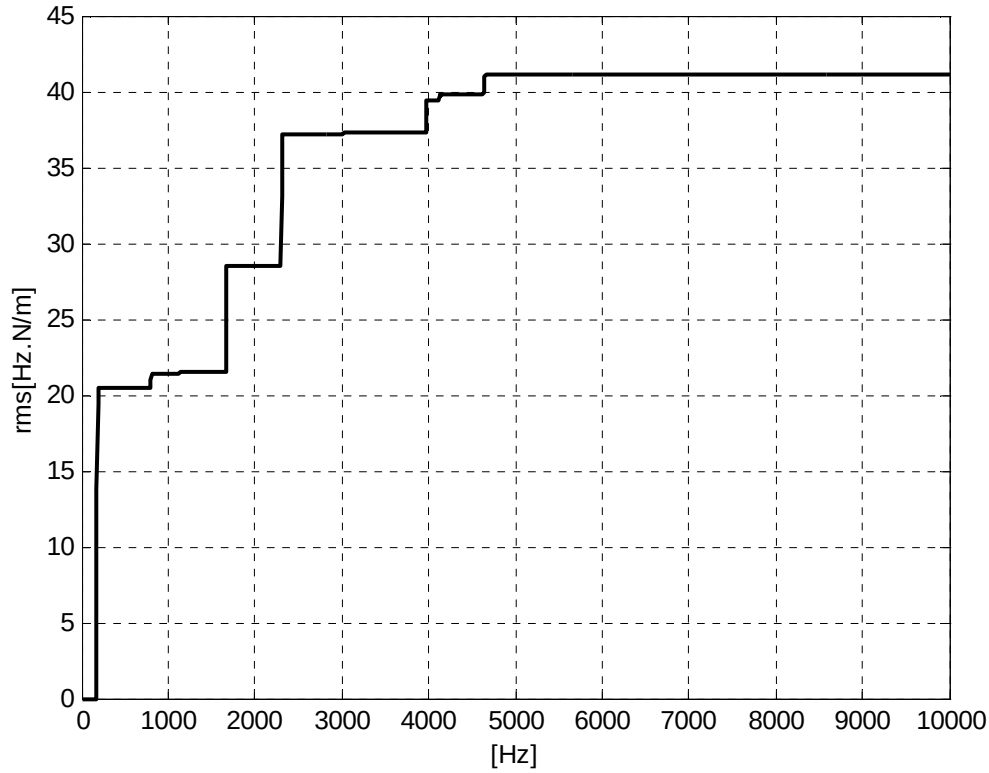

Figure 71 Treuil 2D, courbe *RMScum_CDC$_{12}$*

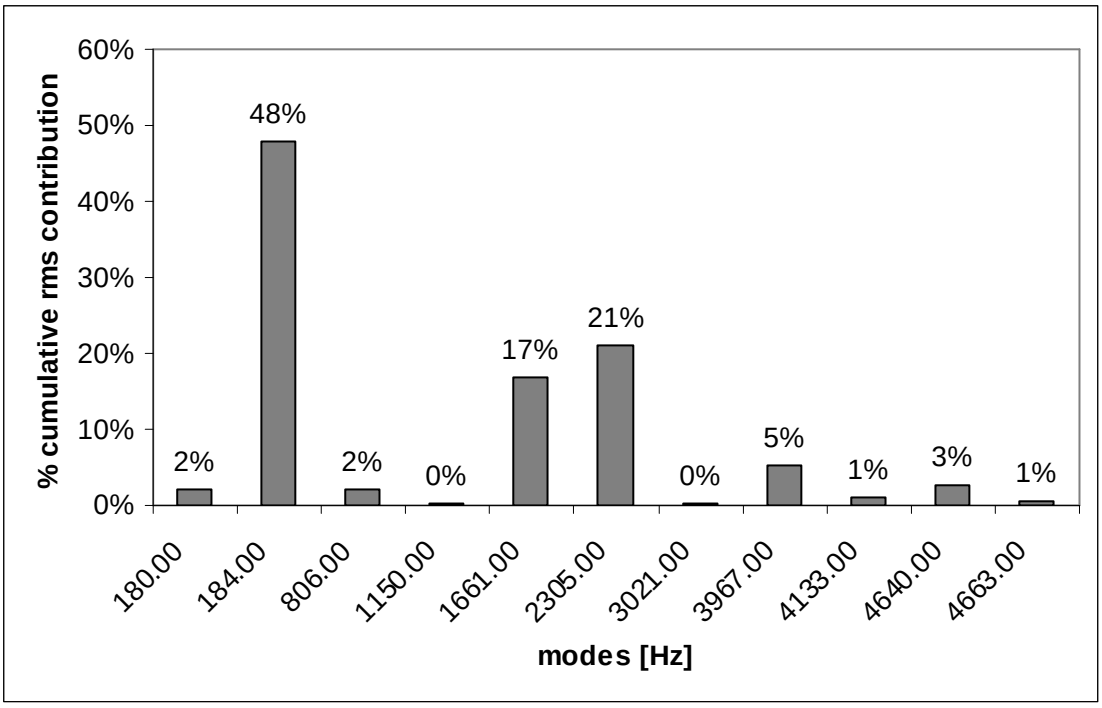

Figure 72 Treuil 2D, Facteur de participation modale %FPM_RMS_CDC$_{12}$

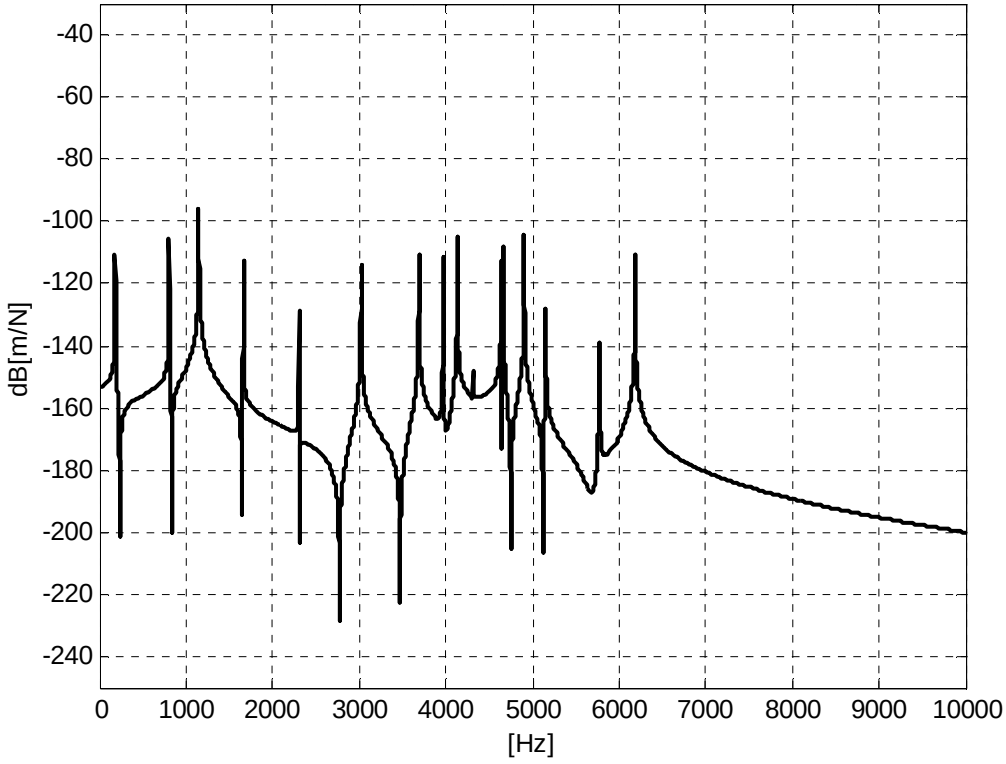

Figure 73 Treuil 2D, courbe H_{22} (f) , RMS_CDC$_{22}$= 31. rms

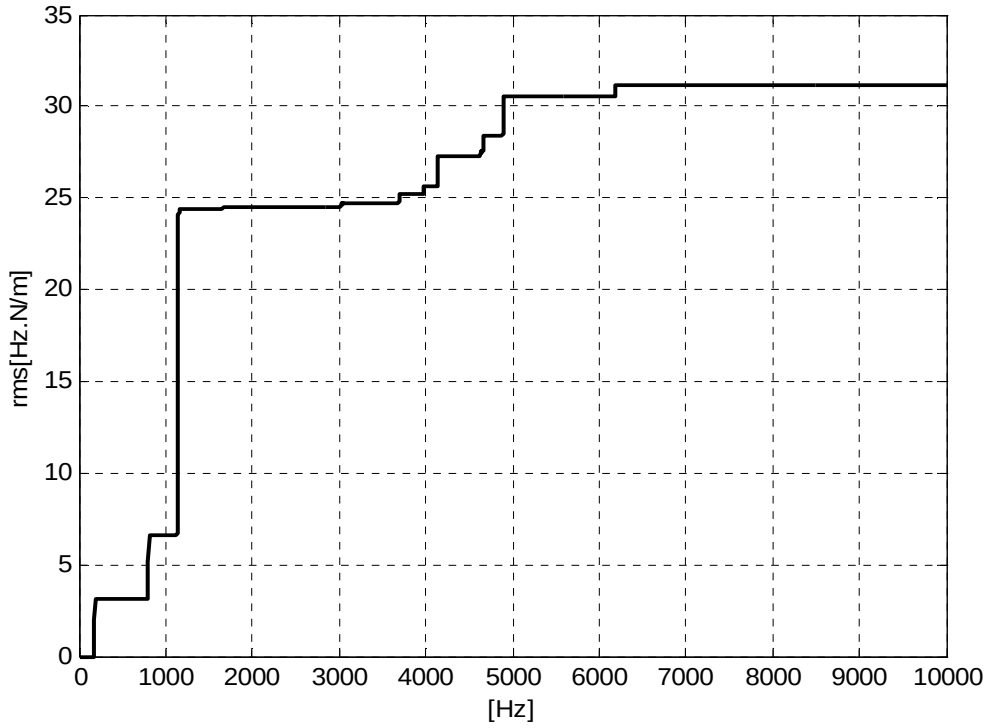

Figure 74 Treuil 2D, courbe *RMScum_CDC*$_{22}$

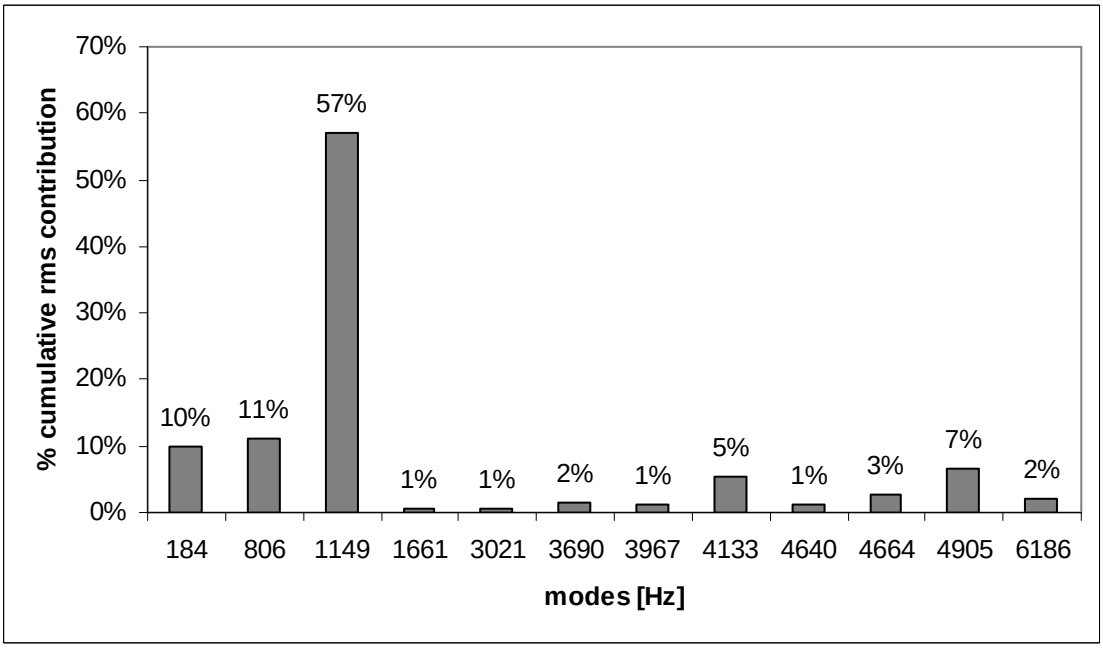

Figure 75 Treuil 2D, Facteur de participation modale %FPM_RMS_CDC$_{22}$

- **Remarque :**

Les surtensions recherchées sur la courbe de RMS cumulée ne sont pas toutes nécessairement des modes de la structure ex : la surtension détectée à 180 Hz (voir Figure 72) n'est pas liée à un mode de structure. Ces surtensions sont dues à quelques erreurs numériques dans le calcul.

A.4.2 Le critère RMS

Le critère RMS du système **B** est une performance globale sur l'ensemble des fonctions de transferts. Ce critère caractérise le système en sa totalité. Le critère est une somme quadratique des critères RMS_{ij}

$$RMS(B) = \sqrt{\sum_{i=1}^{N}\sum_{j=1}^{M}\left(RMS_{ij}(B)\right)^2} = \sqrt{\sum_{i=1}^{N}\sum_{j=1}^{M}\int_{f_{\min}}^{f_{\max}}\left|H_{ij}(f)\right|^2 df} \qquad \text{(A.11)}$$

On trouve comme application au système MIMO la caisse automobile qui subit indépendamment (a) les excitations moteurs et (b) les excitations du bruit de roulement. Le régime moteur est indépendant des conditions du roulage (état de la route).

- **Exemple :**

La valeur de rms totale de l'exemple du treuil 2D est :

$$\begin{aligned} \text{RMS\_CDC} &= \sqrt{\left(\text{RMS\_CDC}_{11}\right)^2 + \left(\text{RMS\_CDC}_{21}\right)^2 + \left(\text{RMS\_CDC}_{12}\right)^2 + \left(\text{RMS\_CDC}_{22}\right)^2} \\ &= \sqrt{(12890.)^2 + (2271.)^2 + (41.)^2 + (31.)^2} = 13089\,\text{rms} \end{aligned} \qquad \text{(A.12)}$$

A.4.3 La courbe de RMS cumulée

La courbe de RMS cumulée pour le système total donne la possibilité de voir quels sont les modes de la structure qui sont en surtension et qui dépassent les références CDC. Notant que ces références CDC sont définies sur chaque transfert.

On définit la fonction de RMS cumulée au niveau du système total comme suit :

$$RMScum\_CDC(f) == \sqrt{\sum_{i=1}^{N}\sum_{j=1}^{M}\left(RMScum\_CDC_{ij}(f)\right)^2} \qquad \text{(A.13)}$$

- **Exemple :**

La Figure 76 illustre la courbe du RMS cumulée du cas d'étude du système treuil. La Figure 77 illustre le %FPM_RMS_CDC qui en découle du même cas d'étude.

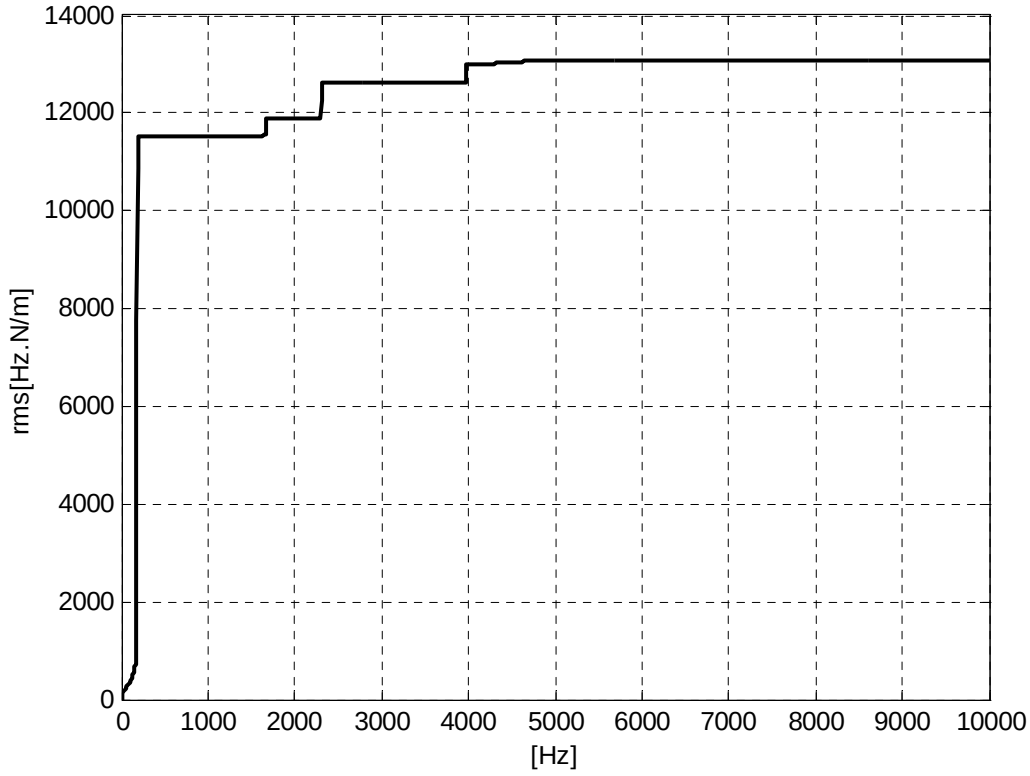

Figure 76s Treuil 2D, courbe *RMScum_CDC*

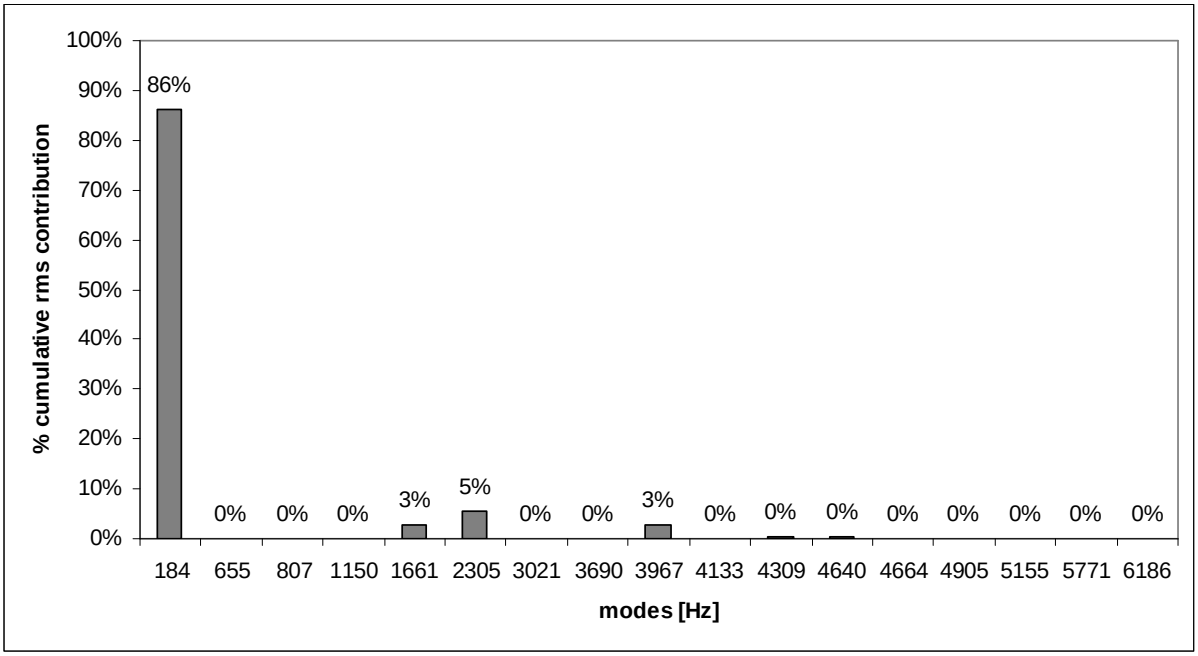

Figure 77 Treuil 2D, Facteur de participation modale %FPM_RMS_CDC

A.4.4 Facteur de participation des voies de transfert : FPV

La fonction de transfert caractérise la voie de passage des vibrations entre les points d'entrée du signal et les points de sortie. Si on ordonne les transferts suivant les valeurs de leurs critères RMS_{ij}, on obtient les voies les plus contributrices au niveau de la valeur du critère globale RMS (du système total). Cette hiérarchisation des transferts est intéressante dans le sens quelle permet de focaliser les modifications dynamiques de la structure sur les voies les plus contributrices. Ce facteur est un outil d'analyse qui permet d'orienter les modifications proposées en conception. Et en complétant par une analyse des contributions modales (%FPM_CDC), on sait orienter encore plus les solutions (dimensionnelles ou topologiques) qu'il faut apporter à la structure.

- **Exemple :**

La illustre Figure 78 le Facteur de participation des voies de transfert (FPV) calculé dans le cadre du cas d'étude du système treuil.

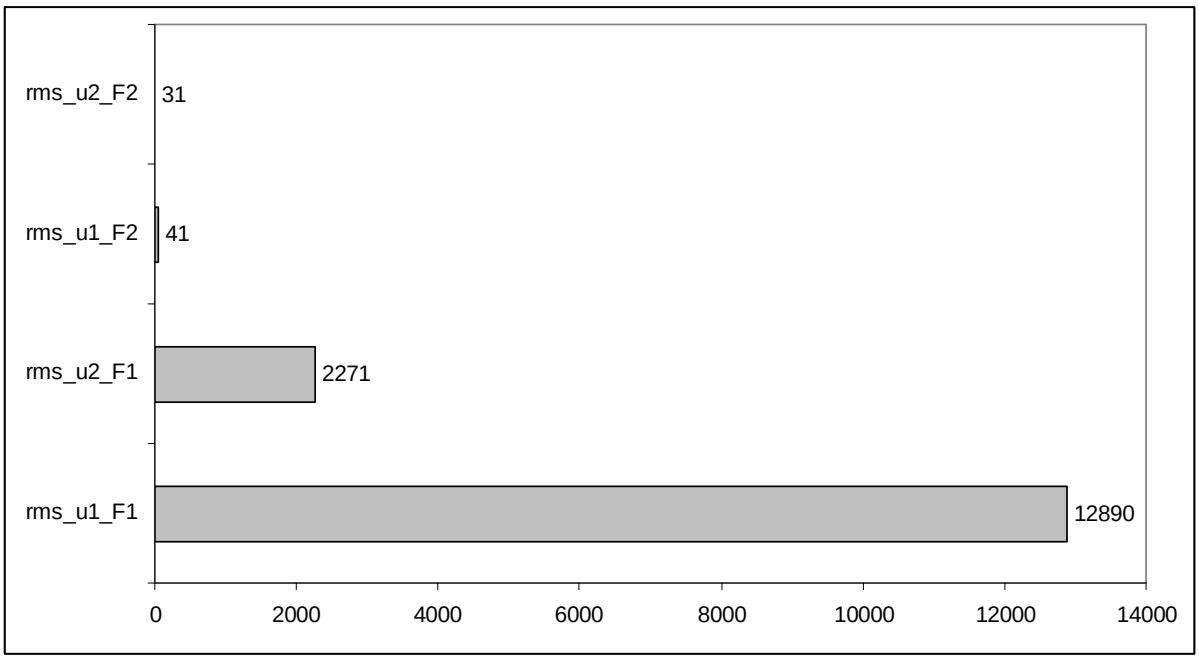

Figure 78 Treuil 2D, Facteur de participation des voies de transfert FPV

Appendix B

Design of Experiments and Metamodeling Techniques

La conception robuste basée sur des modèles d'approximation est très utile pour l'étude des systèmes complexes de grandes-échelles dans un contexte d'ingénierie concurrente. On pourrait voir des exemples d'application dans les travaux de Renaud et Gabriele, 1991 ; Chen, et al., 1996a . Il a été démontré à travers plusieurs articles de recherches (par exemple : Mavris, et al., 1996, Simpson, et al., 1998) que des modèles d'approximation et d'expérimentation pour l'étude et l'analyse des systèmes complexes sont essentiels afin d'être rapide et efficace dans les phases amonts de la conception.

Ces modèles conceptuels :

- constituent des outils d'analyse rapide (fast analysis tool) pour l'exploration de l'espace des concepts puisqu'il s'agit d'approximations à très faible coût de calcul en comparaison aux analyses complètes et coûteuses.
- ils donnent la possibilité de comprendre la relation existante entre les réponses, $\boldsymbol{y}$, du système et les variables de conception, $\boldsymbol{x}$.
- ils facilitent l'intégration des codes d'analyse pour des disciplines interdépendantes dans une stratégie globale de conception.

Cette approximation, ou le modèle des modèles est appelé ***métamodèle*** (Kleijnen, 1987).

Un modèle mathématique d'approximation peut être écrit sous la forme de $y = f(x) \cong \phi(x)$, avec $f(x)$ représente la fonction initiale du modèle étudié, et $\hat{y} = \phi(x)$ est le métamodèle d'approximation à y.

L'élaboration d'un métamodèle implique :

1. le choix d'un plan d'expériences pour la génération des données.
2. le choix d'un modèle représentatif d'approximation des données.
3. l'adaptation du modèle aux données expérimentales.

Toutefois, malgré que l'utilisation des métamodèles permettent une analyse plus rapide que les modèles ingénieurs et complexes d'origine, les métamodèles ajoutent un nouvel élément d'incertitude. Ainsi, il est nécessaire d'avoir des méthodes efficaces d'évaluation afin de permettre l'adaptation des ces métamodèles aux systèmes étudiés.

B.1 La cartographie des techniques de métamodèles

Les techniques d'approximation qui peuvent être utilisées pour les métamodèles (Barton, et al., 1999, Barton , 1992, 1994) sont : *(a)* la régression polynomiale avec la méthodologie de surface de réponse (polynomial regression and response surface methodology), *(b)* les réseaux de neurones (neural networks), *(c)* la corrélation spatiale ou le métamodèle kriging (spatial correlation and kriging models), *(d)* les courbes de régression adaptative à mutli-variables (Multivariate Adaptative Regression Splines: MARS), et *(e)* les fonctions radiales de base (radial basis functions). On fera, dans la suite, l'état de l'art sur ces techniques à partir, principalement, des articles et des travaux de recherches effectués sur les métamodèles :(Chen, et al., 2000 ; Lin, et al., 2000 ; Meckesheimer, et al., 2001, Sasena, 1998).

B.1.1 La régression polynomiale (Polynomial

Regression : PR) et la méthodologie de surface de réponse (Response Surface Methodology :RSM)

Les métamodèles qui vont être présentés à la suite de ce métamodèle, sont des modèles globaux. Ce qui signifie que l'ensemble de l'espace de conception est exploré par un seul métamodèle. A l'inverse, la technique de la méthodologie de surface de réponse est un processus séquentiel d'adaptation de modèles locaux. On présentera par la suite, qu'une définition succincte de la méthodologie de surface de réponse. Pour une plus ample compréhension, un ouvrage de référence dans la matière est recommandé, celui de Myers et Montgomery, 1995.

La régression polynomiale et la méthodologie de surface de réponse ont été appliquées par un certain nombre de chercheurs (Engelund, et al, 1993 ; Unal, et al., 1996 ; Chen, et al., 1996a ; Simpson, et al. 1997) dans la conception des systèmes techniques complexes. Elles sont utilisées afin de bâtir des métamodèles avec des polynômes à faible degré dans une partie relativement limitée de l'espace des facteurs. Un modèle polynomial de second ordre peut être écrit comme suit :

$$\hat{y} = \beta_0 + \sum_{i=1}^{k} \beta_i x_i + \sum_{i=1}^{k} \beta_{ii} x_i^2 + \sum_{i} \sum_{j} \beta_{ij} x_i x_j \qquad \text{(B.1)}$$

Les paramètres β du polynôme sont calculés en utilisant la régression à moindre carré pour adapter la réponse approchée $\hat{y}$ aux données empiriques ou aux données obtenues par simulations et analyses. Ces approximations peuvent être utilisées dans un autre temps comme des modèles de prédiction de la réponse y du système.

En créant le modèle PR, il est possible d'identifier la signification des différents facteurs de conception directement à partir des coefficients dans le modèle de régression normalisé. Pour des problèmes de large dimension, il est plus utile d'utiliser des modèles polynomiaux linéaires ou de second ordre afin de restreindre les variables de conceptions aux plus influentes d'entre elles. Dans le cas d'une optimisation, la possibilité de lissage de la régression polynomiale permet une convergence rapide des fonctions de

perturbation (noise function)(Giunta, et al., 1994). Malgré ces avantages, il y a toujours des faiblesses en appliquant la PR à un modèle de comportement fortement non linéaire. Des polynômes plus haut degré peuvent être utilisés mais l'instabilité du modèle peut augmenter (Barton, 1992), ou il peut être très difficile de prendre un nombre d'échantillons de données suffisants pour l'estimation des tous les coefficients de l'équation polynomiale, particulièrement dans le cas des grandes dimensions.

B.1.2 Les réseaux de neurones et la logique floue

Un point commun aux autres metamodèles ce qu'ils supposent toujours une nature polynomiale des données. Il y d'autres méthodes qui évitent cette supposition en laissant l'adaptation des données se faire d'une manière plus libre. Parmi elles, deux méthodes populaires sont utilisées : la logique floue et les réseaux de neurones.

Pour la première, les variables sont classées suivant des ensembles qui définissent si une entrée est dites " très importante ", " importante " et " peu importante ". Des règles, sont ainsi définies pour décrire comment les variables dépendantes répondent aux différents ensembles d'entrée. En estimant, pour chaque entrée à quel ensemble est-elle plus proche, on définit un modèle approché de la réponse (Ross, 1995).

Les réseaux de neurones sont aussi une méthode très utilisée, où tous ce qui est demandé est seulement un ensemble de données d'entrée et leurs valeurs correspondantes de sortie. Ainsi, le réseau est établi puis entraîné d'une façon qu'il puisse prédire les valeurs de sortie ou la réponse à une nouvelle donnée d'entrée (Ellacott, et al., 1997).

Ces méthodes sont devenues très populaires, puisqu'il n'est pas nécessaire de connaître d'avance le comportement de la réponse.

B.1.3 La corrélation spatiale : le métamodèle kriging

Les métamodèles par corrélation spatiale forment une classe de techniques d'approximation qui se montrent promoteurs pour bâtir des approximations globales et exactes de l'espace de conception (Meckesheimer, et al., 2001).

Dans un métamodèle par corrélation spatiale, les variables de conception seront corrélées à des fonctions de distances dans le modèle de prédiction. Ces métamodèles sont assez flexibles dans le sens qu'ils peuvent ou bien " valoriser les données ", en faisant une interpolation exacte des données, ou bien " lisser les données ", en faisant une interpolation inexacte, suivant le choix de la fonction de corrélation (Simpson, et al., 1997).

Dans les métamodèles de type (a) ou (d) (Regression polynomiale ou les courbes à mutli-variables) l'hypothèse fondamentale est que l'approximation est de la forme : $y(x) = f(x) + \varepsilon$, avec ε considérée comme une distribution normale indépendante et identiquement distribuée $\sim N(0,\sigma^2)$. Mais, l'idée principale des métamodèles avec des fonctions de corrélation spatiale (Spatial Correlation Functions : SCF) est que les valeurs prédites, ε_i, de l'erreur ne sont pas indépendantes. Plus mieux, ces fonctions prennent en compte que les erreurs sont des fonctions systématiques de x. Le métamodèle kriging, $\hat{y}(x) = f(x) + Z(x)$, est constitué de deux parties : une fonction polynomiale $f(x)$ et une déviation fonctionnelle par rapport à cette polynomiale, $Z(x)$.

B.1.4 Les courbes de régression adaptative à plusieurs variables (Multivariate Adaptative Regression Splines: MARS)

Les courbes de régression adaptative à multi-variables (MARS) (Friedman, 1991) sélectionnent d'une façon adaptative un ensemble de fonctions de base pour faire une approximation de la fonction de réponse par une approche itérative d'avance/recule (Chen, et al., 2000).

Pour l'adaptation des données fortement non linéaires, on peut utiliser des courbes définies avec des fonctions polynomiales définies par morceaux, plutôt que d'utiliser une

expression unique pour l'ensemble des données. On adopte, simplement, plusieurs polynômes à faibles degrés qui vont s'adapter aux données, où chacun est défini sur un intervalle séparé et délimité par des noeuds ou points de rupture. Alors, des conditions aux limites sont définies sur les limites des intervalles pour chaque polynôme afin d'assurer que chaque morceau peut nous permettre d'avoir le degré de continuité que nous imposons à la courbe. Plus souvent, les fonctions par morceaux sont choisies comme des polynômes cubiques avec une continuité C^2. En imposant la continuité C^2, les fonctions définies par morceaux ont les mêmes valeurs, tangentes et courbures sur les noeuds qui lient ces morceaux. Dans le cas où on utiliserait des courbes d'interpolation, les noeuds sont l'ensemble des points de données, ainsi la courbe passe, forcement, par chacun des points de données. Cependant, malgré que les courbes d'interpolation soient plus exactes par rapport aux points de l'échantillon par comparaison à la régression polynomiale par moindre carré, elles sont plus ou moins ondulées entre les points de données.

D'une façon Générale, un métamodèle de type courbes de régression adaptative à multi-variables MARS s'écrit de la façon suivante :

$$\hat{y} = \sum a_m B_m(\mathbf{x}) \tag{B.2}$$

où a_m est le coefficient de l'expansion, et B_m, les fonctions de base, est exprimée comme suit :

$$B_m(\mathbf{x}) = \prod_{k=1}^{K_m} \left[s_{k,m} \left(x_{v(k,m)} - t_{k,m} \right) \right]_+^q \tag{B.3}$$

Avec K_m est le nombre des facteurs (ordre d'interaction) dans la m^{ième} fonction de base, $s_{k,m} = \pm 1$, $x_{v(k,m)}$ est la v^{ieme} variable, $1 \le v(k,m) \le n$, et $t_{k,m}$ est la position du noeud pour chacune des variables correspondantes. Le signe " + " signifie que la fonction est une fonction puissance définie par troncature

$$\left[s_{k,m} \left(x_{v(k,m)} - t_{k,m} \right) \right]_+^q = \begin{cases} \left[s_{k,m} \left(x_{v(k,m)} - t_{k,m} \right) \right]^q & s_{k,m} \left(x_{v(k,m)} - t_{k,m} \right) > 0 \\ 0 & \text{sinon} \end{cases} \tag{B.4}$$

Comparée aux autres techniques, l'utilisation de la MARS dans des applications ingénieurs de conception est relativement récente. Buja, et al. (1990) (in Chen, et al.,2000) a utilisé MARS pour une analyse extensive des données concernant l'usage de mémoire dans des contrôleurs électroniques. Wang, et al. (1999), compare des régressions linaires, de second ordre et puis à des degrés plus élevés pour l'étude de cinq variables dans une analyse structurale d'une voiture. Friedman (1991) a utilisé la technique de MARS pour faire l'approximation du comportement de la performance d'un simple circuit de courent alternatif. Sasena (1998) à étudier comparativement les méthodes de MARS et de kriging pour évaluer la performance de consommation d'une voiture à moteur électrique hybride.

B.1.5 les fonctions radiales de base (Radial Basis Functions : RBF)

Les fonctions radiales de base sont développées, initialement, par Hardy en 1971 comme étant un schéma d'interpolation pour des donnés à multi-variables. Quinze ans plus tard, les travaux de Dyn, en 1986, ont rendu les fonctions radiales de base plus utiles en leur donnant la possibilité de lisser les approximations des données en plus de l'interpolation. La méthode utilise une combinaison linéaire de fonctions radiales et symétriques basées sur la distance euclidienne ou d'autres distances similaires pour avoir une approximation aux fonctions de réponses. Une simple fonction radiale de base peut être exprimée de la façon suivante :

$$\hat{y}(\mathbf{x}) = \sum_i \beta_i \left\| \mathbf{x} - \mathbf{x}^i \right\| \tag{B.5}$$

Où, $\|\bullet\|$ représente la norme euclidienne, et la somme est faite sur un ensemble observé de réponses du système $\left\{\left(\mathbf{x}^i, f(\mathbf{x}^i)\right)\right\}, i = 1,\ldots,n$. Les coefficients β_i sont calculés en résolvant le système linéaire obtenu par le remplacement de $\hat{y}(\mathbf{x})$ par $f(\mathbf{x}^i)$ dans l'expression précédente.

Les approximations par fonctions radiales de base se sont révélées assez bonnes pour l'adaptation aux contours arbitraires des fonctions de réponses qu'ils soient déterministes ou stochastiques (Powell, 1987). Tu et Barton (1997) ont trouvé que les RBF donnent des métamodèles assez bon pour la simulation des circuits électronique. Meckesheimer, et al. (2000) utilise la méthode pour construire un métamodèle pour un exemple de problème de conception d'une lampe de bureau qui a des fonctions de réponse continues et discrètes.

B.2 Les plans d'expériences

Les plans d'expériences sont utilisés, dans les métamodèles, pour deux raisons : (1) la première est pour la génération d'un échantillon de données d'entrée et de sortie pour faire l'adaptation du métamodèle au problème ou au modèle étudié, (2) la deuxième est pour avoir des échantillons de données qui serviront pour la validation du métamodèle et pour faire les mesures de performance de celui-ci. En outre, il faut signaler que le choix du plan d'expérience, dans le premier cas (1), est très important pour la bonne réussite du métamodèle. (Wilson, et al, 2000 ; Barton, et al., 1994). En effet, si les points de l'échantillon, obtenus à partir du modèle d'origine, ne sont pas bien choisis, les approximations par le métamodèle conséquent ne seront pas d'une bonne qualité (Meckesheimer, et al., 2001). Cependant, il y a plusieurs critères qui mesurent la performance d'un plan d'expérience(Sasena, 1998). Parmi ces critères, sont (*a*)le nombre nécessaire de points à générer pour remplir au mieux l'espace de conception, (*b*) la symétrie résultante de la distribution de la variance sur l'espace de conception, (*c*) la facilité avec laquelle le plan peut être déployé et (*d*) la capacité d'estimation du plan.

Dans la suite, on citera les cinq types de plans d'expériences les plus communément utilisés dans le domaine d'expérimentations par simulations numériques.

B.2.1 Les plans factoriels (Factorial Design)

Les plans d'expériences factoriels sont les plans les plus répandus (Montgomory, 2001). Ils sont ou bien des plans factoriels complets ou bien des plans factoriels incomplets. Dans un plan d'expériences chaque variable d'entrée (ou de conception) constitue un ***facteur***. Les valeurs qui vont être fixées pour chaque variable sont appelées ***niveaux***. Le plan factoriel complet est un plan dans lequel toutes les combinaisons distinctes de niveaux des facteurs sont toutes présentes (Schimerling, et al., 1998). Le nombre de ces combinaisons de niveaux est égal au produit des nombres de niveaux des facteurs. Dans la plus part des cas les niveaux sont uniformément répartis afin de mieux couvrir l'espace de conception. Mais comme le nombre de combinaisons croît exponentiellement avec le nombre des facteurs, ces plans deviennent vite de faible efficacité et ils sont remplacés par des plans factoriels incomplets. Il reste alors, que l'efficacité de ce type de plans dépend de la nature des réponses étudiées.

B.2.2 Les plans Hypercubes Latins (Latin Hypercube Design)

Les plans Hypercubes Latin ont été introduits, pour la première fois dans les études par simulations numériques, par McKay, et al., 1979. Ils offrent un échantillonnage flexible avec une bonne uniformité sur toute la largeur de l'échantillon. Ils oeuvrent par une distribution aléatoire des points sur tout l'espace de conception. Il a été établit que cette méthode permet d'avoir des échantillons avec une faible variance pour les données de sorties c'est-à-dire les réponses. Mais comme les points d'entrée sont générer aléatoirement, il se peut dans un certain nombre de cas, d'avoir une mauvaise uniformité qui donne des mauvaises approximations ultérieurement. Le meilleur plan est, ensuite, sélectionné sur la base du critère de *D-optimality* (plan optimal) dans lequel le volume de l'ellipsoïde de la confiance pour des valeurs vraies de β autour d'un vecteur aléatoire $\hat{\beta}$ est minimisé, ce qui revient à maximiser le déterminant de la matrice ***X'X***. Et comme on choisit le plan à partir d'un ensemble de plans candidats(et non pas à partir de l'ensemble de tous les plans Hypercube Latin qui sont possible pour cette dimension de problème), on dit alors qu'il s'agit d'un plan D-best (le meilleur plan) au lieu de dire qu'il est un D-optimal (le plan optimal).

B.2.3 Les plans orthogonaux (Orthogonal Array Design)

On considère, dans la suite, les plans d'expérience avec des modèles qui prennent uniquement les *facteurs* comme *actions*[1]. Un plan de ce type est dit orthogonal, si seulement si, pour chaque couple d'actions (ici de facteurs), tous ses couples de nivaux possibles sont présents un même nombre de fois dans ce plan (Schimerling, et al., 1998). Owen, 1992 et Barton 1994, présentent dans leurs articles la méthode des plans orthogonaux. L'intérêt de l'orthogonalité d'un plan est que les coefficients relatifs à des actions distinctes ne sont pas corrélés et donnent une variance plus faible que dans le cas des autres types de plans.

D'autre type de plans d'expérience, destinés aux expérimentations par simulations numériques, tels que les plans de type ***Hammersley Sampling Sequence***(Kalagnanam, et al., 1997) et les ***plans uniformes*** (uniform design) (Venter, et al., 1998) existent en littérature. Des études comparatives pour les plans d'expériences utilisés pour l'adaptation des modèles ont montré la faiblesse de ces plans par rapport aux autres types de plan (Lin, et al., 2000).

B.3 Le métamodèle kriging

B.3.1 La formulation du métamodèle kriging

Il a été dit précédemment dans le paragraphe §B.1.3 que le métamodèle kriging est basé sur l'hypothèse qui considère que les écarts $\varepsilon(x_i)$ ne sont pas indépendants. Pour mieux comprendre cette hypothèse, on considère l'illustration suivante où une fonction quadratique est utilisée pour approcher avec la méthode de moindres carrés un échantillon d'un ensemble de donnée (Figure 79):

---

[1] par définition une action est un facteur ou une interaction entre facteurs (Schimerling, et al., 1998)Schimerling, P., Sisson, J. C. and Zaïdi, A. (1998). Pratique des Plans d'Expériences, Technique & Documentation, Paris..

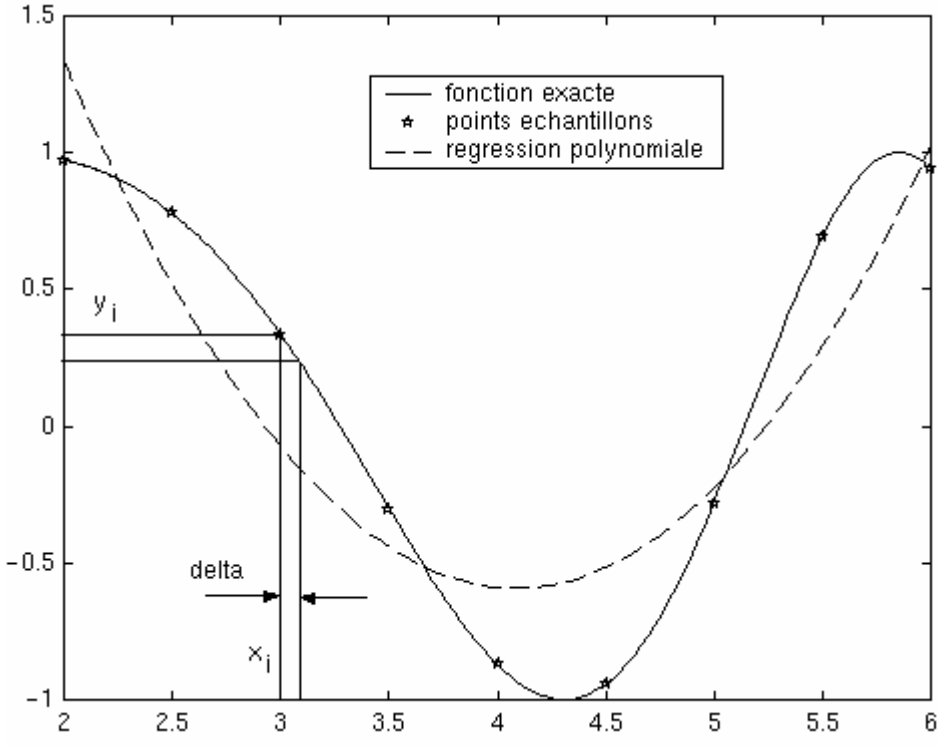

Figure 79. Illustration de l'hypothèse de la distribution d'erreur pour le métamodèle kriging

On peut constater qu'à chaque fois que la valeur prédite $f(x_i)$ est très différente de la valeur exacte $y(x_i)$, on peut dire, alors qu'à un point très proche de x_i, la valeur prédite $f(x_i+\delta)$ est très différente de la valeur $y(x_i+\delta)$. Ceci, est due au fait que pour une approximation de moindres carrés, une erreur est systématiquement associée à la fonction de prédiction $f(x)$.

Un métamodèle kriging est une combinaison d'un modèle polynomial plus une déviation par rapport à ce modèle qui se présente sous la forme suivante :

$$\hat{y}(x) = f(x) + Z(x) \tag{B.6}$$

où $\hat{y}(x)$ est la fonction à déterminer et $f(x)$ est donnée comme une fonction polynomiale de x. $Z(x)$ est considérée comme une réalisation d'un processus stochastique avec une moyenne nulle, et une fonction de corrélation spatiale. $Z(x)$ représente l'incertitude autour de la valeur moyenne de $\hat{y}(x)$.

Dans ce modèle $f(x)$ est une approximation globale de l'espace de conception, alors que $Z(x)$ crée des déviations locales, c'est ainsi que le métamodèle kriging fait l'interpolation sur l'ensemble de l'échantillon des n_s points de données.

Typiquement dans la plupart des cas (Simpson, et al., 1998 ; Sacks, et al., 1989 ; Koehler, et al., 1996), la fonction $f(x)$, dans l'équation (B.6), est considérée comme un terme constant.

La fonction de corrélation spatiale dans $Z(x)$ est donnée par :

$$\mathbf{Cov}[Z(x^i), Z(x^j)] = \sigma^2 \mathbf{R}[R(x^i, x^j)] \qquad \text{(B.7)}$$

avec σ^2 est la variance du processus et $R(x^i, x^j)$ est la fonction de corrélation entre tous deux points x^i et de l'ensemble de l'échantillon des n_s points de données. $\mathbf{R}$ est une matrice symétrique (n_s x n_s) avec des uns sur toute sa diagonale. C'est le choix de R, la fonction de corrélation spatiale, qui détermine comment le métamodèle va approcher les données. Il y a le choix entre plusieurs fonctions suivant la rapidité et la finesse avec lesquelles la fonction va d'un point x^i à un point x^j.

Une variété de fonctions de corrélation est présentée dans l'article de (Simpson, et al., 1998) ; Mais, la fonction Gaussienne de corrélation proposée dans (Sacks, et al., 1989) est la plus utilisée. Par exemple, cette fonction est bien adaptée à la méthode de formulation des objectifs par " minimisation de la variance autour d'un point central " (Lin, et al., 1999).

Un résumé des fonctions de corrélation les plus couramment utilisées est présenté dans le tableau (Table 3) (Sacks, et al., 1989 ; Mitchell et Morris, 1992). Dans les expressions de ces fonctions, n représente le nombre des variables de conception, θ_m sont les paramètres indéterminés de la corrélation utilisés pour approcher le modèle, et $d_m = x_m^i - x_m^j$ est la distance entre les m^{iemme} composantes des points $\boldsymbol{x}^i$ et $\boldsymbol{x}^j$ de l'échantillon de donnée.

Nom de la fonction de corrélation spatiale	Expression de la fonction	N° de l'eq.
Exponentielle	$\prod_{m=1}^{n} \exp(-\theta_m \lvert d_m \rvert)$	(B.8)
Gaussienne	$\prod_{m=1}^{n} \exp(-\theta_m \lvert d_m \rvert^2)$	(B.9)
Cubique	$\prod_{m=1}^{n} \begin{cases} 1-6\left(\theta_m \lvert d_m \rvert\right)^2+6\left(\theta_m \lvert d_m \rvert\right)^3 & \theta_m \lvert d_m \rvert \\ 2\left(1-\theta_m \lvert d_m \rvert\right)3 & \frac{1}{2} \le \theta_m \lvert d_m \\ 0 & \theta_m \lvert d_m \end{cases}$	(B.10)
Fonction linéaire de Matérn	$\prod_{m=1}^{n} \left[\left(1+\theta_m \lvert d_m \rvert\right) \exp\left(-\theta_m \lvert d_m \rvert\right)\right]$	(B.11)
Fonction cubique de Matérn	$\prod_{m=1}^{n} \left[\left(1+\theta_m \lvert d_m \rvert+\frac{{\theta_m}^2 \lvert d_m \rvert^3}{3}\right) \exp\left(-\theta_m \lvert d_m \rvert\right)\right]$	(B.12)

Table 3. Résumé des fonctions de corrélation spatiale (Lin, et al., 2000)

Etant donné, que tous les θ_m>0 ,On constate que quelque soit le choix de la fonction de corrélation, la fonction tant vers 0 quand la valeur de $|d_m| = |x_m^i - x_m^j|$ augmente. Ceci montre que l'influence de l'échantillon des points de données sur le point à prédire devient de plus en plus faible quand les points de l'échantillon sont de plus en plus éloigné les uns des autres. La valeur de θ_m détermine la rapidité de la détérioration de cette influence.

Si on restreint la fonction polynomiale $f(x)$ à un terme constant β, l'estimation de la réponse $y(x)$ pour des nouvelles valeurs de $\boldsymbol{x}$ (qui n'existaient pas dans l'échantillon et pour lesquelles la réponse est encore non calculée) , notée $\hat{y}(x)$, est donnée sous la forme suivante :

$$\hat{y} = \hat{\beta} + \mathbf{r}^T(\boldsymbol{x})\mathbf{R}^{-1}(\mathbf{y}-\mathbf{f}\hat{\beta}) \qquad \text{(B.13)}$$

Où $\mathbf{y}$ est un vecteur colonne de taille n_s qui contient les réponses observées à chaque point de l'échantillon, et $\mathbf{f}$ est un vecteur colonne de taille n_s remplis avec des uns dans le cas où $f(x)$ serait une constante. $\mathbf{R}$ est la matrice symétrique de corrélation entre les points de l'échantillon de données de taille $n_s \times n_s$ avec des uns sur toute sa diagonale, et $\mathbf{r}^T(\boldsymbol{x})$ est le vecteur de corrélation de taille n_s entre les points de l'échantillon de données $\{\boldsymbol{x}^1, \boldsymbol{x}^2, \ldots, \boldsymbol{x}^{ns}\}$ et le nouveau point $\boldsymbol{x}$ où la réponse est encore non calculée.(Mitchell, et al., 1992)

$$\mathbf{r}^T(\boldsymbol{x}) = [R(\boldsymbol{x},\boldsymbol{x}^1), R(\boldsymbol{x},\boldsymbol{x}^2), \ldots, R(\boldsymbol{x},\boldsymbol{x}^{ns})]^T \quad \text{(B.14)}$$

B.3.2 Adaptation du métamodèle

Les seuls paramètres qui appairaient dans le métamodèle kriging sont les coefficients $\boldsymbol{\beta}_m$, associés avec la partie polynomiale $f(\boldsymbol{x})$ et les paramètres θ_m, associés avec le processus stochastique $Z(\boldsymbol{x})$. Les articles de Mitchell, et al., 1992 et Sacks, et al. 1989 rapportent que le modèle de régression $f(\boldsymbol{x})$ n'a pas de grande influence sur l'adaptation du ce métamodèle. A la différence, des méthodes de régression polynomiale avec des moindres carrés et les courbes de régression, il n'y a plus besoin de déterminer une forme fonctionnelle spécifique pour le métamodèle kriging. Il en résulte une flexibilité, qui donne à ce métamodèle un avantage particulier par rapport aux méthodes les plus " classiques ". Dans la plus part des cas, un simple coefficient $\boldsymbol{\beta}$ est utilisé pour la fonction $f(\boldsymbol{x})$, alors l'utilisation d'un polynôme linéaire est de très rare cas. Ce phénomène atteste la puissance des hypothèses à partir des quelles le métamodèle kriging est construit. En assumant que les écarts sont corrélés en fonction de $\boldsymbol{x}$, on ait capable d'utiliser seulement les paramètres, θ_m, de la fonction de corrélation pour adapter, avec une précision acceptable, le métamodèle à l'ensemble des données.

L'estimation de $\hat{\boldsymbol{\beta}}$, dans l'équation d'évaluation (B.13), est donnée par :

$$\hat{\boldsymbol{\beta}} = (\mathbf{f}^T\mathbf{R}^{-1}\mathbf{f})^{-1}\mathbf{f}^T\mathbf{R}^{-1}\mathbf{y} \quad \text{(B.15)}$$

L'estimation de la variance, $\hat{\sigma}^2$, d'un échantillon de données, noté **y**, à partir du modèle global en question (qui n'est pas la variance des données déjà observées) est donnée par :

$$\hat{\sigma}^2 = \frac{(\mathbf{y} - \mathbf{f}\hat{\beta})^T \mathbf{R}^{-1} (\mathbf{y} - \mathbf{f}\hat{\beta})}{n_s} \tag{B.16}$$

avec **y** est le vecteur des valeurs y et $f(\boldsymbol{x})$ est représentée par la constante $\hat{\beta}$. En rappelant que la variance σ^2 et la matrice de covariance **R** citées en haut sont des fonctions de θ_m, il est convenue de trouver les paramètres θ_m par une estimation de la plus grande vraisemblance (maximum likelihood estimate) en maximisant l'expression suivante :

$$\max_{\theta>0, \theta \in \Re^{n_s}} -\frac{\left[n_s \ln\left(\hat{\sigma}^2\right) + \ln|\mathbf{R}|\right]}{2} \tag{B.17}$$

Alors, que n'importes quelles valeurs de θ_m permet d'obtenir un modèle d'interpolation, le meilleur métamodèle kriging est obtenue en résolvant le problème d'optimisation non linéaire, sans contraintes et de dimension m exprimé par l'équation (B.17). Il est à noter, que la résolution d'un tel problème peut engendrer un coût de calcul élevé.

B.3.3 Critères et métriques pour les mesures de performance du métamodèle kriging

En général, la performance d'un métamodèle, et en particulier le kriging, est mesurée suivant plusieurs aspects et critères. Parmi ces critères on cite :

- ***La précision*** : est la capacité de prédire les réponses du système sur la région étudiée de l'espace conception.
- ***La robustesse*** : est la capacité du métamodèle d'avoir une bonne précision pour différents types et différentes tailles de problèmes.

- ***l'efficacité*** : est le coût de calcul nécessaire pour (1) l'élaboration du métamodèle et (2) pour l'estimation des réponses prédites pour un nouveau ensemble de points par le métamodèle.
- ***La transparence*** : est la capacité d'illustrer une relation explicite entre les variables d'entrée et les réponses.
- ***La simplicité conceptuelle*** :est le degré de simplicité de l'implémentation. Les méthodes simples nécessitent un nombre limité d'entrée par l'utilisateur et la possibilité de s'adapter facilement à chaque type de problème.

Pour la mesure de précision, il est souvent nécessaire d'avoir un nombre de points plus important du nombre des points utilisés pour l'élaboration du métamodèle.

Pour avoir une idée sur la précision du métamodèle, trois types de distance sont utilisés :

- **La racine de la moyenne des carrés des erreurs (Root Mean Square Error) :**

$$RMSE=\sqrt{\frac{1}{n}\sum_{i=1}^{n}\left(\hat{y}_i - y_i\right)^2} \tag{B.18}$$

avec $\hat{y}_i$ est la valeur prédite corresponde à la réponse observée y_i. La racine de la moyenne des carrées des erreurs représente la déviation du métamodèle par rapport au modèle réel étudié. La précision du métamodèle est d'autant plus bonne que la valeur du RMSE soit plus faible.

On utilise aussi la valeur relative de la racine de la moyenne des carrés des erreurs (Normalized Root Mean Square Error) définie ainsi :

$$NRSME = \frac{RSME}{STD} = \frac{\sqrt{\frac{1}{n}\sum_{i=1}^{n}\left(\hat{y}_i - y_i\right)^2}}{\sqrt{\frac{1}{n}\sum_{i=1}^{n}\left(y_i - \bar{y}\right)^2}} \quad \text{(B.19)}$$

avec $\bar{y}$ est la moyenne des réponses observées à partir des données. La variance (Standard Deviation :STD) donné une idée sur les irrégularités des données du problème.

- **La moyenne de la valeur absolue des erreurs(Mean absolute error) :**

$$MAE=\frac{1}{n}\sum_{i=1}^{n}\left|\hat{y}_i - y_i\right| \quad \text{(B.20)}$$

On définit aussi la valeur relative de la moyenne de la valeur absolue des erreurs(Normalized Mean absolute error) comme suit :

$$NMAE = \frac{\frac{1}{n}\sum_{i=1}^{n}\left|\hat{y}_i - y_i\right|}{STD} \quad \text{(B.21)}$$

Le métamodèle est d'autant plus précis que la valeur de la *MAE* et de la *NMAE* sont plus faible

- **la valeur maximale de la valeur absolue des erreurs (Maximum Absolute error) :**

$$MAX=\max_i\left|\hat{y}_i - y_i\right| \quad \text{(B.22)}$$

Il est commode aussi d'évaluer la valeur maximale relative de la valeur absolue de l'erreur (Normalized Maximum Absolute error) définie par :

$$NMAX = \frac{\max_i \left| \hat{y}_i - y_i \right|}{STD} \tag{B.23}$$

Alors que la *MAE* (*NMAE*), est fortement corrélée à la *RMSE* (*NRSME*), il se trouve que ce n'est pas le cas pour la *MAX*(*NMAX*). Une importante valeur de la MAX indique qu'il y a une erreur importante dans une région de l'espace de conception, même si la précision générale sur l'ensemble de l'espace du métamodèle, donnée par les valeurs de la *RMSE* et la *MAE*, est relativement bonne. De faibles valeurs de la *MAX* sont plutôt préférées, Cependant, cette distance ne peut renseigner sur la précision globale du métamodèle, d'où l'importance de la *RMSE* et la *MAE*.

Une étude comparative suivant les différents critères de performance des différentes techniques de métamodèles, a été élaborée par Chen, et al., 2000.

B.3.4 Implémentation du métamodèle kriging sous Matlab

Toutes les traitements qui concernent l'élaboration des métamodèles kriging ont été codés sous Matlab. Matlab permet une manipulation aisée des matrices et n'impose pas trop de contrainte sur leurs tailles. Pour une partie des fonctions Matlab, elles ont été adoptées et modifiées, suivant nos besoins, depuis le travail de Sasena, 1998. Des fonctions Matlab spécifiques à notre cas ont été élaborées pour permettre le traitement et la présentation des données suivant les nécessités de notre étude.

B.3.5 Exemple d'application du métamodèle kriging

Dans l'exemple suivant, on va tester les capacités d'approximation des métamodèles kriging à un modèle analytique donné. Tout en gardant en tête que le but des métamodèles est non pas de faire l'approximation d'un modèle qu'on peut facilement l'exprimer analytiquement et le manipuler sous cette forme. Mais le but d'un métamodèle est d'avoir des modèles simplifiés d'un modèle de simulation plus complexe.

En effet, vu le temps alloué à chaque simulation pour étudier un seul point de l'espace de conception, on voit mal de tester un nombre important de points en vue d'avoir une solution optimale suivant les contraintes auxquelles est assujetti le modèle du système.

Pour cet exemple, on va faire l'approximation de la fonction de deux variables suivante :

$$f(x_1, x_2) = 2 + 0.01(x_2 - x_1^2)^2 + (1 - x_1)^2 + 2(2 - x_2)^2 + 7\sin(0.5x_1)\sin(0.7x_1x_2) \quad \text{(B.23)}$$

L'implémentation de l'exemple est faite sous Matlab. Vous pouvez trouver le script de l'exemple dans l'annexe A.

La Figure 80 montre le tracé de la surface et des contours de la fonction sur le domaine [0..5]x[0..5].

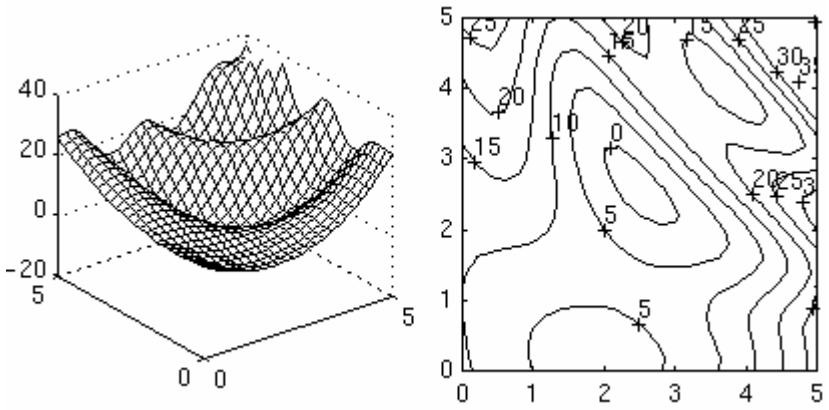

Figure 80. Surface et contours de la fonction analytique

Pour l'élaboration du métamodèle, on a choisi de générer 25 points par un plan factoriel (le plus facile à adopter dans ce cas). L'adaptation du métamodèle kriging a été faite sur la base de ces 25 points (les points en ronds sur la Figure 81 -b).

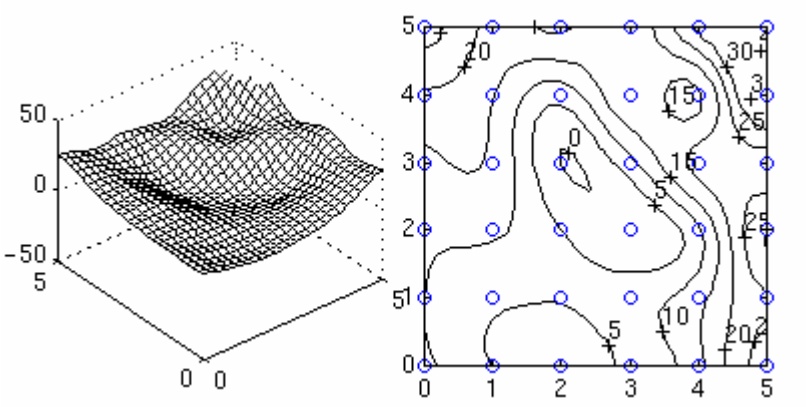

(a) (b)

Figure 81. (a & b) : Surface et contours de l'approximation par le métamodèle kriging (25 points d'un plan factoriel pour l'adaptation)

Le métamodèle qui apparaît dans la Figure 81-a semble avoir, globalement, la même forme que la fonction d'origine sans être très exacte. Sur le tracé des contours on peut mieux voir à quel point le métamodèle épouse-t-il la forme d'origine. Le métamodèle, ainsi obtenue après des cycles d'estimations de la plus grande vraisemblance (MLE : Maximum Liklihood Estimate) pour les valeurs de θ, a donné pour ces valeurs $\theta = (22.74 , 34.468)$.

Pour la validation du métamodèle, on a généré par le biais d'un plan factoriel 625 (25x25) points de validation.

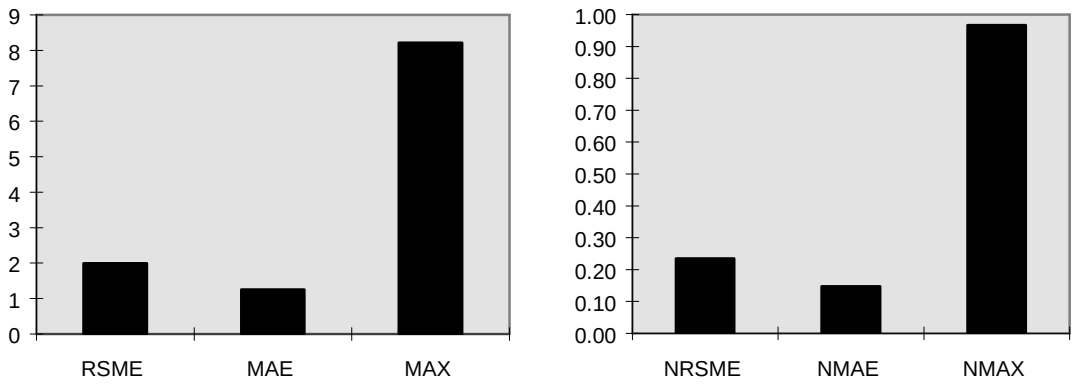

Figure 82. Différents types d'erreurs d'approximation du métamodèle kriging (25 points d'un plan factoriel pour l'adaptation du métamodèle)

Bien que l'adaptation de ce métamodèle soit relativement rapide, 14s, (on considère le temps de génération des points par le plan d'expériences et le temps de calcul de θ, le calcul étant effectué sous Matlab avec une station de travail Silicon Graphics de 1 GHz), les résultats de l'approximation sont pauvres. On remarque bien que l'erreur relative NMAX, de 0.97, est une erreur très importante (voir Figure 82). Ce qui signifie, dans ce cas, que le métamodèle peut donner des réponses locales avec un écart important par rapport aux réponses réelles.

Pour pousser un peu les limites d'approximation du métamodèle kriging, dont la précision dépend essentiellement, comme tout autre métamodèle, du nombre des points de l'échantillon, on a essayé d'augmenter le nombre des points générer par le plan d'expérience pour passer de 25 points à 100 points. Il est à noter que dans la pratique, où il s'agit de problème industriel avec des simulations numériques qui durent quelques minutes (1 à 10mn suivant la complexité du problème et la puissance de l'ordinateur), le nombre de points à générer reste très limité.

Les résultats obtenus pour ce nombre de points sont nettement meilleurs. On voit sur la Figure 83-b que le métamodèle reproduit avec une grande précision les contours de la fonction d'origine.

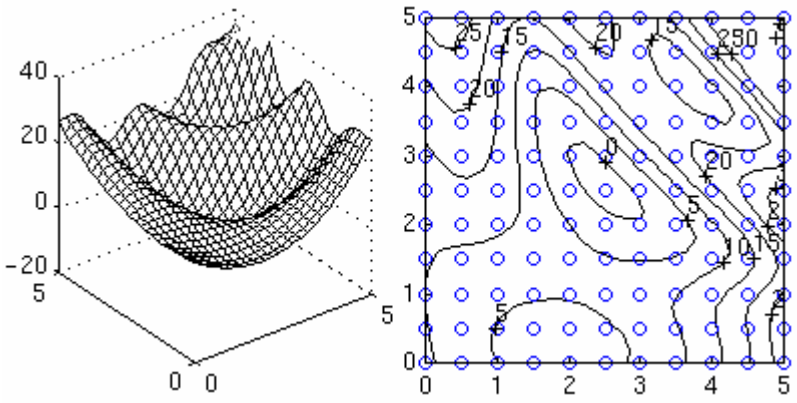

(a) (b)

Figure 83. (a & b) : Surface et contour de l'approximation par le métamodèle kriging (100 points d'un plan factoriel pour l'adaptation)

Les valeurs obtenues de θ sont (25.0 , 25.0). Ces valeurs, sont en réalité les valeurs des bornes inférieures de la MLE qu'on s'est fixées. En effet, des valeurs plus faibles conduisent à la singularité de la matrice de corrélation $\mathbf{R}$.

Après un temps de calcul de 37.5s, nécessaires pour la génération des points du plan factoriel et de l'adaptation du métamodèle, tous les type d'erreurs d'approximation obtenues sont assez faibles.

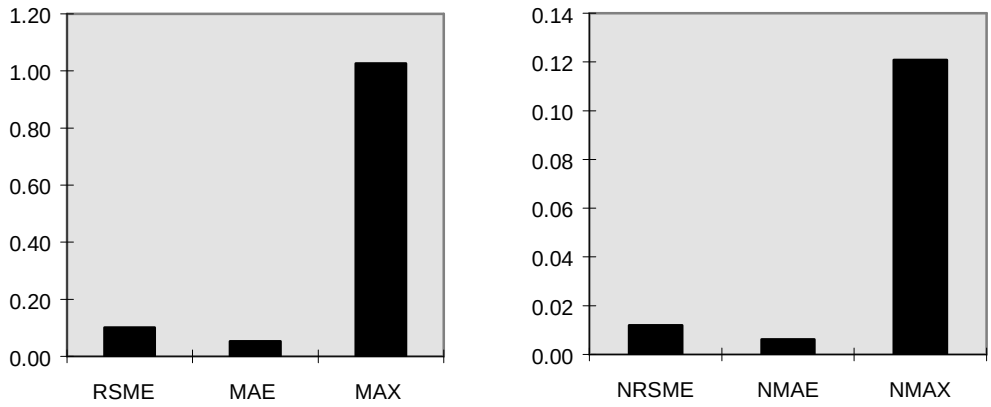

Figure 84. Différents types d'erreurs d'approximation du métamodèle kriging (100 points d'un plan factoriel pour l'adaptation du métamodèle)

Avec une erreur relative *NRSME* de 0.01 le métamodèle reproduit globalement avec une très bonne précision les réponses du modèle d'origine (voir Figure 84). Même si la fonction qui a servi d'exemple est non linéaire, la valeur maximale relative de la valeur absolue des écarts *NMAX* ne dépasse guère les 12 %.

Ces résultats montrent que les approximations du métamodèle s'améliorent sensiblement en adoptant un nombre plus important de points d'échantillon.

Appendix C

The Normalized Normal Constraint Method for Generating Pareto Frontiers

Messac and Ismail-Yahaya [Ismail-Yahaya et Messac 2002a] developed first the Normal Constraint (NC) method. And, because the original NC method does not fulfill criterion #3 of the generation methods – the ability of the method to generate only Pareto solutions – they improved the method by presenting the **Normalized Normal Constraint** (NNC) Method. For more details of the last method, the reader is invited to read [Messac et al. 2003] [Messac et Mattson 2004].

The NNC method is a Pareto frontier generator that validates the four criteria about generation methods for Pareto frontier. The method (i) generates an even distribution of Pareto points along the complete Pareto frontier (see definition of even distribution in section §C.5), (ii) it is insensitive to design objective magnitude, (iii) it is valid for an arbitrary number of design objectives, and (iv) it is relatively easy to implement.

So, in this section we present, first, requisite mathematical preliminaries. Then, we present through section §C.2 to section §C.7 the normalized normal constraint method. After that, we present the Pareto filter, which eliminates dominated solutions from the generated set of points. And finally we provide numerical examples to illustrate the method.

But before beginning, here is the nomenclature used for the further developments in this section.

- **Nomenclature**

x	Vector of design parameters
μ	Vector of design Performances (metrics or objectives)
g	Vector of inequality constraints
h	Vector of equality constraints
μ^{i*}	i-th anchor point
x^{i*}	x corresponding to μ^{i*}
$\vec{v}_i$	Vector from anchor points i to point j, $(i \neq j)$
p	Vector of points on the utopia plane
n_p	Number of generated Pareto points
α	Non-dimensional parameter
δ^i	i-th fixed increment
n	Number of design objectives
n_x	Number of design parameters

Subscripts and Superscripts

$\bar{(\ )}$	Normalized form of variable $(\ )$
$*$	Indicates optimum
U	Indicates utopia (ideal)
N	Indicates nadir (worst)
i, j, k, r	Dummy indices
l	Minimal value or Lower bound
u	Maximal value or Upper bound

C.1 Mathematical Preliminaries

This section provides requisite mathematical preliminaries. A generic formulation of the multiobjective optimization problem is presented.

The Multiobjective Optimization Problem (MO)

For mechanical design, engineers need to carry out the optimization of the multiple performance criteria subject to different constraints. The multiobjective optimization represents this activity. We define the mathematical representation of the multiobjective optimization problem as follows:

Problem P1

$$\min_x \{\mu_1(x)\, \mu_2(x) \ldots \mu_n(x)\} \qquad (n \geq 2) \tag{C.1}$$

subject to

$$g_j(x) \leq 0 \qquad (1 \leq j \leq r) \tag{C.2}$$

$$h_k(x) = 0 \qquad (1 \leq k \leq s) \tag{C.3}$$

$$x_{li} \leq x_i \leq x_{ui} \qquad (1 \leq i \leq n_x) \tag{C.4}$$

The vector $x \in R^{n_x}$ denotes the design parameters and μ_i denotes the ith generic design metric (i.e., objective). In Problem P1, g in equation (C.2) and h in equation (C.3) are inequality and equality constraint vectors, respectively; and in equation (C.4) is the lower and upper bounds of the design parameters. As stated, Problem P1 does not yield a unique solution.

Associated with every MO problem is a ***feasible performance space***. By definition, a design solution within the feasible performance space satisfies the constraints. Figure 85 shows a feasible performance space (shaded surface) for a bi-objective case. The mutually orthogonal axes represent individual design objectives. For problems of three objectives the feasible performance space is a volume and for more than three objectives, the feasible performance space is a hyper volume. Note that it can be a non-convex volume.

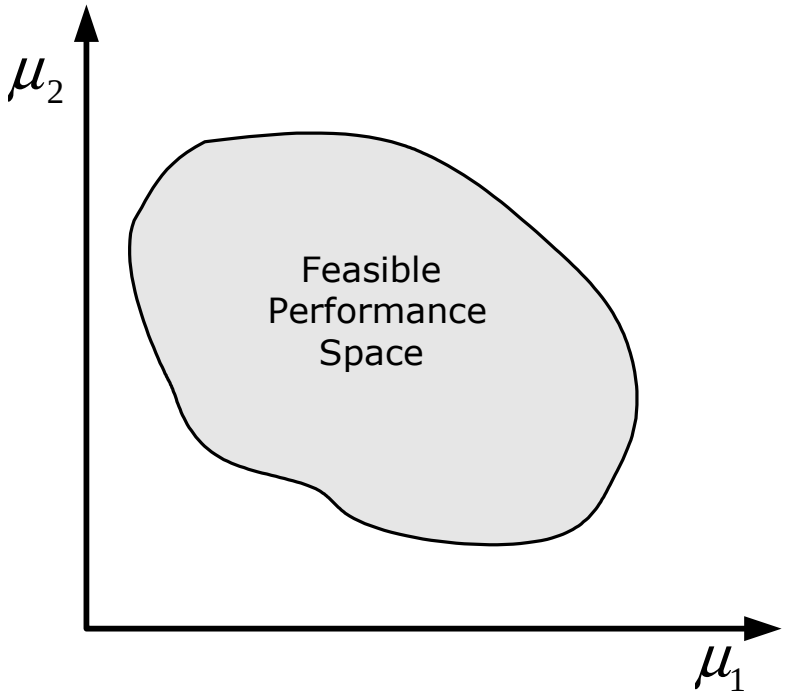

Figure 85. Feasible performance space (shaded surface) for bi-objective case

C.2 Reference Points and Planes

For every MO problem and for a better understanding of the Normal Constraint method principles, some important references consisting of particular points, vectors, and planes are defined in the following.

Design Performances Points are any of the designs in the performance design space that correspond to the set of the n design objectives. We denote design performance as μ. And it is written as follows:

$$\mu = \{\mu_1, \mu_2, \ldots, \mu_n\} \tag{C.5}$$

Anchor Points (or, the end points of the Pareto frontier) are specific designs, in the feasible performance space. They correspond to the best possible values for respective individual objectives. We denote anchor points as μ^{i*}.The ith anchor point is obtained when the ith objective μ_i is minimized independently. For a bi-objective problem, the anchor points are labeled as μ^{1*} and μ^{2*} in Figure 86.

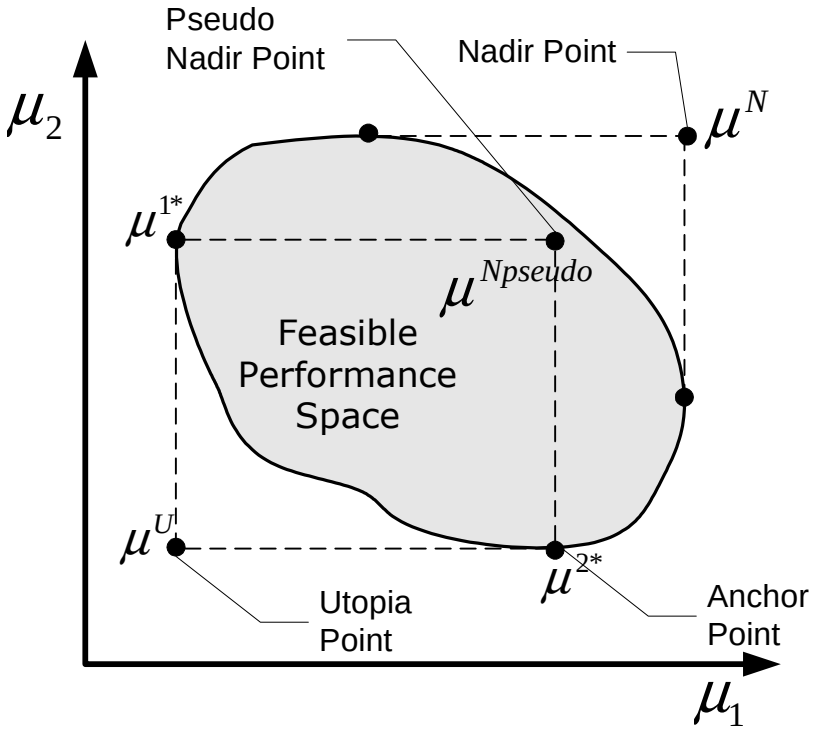

Figure 86. Graphical Description of multiobjective reference points

The anchor points (or optimum vertices) are obtained by solving Problem PU*i*, defined as follows.

Problem PU*i*

$$\min_x \{\mu_i(x)\} \qquad (1 \le i \le n) \tag{C.6}$$

subject to

$$g_j(x) \le 0 \qquad (1 \le j \le r) \tag{C.7}$$

$$h_k(x) = 0 \qquad (1 \le k \le s) \tag{C.8}$$

$$x_{li} \le x_i \le x_{ui} \qquad (1 \le i \le n_x) \tag{C.9}$$

So, the *i*th anchor point can be written as:

$$\mu^{i*} = \left[\mu_1\left(x^{i*}\right)\ \mu_2\left(x^{i*}\right) \cdots\ \mu_n\left(x^{i*}\right)\right]^T \tag{C.10}$$

where x^{i*} is the optimal decision (i.e. solution) vector for problem PUi ($x^{i*} \in R^{n_x}$).

Anchor points are important for the definition of the latter following reference points and hyper-planes. They are important for the effectiveness of NNC method. So it is important for each anchor point to find the global minimum for the problem PUi. The classic optimization techniques can converge to a local minimum if the provided starting point in the algorithm is near a local minimum. To be sure to obtain a global minimum for the problem PUi, we use, in a first step, ***Direct***[1] as a global optimization algorithm. The *Direct* algorithm approximates the global minimum. Then in a second step we use the approximate global minimum as a starting point for a classic optimization technique. The obtained minimum is a global minimum for problem PUi.

Utopia Point is a specific point, generally outside of the feasible performance space, that corresponds to all objectives simultaneously being at their best possible values. The utopia point is denoted as μ^U in Figure 86, and is written as:

$$\mu^U = \left[\mu_1\left(x^{1*}\right)\ \mu_2\left(x^{2*}\right) \cdots\ \mu_n\left(x^{n*}\right)\right]^T \tag{C.11}$$

Nadir Point is a point in the performance space where all objectives are simultaneously at their worst values. The nadir point is written as:

$$\mu^N = \left[\mu_1^N\ \ \mu_2^N\ \cdots\ \mu_n^N\right]^T \tag{C.12}$$

where μ_i^N is defined as

$$\mu_i^N = \max_x \mu_i\left(x\right) \tag{C.13}$$

subject to Eqs. (C.2–C.4).

---

[1] Direct is an optimization algorithm that searches for the global minimum. The name DIRECT comes from the shortening of the phrase "DIviding RECTangles", which describes the way the algorithm moves towards the optimum. More details can be found at: http://www4.ncsu.edu/~definkel/research/index.html

Pseudo Nadir Point is a point in the performance space with the worst design objective values of the anchor points (see Figure 86). The pseudo nadir point is denoted as $\mu^{Npseudo}$ and written as:

$$\mu^{Npseudo} = \left[\mu_1^{Npseudo} \;\; \mu_2^{Npseudo} \;\; \cdots \;\; \mu_n^{Npseudo}\right]^T \tag{C.14}$$

where $\mu_i^{Npseudo}$ is defined as

$$\mu_i^{Npseudo} = \max\left\{ \mu_i\left(x^{1*}\right), \cdots, \mu_i\left(x^{n*}\right) \right\} \tag{C.15}$$

Utopia Line is the line joining two anchor points in the bi-objective cases (see Figure 87), and **Utopia Plane** is a hyperplane constructed such that it comprises all anchor points. The word Utopia is used here to indicate that the plane contains the n optimum vertices, components that form the Utopia point. We note that since the Utopia point is generally unattainable, it is not part of the Utopia plane.

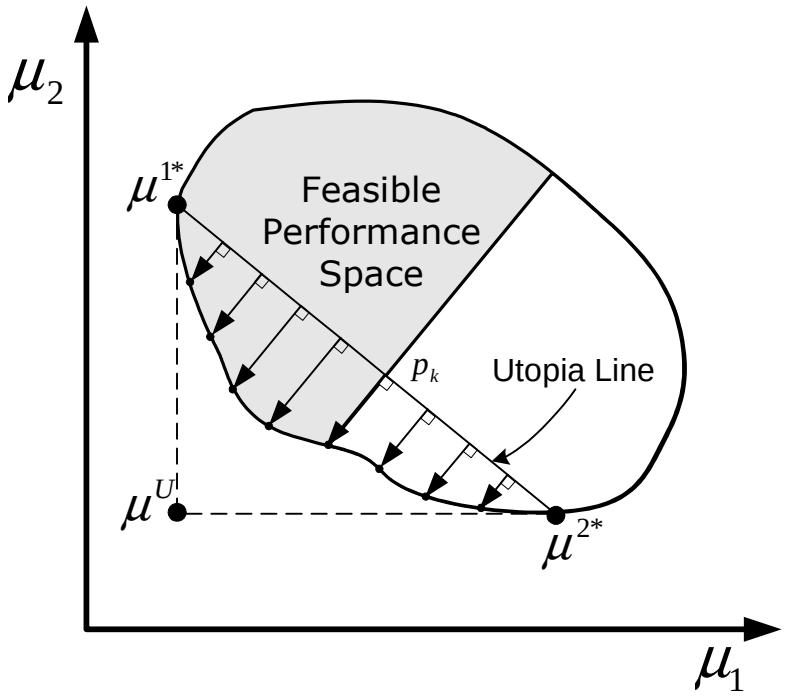

Figure 87. Performance space reduction under the Normal Constraint method for a bi-objective case

The principle of the NNC method is to obtain a set of evenly distributed Pareto solutions for a generic MO problem (Problem P1) by performing a series of optimizations. Each optimization in the series is performed after being subject to a reduced feasible performance space. With each performance space reduction, a single Pareto solution is obtained by (i) transforming the original MO problem to a single objective problem, and (ii) minimizing the single objective subject to the reduced performance space. Starting with the original feasible performance space and reducing it until the entire performance space has been explored, the NNC method generates Pareto solutions throughout the Pareto frontier.

C.3 Normalization

In most practical design case, the design objectives in Problem 1 have different magnitudes. The objectives must first be normalized in order to obtain a set of Pareto solutions that well represents the Pareto frontier. The objectives can be normalized by the following approach.

The normalized value of the design performance point, denoted as $\bar{\mu}$, can be computed using the utopia point and pseudo nadir point. The following equation is used to perform the mapping.

$$\bar{\mu} = \left\{\bar{\mu}_1, \bar{\mu}_2, \ldots, \bar{\mu}_n\right\} \tag{C.16}$$

where

$$\bar{\mu}_i = \frac{\mu_i - \mu_i^U}{\mu_i^{Npseudo} - \mu_i^U} \quad for\ each\ i \in \{1, \ldots, n\} \tag{C.17}$$

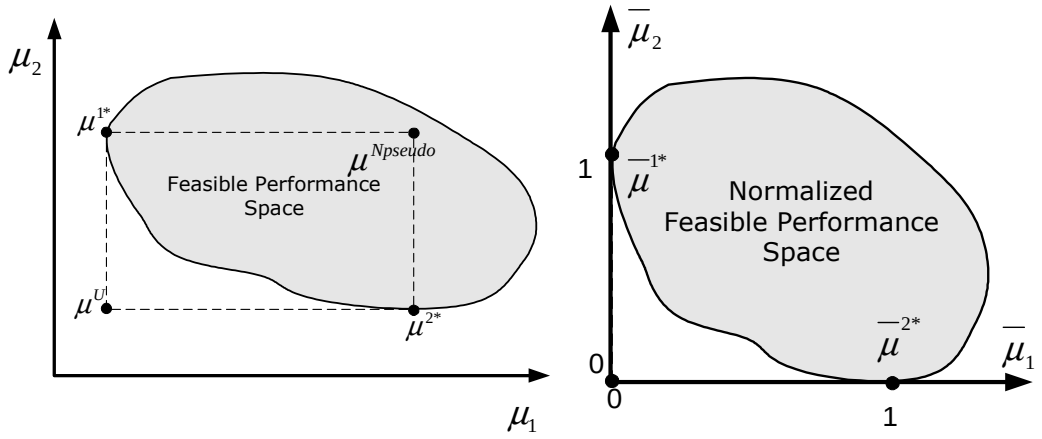

General Design performance Space Normalized Design Performance Space

Figure 88. Normalized Design performance space for a bi-objective case

Note that the normalization is performed in the performance (objective) space – not the design parameter space -. From here, further problems and expressions are expressed when needed with the normalized form $\bar{(\cdot)}$. Figure 88 shows the feasible performance space before and after normalization.

C.4 The NNC Method description

The NNC method entails two critical aspects that result in the generation of an evenly distributed set of Pareto solutions. The first aspect is that of judiciously reducing the feasible performance space. The second aspect is that of choosing a sequence of reductions and optimizations that result in an evenly distributed set of Pareto solutions. In the next sections, the notion of even distribution is detailed. Then, the reduction of the performance space is presented. And finally, the process of sequential reduction and optimization for the generation of Pareto points is given. Figure 89 illustrates the process of the NNC method.

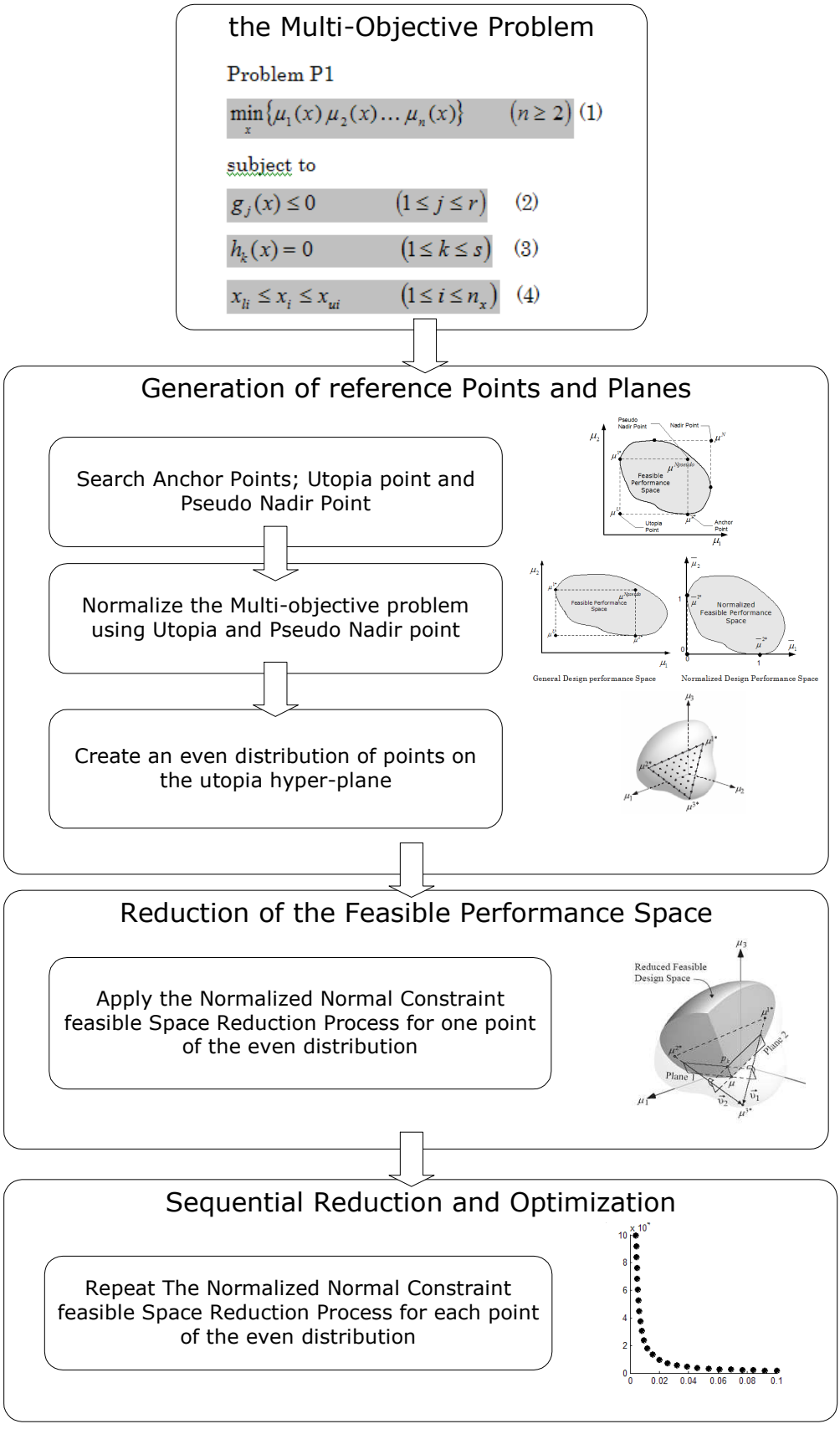

Figure 89. The process of the Normalized Normal Constraint (NNC) Method

C.5 Even Distribution

Distribution means sampling. A set of points is evenly distributed over a region if no part of that region is over or under represented in that set of points, compared to other parts. A measure of distribution evenness is described in the following. We note that the objective space is normalized.

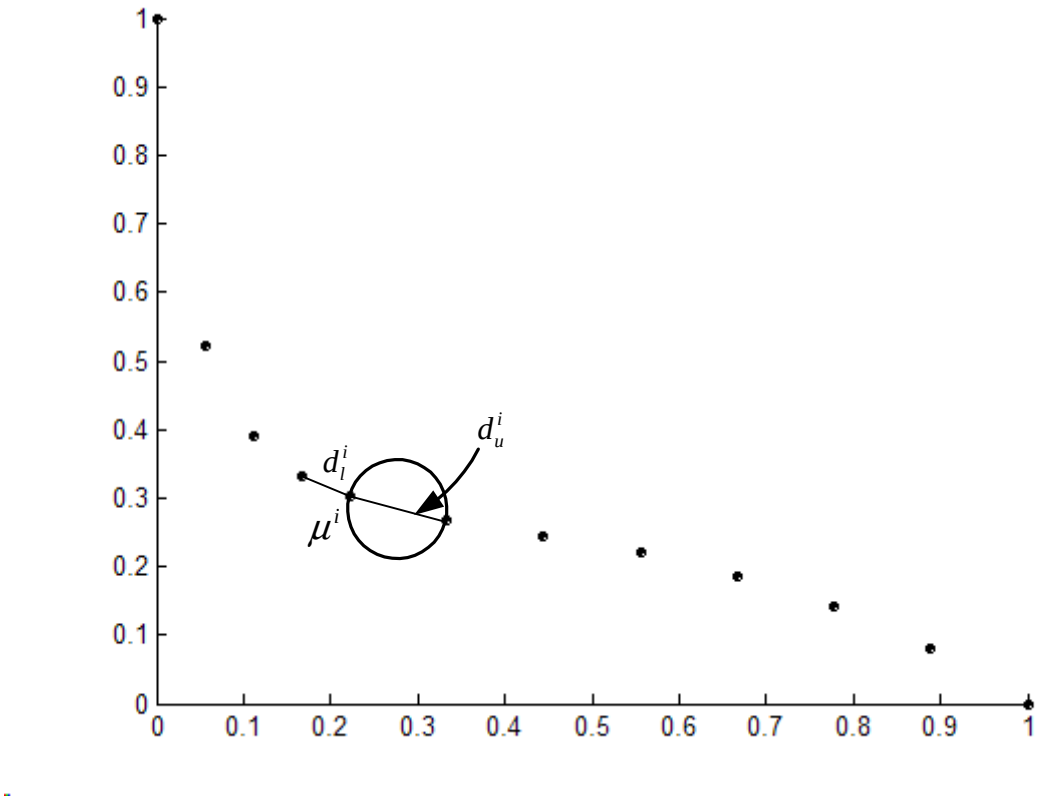

Figure 90. Graphical description of factors contributing to the evenness of a distribution of points

One approach for measuring the evenness of a distribution of points can be understood through the illustration in Figure 90. In this figure, each axis represents a design objective. To measure the evenness of the distribution of points in Figure 90, we measure the distances between each point, $\bar{\mu}^i$, and the rest of points in the set. For each point in the set, we take into account two distances. The first distance is the smallest distance that can be found between the point $\bar{\mu}^i$ and any other point in the set. We find the nearest neighbor point to $\bar{\mu}^i$. This distance is denoted as d_l^i. And it is expressed as

$$d_l^i = \min_{j \neq i}\left(\left\|\bar{\mu}^i - \bar{\mu}^j\right\|\right) \tag{C.18}$$

The second distance is the diameter of the largest circle that can be constructed between the point $\bar{\mu}^i$ and any other point in the set such that no point in the set is within the circle. The distance is denoted as d_u^i. And it is expressed as:

$$\begin{aligned} d_u^i &= \max_{j \neq i}\left(\left\|\bar{\mu}^i - \bar{\mu}^j\right\|\right) \text{ Such that } \textit{None of } \bar{\mu}^k \textit{ is interior to the circle } (\bar{\mu}^i, \bar{\mu}^j) \;\; \forall\, k \neq j \neq i \\ &= \max_{j \neq i}\left(\left\|\bar{\mu}^i - \bar{\mu}^j\right\|\right), \quad \bar{\mu}^j \textit{ is taken such that } \left\|\bar{\mu}^k - \theta^{ij}\right\|^2 \succ \left(\frac{\left\|\bar{\mu}^i - \bar{\mu}^j\right\|}{2}\right)^2 \;\; \forall\, k \neq j \neq i \end{aligned} \tag{C.19}$$

where $\theta^{ij} = \dfrac{\bar{\mu}^i + \bar{\mu}^j}{2}$ is the center of the circle formed between $\bar{\mu}^i$ and $\bar{\mu}^j$

A measure of the evenness is given by the expression

$$\xi = \sigma_d / \hat{d} \tag{C.20}$$

where $\hat{d}$ and σ_d denote the mean and standard deviation of d, respectively; and where $d = \left\{d_l^1, d_u^1 \ldots, d_l^i, d_u^i, \ldots, d_l^{n_p}, d_u^{n_p}\right\}$. A set of points is evenly distributed when $\xi = 0$.

Figure 91 gives a numerical example, based on the case study in the section §C.10, of the evenness of a distribution. The set of points in Figure 91 (a) with measure of $\xi = 0.1631$ is better distributed than the set of points in the Figure 91 (b) with an evenness of $\xi = 0.8309$.

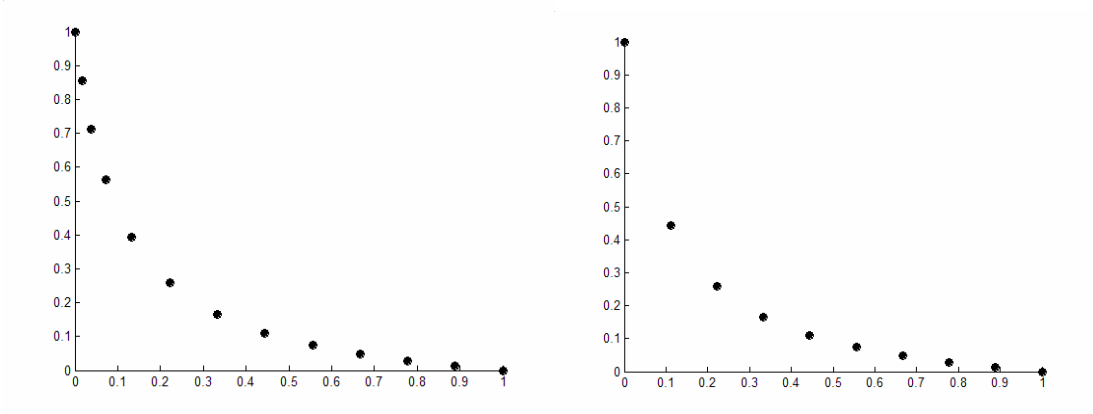

(a) $\xi = 0.1631$ (b) $\xi = 0.8309$

Figure 91. Numerical example of the evenness measure of a distribution

C.6 Reduction of the Feasible Performance space

An evenly distributed set of points on the utopia plane can be used to define reduction constraints that lead to good evenly distributed points on the Pareto frontier. A good even distribution of points on the Pareto frontier occurs when reduction constraints are made normal to the utopia plane. Figure 87 shows that the reduction constraints, which are normal to the utopia line (utopia plane in the multi-objective case), result in an even distribution of Pareto solutions for a bi-objective case. This important characteristic is what makes the NC method effective at generating even distributions of points on the Pareto frontier. FromFigure 87, it can be seen that obtaining an even distribution requires similar scales for the design objectives. Importantly, the section §C.3 provides a normalization approach that overcomes scaling problems, and ensures obtaining a set of Pareto solutions that well represents the Pareto frontier.

In this section, the development of NC based performance space reduction is presented, while the next section examines the sequence of reductions and optimizations.

Figure 93 shows the NC based approach to performance space reduction. Planes 1 and 2, and the corresponding optimization constraints, are obtained using the process below.

The Normalized Normal Constraint feasible Space Reduction Process (NNCSR)

Stage 1 Compute $n-1$ vectors. One vector from the i-th anchor point to the j-th anchor point for all $i \neq j$, where j is an index of an arbitrarily given design objective.

$$\vec{v}_i = \bar{\mu}^{j*} - \bar{\mu}^{i*} \qquad \forall i \in \{1,\ldots,n\}; \quad i \neq j \tag{C.21}$$

Stage 2 **POINT GENERATION ON UTOPIA PLANE:** In this stage we choose a generic point, $\bar{p}_k$, on the utopia plane.

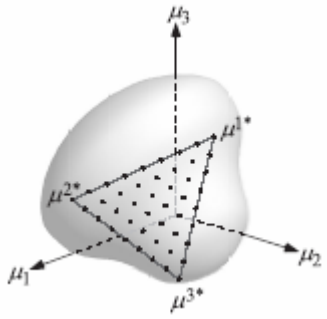

Figure 92. A set of evenly distributed points on the utopia plane, from [Messac et Mattson 2004].

To illustrate the generation of the evenly distributed points on the utopia plane, we again consider a three-objective case as shown in Figure 92. Here, a section of the utopia plane is shown as a triangle with the anchor points at the vertices. A set of evenly distributed points is shown on the utopia plane. Any point on the utopia plane can be defined as a function of the anchor points.

In general, the i-th point on the polygon formed by the anchor points (triangular section of the utopia plane for the three-objective case) can be written as:

$$\bar{p}_k = \sum_{j=1}^{n} \alpha_k^j \bar{\mu}^{j*} \tag{C.22}$$

where the non-dimensional parameter α_k^j satisfies

$$0 \leq \alpha_k^j \leq 1 \qquad \forall j \in \{1,\ldots,n\} \tag{C.23}$$

and

$$\sum_{j=1}^{m} \alpha_k^j = 1 \tag{C.24}$$

By varying α_k^j from 0 to 1 with a fixed increment of δ^j, an even distribution of points on the utopia plane can be generated.

The increment δ^j can be computed after choosing a number *m*, which is the number of the sampling points along a line between two anchor points. The increment δ^j) can be written as:

$$\delta^j = \frac{1}{m-1} \tag{C.25}$$

The total number, n_p , of the generated points on the utopia hyper-plane, which is the number of Pareto points to find on the Pareto frontier, is depending on the choice of the number *m*.

***Stage 3*: PERFORMANCE SPACE REDUCTION** at each point $\bar{p}_k$ the feasible performance space is reduced by enforcing the following set of plane constraints:

$$\vec{v}_i \cdot \left(\bar{\mu} - \bar{p}_k\right) \le 0 \qquad \forall i \in \{1,\ldots,m\};\ i \neq j \tag{C.26}$$

where $\bar{\mu}$ is a generic point in the feasible performance space. When Eq. (C.26) is equal to zero, it represents the equation of a plane that is perpendicular to the utopia plane containing point $\bar{p}_k$.

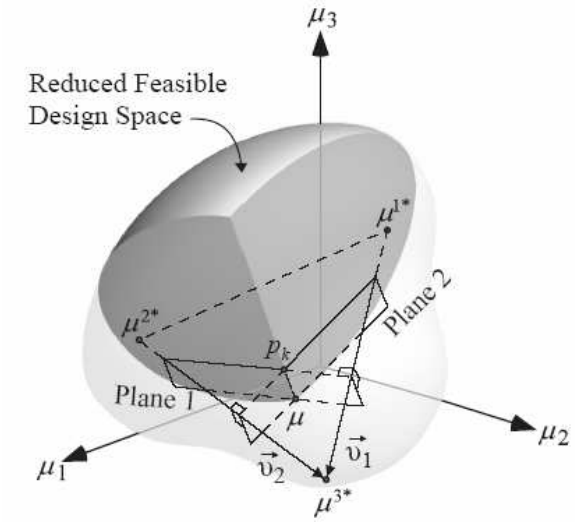

Figure 93. Normal Constraint based reduction of feasible performance space, from [Messac et Mattson 2004]

For the purpose of illustration, Figure 93 shows the reduced feasible performance space that can be described by the set of optimization constraints as follows:

$$g_j(x) \le 0 \qquad (1 \le j \le r) \tag{C.27}$$

$$h_k(x) = 0 \qquad (1 \le k \le s) \tag{C.28}$$

$$x_{li} \le x_i \le x_{ui} \qquad (1 \le i \le n_x) \tag{C.29}$$

$$\vec{\bar{v}}_i \cdot \left(\bar{\mu} - \bar{p}_k\right) \le 0 \qquad \forall i = 1,2 \tag{C.30}$$

$$\vec{\bar{v}}_i = \bar{\mu}^{3*} - \bar{\mu}^{i*} \qquad \forall i = 1,2 \tag{C.31}$$

The solid volume with two flat surfaces represents the reduced feasible performance space. A section of the utopia plane is shown as a triangle with the anchor points at the vertices. Planes 1 and 2 define the flat surfaces of the reduced feasible performance space and correspond to optimization constraints that make all but the shaded volume infeasible.

Stage 4 GENERATION OF PARETO POINTS

The benefit of stage 3 is that after feasible performance space reduction, at each point $\bar{p}_k$, a single objective optimization, described by Problem P2, can be effectively resolved. The optimization results in a single Pareto solution for the original multiobjective problem.

Using the set of evenly distributed points on the Utopia plane (generated in stage 2), a corresponding set of Pareto points can be generated by solving a succession of optimization runs of Problem P2. Each optimization run corresponds to a point on the Utopia Plane. For each generated point $\bar{p}_k$ on the Utopia plane, the following problem is solve for the *j* th point.

Problem 2 (for the *j*th point)*: Normalized Normal Constraint Generic Optimization Problem for Point* $\bar{p}_k$

$$\min_x \left\{\bar{\mu}_j(x)\right\} \tag{C.32}$$

subject to

$$g_j(x) \le 0 \qquad (1 \le j \le r) \tag{C.33}$$

$$h_k(x) = 0 \qquad (1 \le k \le s) \tag{C.34}$$

$$x_{li} \le x_i \le x_{ui} \qquad (1 \le i \le n_x) \tag{C.35}$$

$$\vec{\bar{v}}_i \cdot \left(\bar{\mu} - \bar{p}_k\right) \le 0 \qquad \forall i \in \{1,\ldots,n\}, \quad i \ne j \tag{C.36}$$

$$\vec{\bar{v}}_i = \bar{\mu}^{j*} - \bar{\mu}^{i*} \qquad \forall i \in \{1,\ldots,n\}, \quad i \ne j \tag{C.37}$$

The NNCSR process reduces the performance space for a generic point $\bar{p}_k$ on the utopia plane.

C.7 Sequential Reduction and Optimization

Performed repeatedly for a set of evenly distributed points, Problem 2 will yield an even distribution in the normalized space. This distribution in the normalized space directly leads to a set of Pareto solutions that well represents the objectives ranges in the non-normalized space.

C.8 Complete representation of Pareto frontier with the Normalized NC method

The Normalized NC as presented above can not guarantee the complete representation of the Pareto frontier for problems of more than two objectives. In some cases, some regions in the Pareto frontier are left unexplored. Messac and Mattson [Messac et Mattson 2004] present a method to overcome the limitations of the originally developments of the NNC method. The method consists in two main aspects. The first one is to encompass the entire feasible space by a hypercube, which is constructed such that the utopia and nadir points occupy the opposite corners. The second aspect is to resize the utopia plane section by enlarging the utopia plane section until it encloses the normal projection of the hypercube onto the utopia plane.

We do not integrate the complete representation of the Pareto frontier as it is described by [Messac et Mattson 2004] into our development, considering that the unattainable regions are small parts of the Pareto frontier [Das et Dennis 1998] and the computing developments to implement the method are out of the scope of this work.

C.9 Pareto filter

- **Local or non-Pareto solutions**

There are some special cases where the Normalized NC method results in locally Pareto or non-Pareto solutions (in addition to all the Pareto points). To overcome this deficiency, a simple Pareto filter, described in [Messac et al. 2003] and [Mattson et al. 2002], can be used. Pareto filters examine a set of candidate solutions and remove all that are not globally Pareto optimal.

C.10 Academic Case Study: Generation of Pareto Frontier

The case study involves a multi-objective 2-bar truss problem adapted from Azarm, Reynolds, & Narayanan [Azarm et al. 1999] (see Figure 94) described also in [Eddy et Lewis 2001]. We take the case study to illustrate the use of the normal constraint method for the populating of the Pareto Frontier. While the case study is a bi-objective one, we remind that the normal constraint method works well for multi-objective problems.

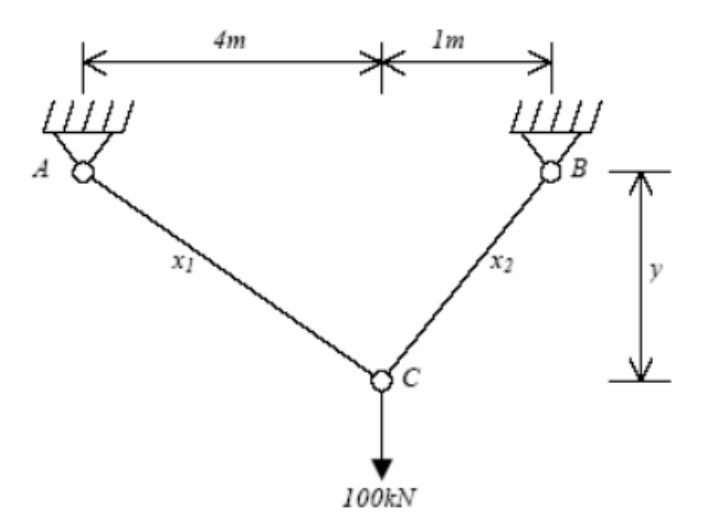

Figure 94. The truss case study, from [Azarm et al. 1999]

The problem formulation is givent as fallows:

Minimize:

$$f_{volume} = x_1\sqrt{16+y^2} + x_2\sqrt{1+y^2} \tag{C.38}$$

$$f_{stressAC} = \frac{20\sqrt{16+y^2}}{yx_1} \tag{C.39}$$

Subject to:

$$g_1(\bar{x}, y) \qquad f_{volume} \le 0.1 \tag{C.40}$$

$$g_2(\bar{x}, y) \qquad f_{stressAC} \le 100000 \tag{C.41}$$

$$g_3(\bar{x}, y) \qquad \frac{80\sqrt{1+y^2}}{yx_2} \le 0.1 \tag{C.42}$$

$$1 \le y \le 3 \tag{C.43}$$

$$0.0001 < x_1 < 0.1 \tag{C.44}$$

$$0.0001 < x_2 < 0.1 \tag{C.45}$$

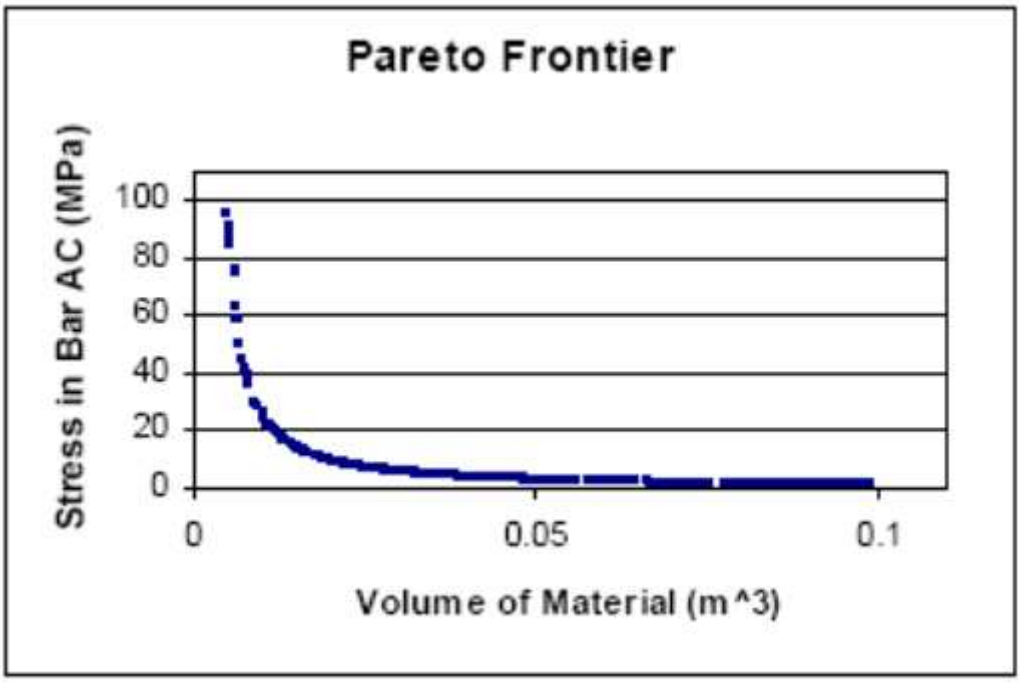

Figure 95. Pareto Set Generation. From [Azarm et al. 1999]

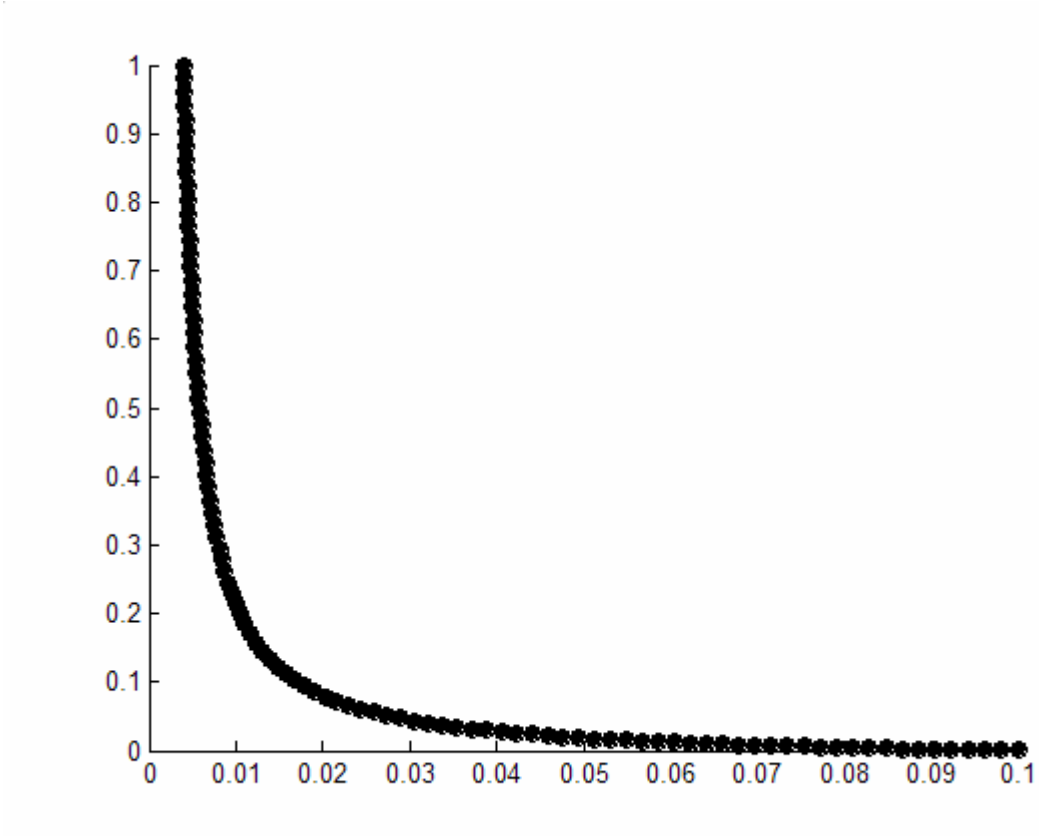

Figure 96. Pareto Set Generation in the normalized space using the NNC method

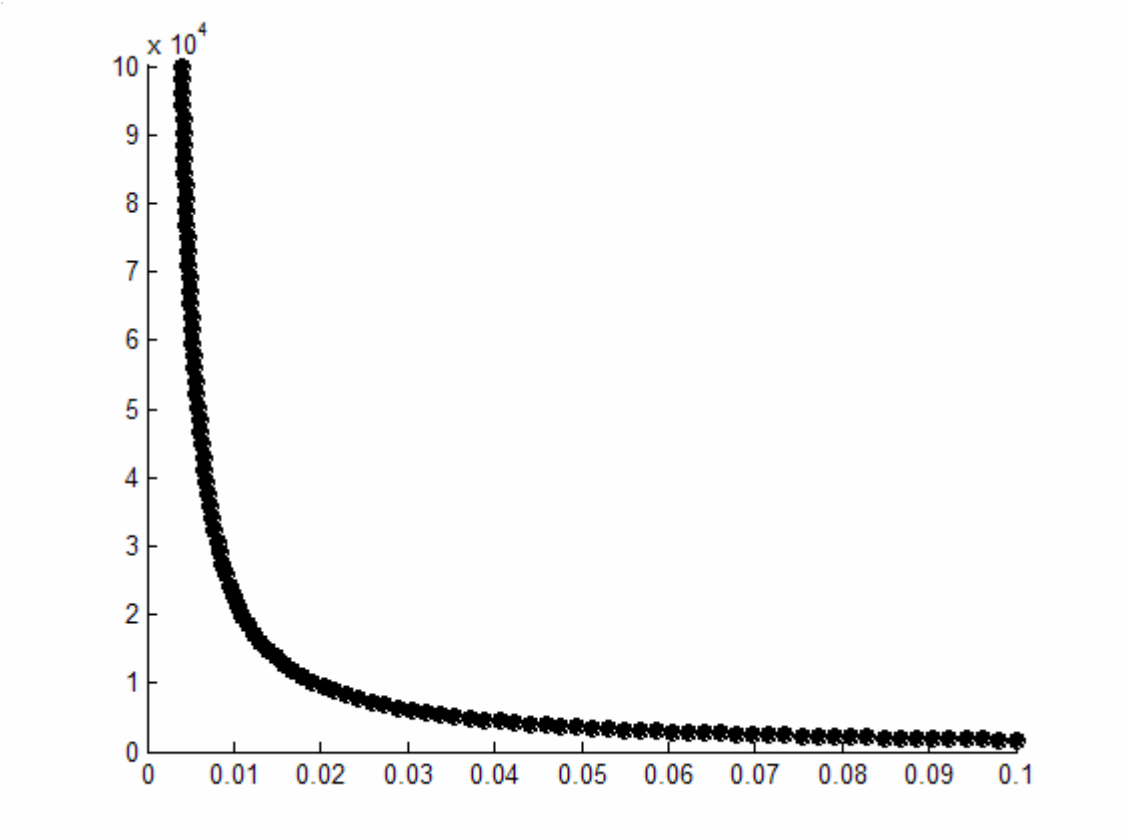

Figure 97. Pareto Set Generation in the performance space using the NNC method

From Figure 96 and Figure 97,we can see that the NNC method generate a better evenly distributed Pareto set. The Pareto set in Figure 95 was generated using Genetic Algorithm methods.

Abstract

In this thesis, we propose, for the preliminary design stage of automotive vehicle, a methodological framework to achieve a compromise between the architectural constraints of the mechanical subsystems and their contribution to reduce the noise inside the vehicle compartment.

Using the methodology, we make possible to engage trade-offs between automobile architects and mechanical engineers about the respect or the non-respect of architectural constraints and the fulfillment of noise performance targets.

The proposed methodological framework consists of five stages: (1) modeling the design problem, including (a) noise performances modeling and (b) architectural constraints modeling, (2) metamodeling the resulting design problem with kriging metamodels, (3) formulating the design problem as a Multi-Objective Optimization Problem, (4) generating with the use of the already generated metamodels the Pareto frontier of the Multi-Objective Optimization Problem with the Normalized Normal Constraint Method, and finally (5) leading negotiations based on the Pareto frontier representation in order to obtain a design compromise between architectural constraints and mechanical design performances of the subsystem.

To deal with the architectural constraints in the preliminary design stage, we introduce an architecture criterion that expresses the respect or the non-respect of the geometrical constraints. The originality of the method consists in shifting the incorporation of the stage of the volume allocation from the CAD environment to CAE environment using FEM models.

We introduce also a method of aggregating noise performances into a single real value criterion. The technique enables an efficient reduction of the high dimensionality of the design problem inherent to to the multiple noise performances of a mechanical subsystem.

The application of the methodology to an automotive case study has revealed its efficiency to improve the NVH performances of a car Body in White while respecting the tight architectural constraints in the neighborhood of the volume envelope allocated to the vehicle powertrain.

Finally, with this methodological framework, the negotiations between architects and design engineers are no longer based on qualitative judgments but they are, now, based on quantitative criteria for both of the architectural constraints and the mechanical performances.

Keywords Automotive, NVH, Volume Allocation, Pareto Frontier, Metamodel, Design of Experiments, Performance Aggregation, Preliminary Design, Compromise Negociation.

Résumé

Dans cette thèse, nous proposons un cadre méthodologique en phase de conception préliminaire dans l'industrie automobile, afin de gérer le compromis entre, d'une part, les contraintes d'architecture auxquelles est soumis un sous-système mécanique, et d'autre part une contribution satisfaisante du sous-système à la minimisation du bruit dans l'habitacle véhicule.

La méthodologie proposée, nous permet d'engager des négociations entre les architectes de l'automobile et les ingénieurs mécaniciens sur le respect ou le non-respect de contraintes d'architecture d'un sous-système ou d'un organe, ainsi que sur l'atteinte des cibles du cahier des charges en ce qui concerne les performances vibro-acoustiques.

Le cadre méthodologique proposé se compose de cinq étapes : (1) la modélisation du problème de conception, comprenant (a) la modélisation des performances vibro-acoustiques et (b) la modélisation des contraintes d'architecture (2) la métamodélisation (approximation mathématique) du problème de conception résultant en utilisant les métamodèles de type kriging, (3) la formulation du problème de conception sous la forme d'un problème d'optimisation multi-objectifs, (4) la génération grâce au métamodèle de la frontière de Pareto de ce problème d'optimisation multi-objectif par la méthode des contraintes normales et normalisées, (5) une étape de négociation entre les contraintes d'architecture et les performances du sous-système mécanique.

Pour gérer le problème des contraintes d'architecture, dans la phase de conception préliminaire, nous introduisons une méthode pour exprimer, par un critère dit d'architecture, le respect ou le non-respect des contraintes géométriques. L'originalité de cette méthode consiste dans le fait de migrer l'étape de l'allocation de volumes enveloppes sous un système de CAO vers un système d'IAO plus accessible aux ingénieurs puisque c'est dans ce système qu'ils gèrent leurs modèles éléments finis.

Nous introduisons, en outre, une méthode d'agrégation des performances vibro-acoustiques d'un sous-système mécanique en un seul critère (indicateur) à valeur réelle. Cette technique permet une réduction efficace de la dimension importante d'un problème de conception lié à l'étude d'un sous-système mécanique avec des multiples performances vibro-acoustiques.

L'application de la méthodologie à un cas d'étude, dans le domaine automobile, a permis de démontrer son efficacité à améliorer sensiblement les performances vibro-acoustiques d'une caisse en blanc (caisse nue d'une automobile) tout en respectant des contraintes d'architecture serrées à cause d'un volume enveloppe alloué au groupe motopropulseur du véhicule.

Finalement, avec ce cadre méthodologique, les négociations entre les architectes et les ingénieurs ne sont plus fondées sur des jugements qualitatifs, mais elles sont à présent fondées sur des critères quantitatifs à la fois pour les contraintes d'architecture et les performances mécaniques.

Mots-clefs automobile, vibro-acoustique, allocation de volume, frontière de Pareto, métamodèle, plan d'expérience, agrégation des performances, conception préliminaire, négociation de compromis.